JCBFM
Journal of Cerebral Blood Flow & Metabolism
2017, Vol. 37(1S) 240–311

DOI: 10.1177/0271678X17695987
journals.sagepub.com/home/jcbfm
SAGE

BRAIN & BRAIN PET 2017
Poster Viewing Session III

PS03-001

Poster Viewing Session III

The relationship between cerebral vascular and mitochondria oxygenation during arterial desaturations is predictive of injury severity in neonates with hypoxic-ischaemic encephalopathy

G. Bale[1], S. Mitra[2], I. De Roever[1], J. Meek[1], N. Robertson[2] and I. Tachtsidis[1]
[1]University College London, Medical Physics and Biomedical Engineering, London, United Kingdom
[2]University College London, Department of Neonatology, Institute for Women's Health, London, United Kingdom

Abstract

Objectives: The hypothesis is that the relationship between brain vascular and brain tissue mitochondrial oxygenation will differ with the severity of hypoxic-ischaemic injury that has been sustained by newborn infants. The aim was to test this hypothesis using broadband near-infrared spectroscopy (NIRS) to monitor changes in brain vascular oxygenation (HbD = oxyhaemoglobin (HbO_2)-deoxyhaemoglobin (HHb)) and brain tissue metabolism (oxidation of cytochrome-c-oxidase (oxCCO))[1].

Methods: 24 term neonates (9 severe, 15 mild) with hypoxic-ischaemic encephalopathy (HIE) were monitored with an in-house broadband NIRS device[2] during therapeutic hypothermia ($\leq 35^{\circ}C$) over postnatal days 1–4. Arterial saturation (SpO_2) decreases (>10%) were identified ($n = 54$, $n_{mild} = 43$, $n_{severe} = 11$). The changes in the concentration of haemoglobin and oxCCO signals per percentage SpO_2 change were averaged and grouped by the severity of injury (determined by MRS-measured lactate-to-NAA ratio).

Results: Fig.1 shows that the changes in the NIRS-haemoglobin signals were similar between the groups, whereas the oxCCO reduction in the infants with severe HIE was much larger than the infants with mild HIE. Further, the

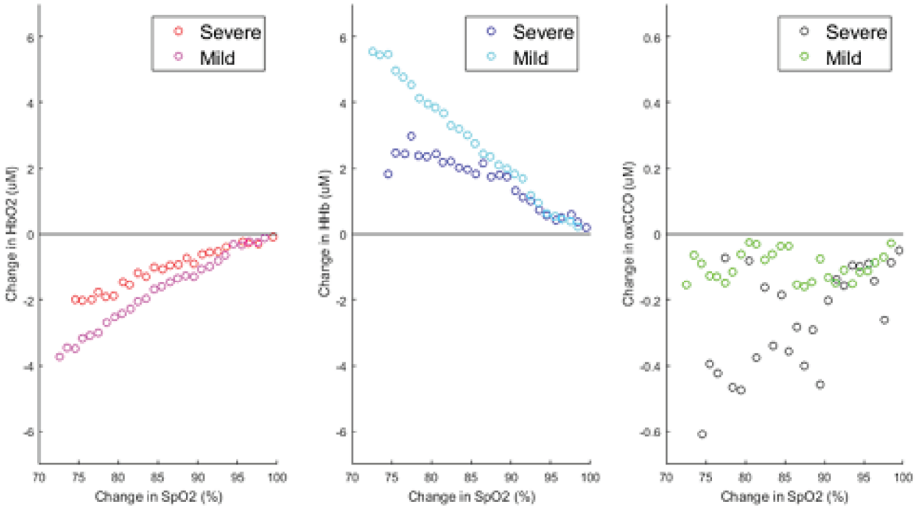

Fig 1: Mean cerebral concentration changes per SpO_2 percentage change for the mild and severe HIE groups.

HbD/oxCCO gradient was predictive of injury severity with a gradient greater than 0.1uM oxCCO per unit HbD change indicates severe injury (ROC curve area-under-the-curve = 0.81:73% sensitivity, 86% specificity).
Conclusions: We have found that the degree of drop in brain tissue mitochondrial oxygenation for a similar brain vascular oxygenation change is larger in infants with severe HIE. This could be due to a greater ability of the brain tissue to buffer the metabolic changes during brief hypoxic episodes in the infants with mild HIE. In conclusion, we have shown that HIE injury severity is linked to metabolism rather than vascular oxygenation, which is supported by other studies[3].

References

1. Bale et al. *J Biomed Opt*, *21*(9):091307(2016);
2. Bale et al. *Biomed Opt Exp*, *5*(10):3450–66(2014);
3. Dehaes et al. *J Cereb Blood Flow Metab, 34*(1):87–94(2014).

PS03-002

Poster Viewing Session III

Cerebral hemodynamic response to change of body position in patients with obstructive sleep apnea by diffuse correlation spectroscopy

C. Gregori-Pla[1], G. Cotta[1], I. Blanco[1], P. Zirak[1], A. Fortuna[2], M. Mayos[2,3] and T. Durduran[1,4]

[1]ICFO-Institut de Ciències Fotòniques, Castelldefels, Spain
[2]Hospital de la Santa Creu i Sant Pau, Barcelona, Spain
[3]CIBER Enfermedades Respiratorias (CiberRes) CB06/06, Madrid, Spain
[4]Institució Catalana de Reserca i Estudis Avançats (ICREA), Barcelona, Spain

Abstract

Objectives: Breathing is repeatedly interrupted in obstructive sleep apnea (OSA) syndrome during sleep. Left untreated, OSA may lead to increased cardiovascular risk and ischemic stroke.
We have evaluated the impairment of cerebral vasoreactivity (CVR) in OSA patients by an easy-to-do head-of-bed (HOB) [1] protocol; we have also evaluated if continuous positive air pressure (CPAP) treatment, the standard treatment for OSA patients, improves CVR after two years.
Methods: We have used diffuse correlation spectroscopy (DCS) [2] to follow microvascular cerebral blood flow (CBF) changes in the frontal lobes during a HOB challenge. We measured control and obstructive sleep apnea patients of different severities in different head-of-bed positions (supine to 30° to supine). Part of the severe patients were measured again after two years of treatment.
Results: Sixty-eight OSA patients (twenty-eight severe, twelve moderate, twenty-eight mild) and fourteen controls were recruited.
No difference in CBF response was found between different OSA severity groups in the first HOB change (supine to 30°) but moderate-to-severe OSA patients did not recover to baseline levels (30° to supine, Fig.1). This alteration was correlated to OSA severity, number of apneas/hypoapneas per hour of night sleep, and mean oxygen saturation by pulse-oximetry whole night.
This alteration disappeared after two years of CPAP treatment, blood flow response in the severe group (thirteen remeasured) recovered to baseline as controls.
Conclusions: CBF response to a mild head-of-bed challenge suggests that moderate and severe OSA patients do not recover to baseline CBF due to damaged CVR. In addition, this protocol suggests improved CVR in the severe group after two years of treatment.

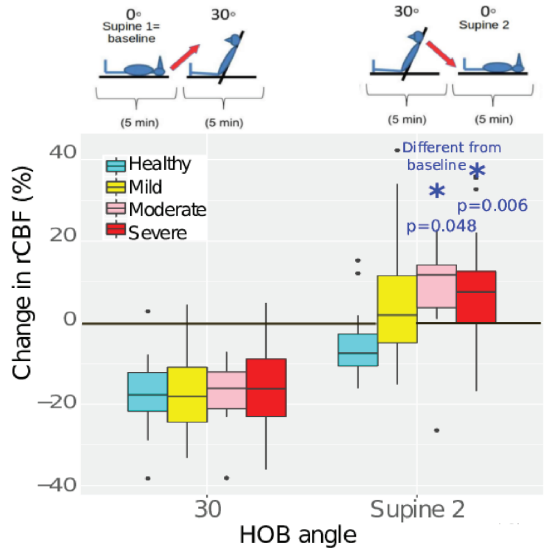

[Figure1]

Figure 1: Relative cerebral blood flow responses to different head-of-bed changes in different OSA severity groups.

References

1. Favilla et al. Stroke (2014)
2. Durduran et al. NeuroImage (2014)

PS03-003

Poster Viewing Session III

Acute high-intensity interval training, but not moderate-intensity aerobic exercise, decreases mu-opioid receptor availability in humans

T. Saanijoki[1], L. Tuominen[1,2], J.J. Tuulari[1], L. Nummenmaa[1], E. Arponen[1], K. Kalliokoski[1] and J. Hirvonen[1,3]

[1]University of Turku, Turku PET Centre, Turku, Finland
[2]Massachusetts General Hospital & Harvard Medical School, Boston, MA, United States
[3]Turku University Hospital, Department of Radiology, Turku, Finland

Abstract

Objectives: Physical exercise reduces stress and anxiety and induces positive mood changes, and exercise intensity regulates these effects. Previous positron emission tomography (PET) studies suggest that endogenous opioid system and μ-opioid receptors (MOR) underlie the euphoric sensations following prolonged exercise, yet the influence of exercise intensity on MOR in human brain remains elusive. Here we studied the effects of acute high-intensity interval training (HIIT) and moderate intensity continuous training (MICT) on MOR availability in healthy men.

Methods: Twenty two healthy men (age: 26 ± 5 years, BMI: 23.4 ± 1.7) were studied with PET using a bolus injection of MOR-selective radioligand [^{11}C]carfentanil. MOR binding was studied in three conditions in random order: 1) after 60 min of rest, 2) after MICT session (60 min of aerobic endurance cycling), and 3) after HIIT session (5×30 s all-out cycling efforts interspersed with 4 min recovery periods). All of the participants were scanned after rest and MICT, and twelve of them additionally after HIIT. Voxel-wise μ-opioid receptor availability was quantified with simplified reference tissue model using occipital cortex as the reference region, and statistical parametric mapping was used to compare MOR availability maps between the conditions.

Results: Acute HIIT significantly decreased MOR availability selectively in frontolimbic brain regions relevant for processing pain and pleasure, such as thalamus, insula, prefrontal cortex, amygdala, hippocampus, and anterior cingulate cortex (cluster-level FDR-corrected p-value < 0.05). In contrast, MOR availability after acute MICT showed no significant differences compared with the rest condition.

Conclusions: Intensity of physical exercise modulates the MOR availability in healthy men. HIIT-induced decreased MOR availability is consistent with endogenous opioid release, which may be a means to modulate pain perception and affective responses.

PS03-004

Poster Viewing Session III

Noninvasive optical method can predict hydrocephalus treatment and brain outcomes-initial experiences with post-infectious hydrocephalus infants in Uganda

P.-Y. Lin[1], J. Sutin[1], P. Farzam[1], J. Selb[1], F.-Y. Cheng[1], P. Ssenyonga[2], E. Mbabazi[2], J. Kimbugwe[2], J. Nalwoga[2], E. Nalule[2], B. Kaaya[2], K. Hagan[1], P.E. Grant[3], B. Warf[2,4] and M.A. Franceschini[1]

[1]Massachusetts General Hospital, Martinos Center for Biomedical Imaging, Charlestown, United States
[2]CURE Children's Hospital of Uganda, Mbale, Uganda
[3]Boston Children's Hospital, Fetal-Neonatal Neuroimaging and Developmental Science Center, Boston, United States
[4]Boston Children's Hospital, Departments of Neurosurgery and Global Health and Social Medicine, Boston, United States

Abstract

In Sub-Sahara Africa every year 200,000 infants are affected by post-infectious hydrocephalus (PIH). The majority of these infants go untreated suffering severe brain damage and death. CURE Children Hospital of Uganda (CCHU) treats over 1,000 hydrocephalus patients per year. Uncertainty remain over which children respond to surgical treatment. We partnered with CCHU to test whether our novel technology, which combines frequency-domain near-infrared spectroscopy (FDNIRS) and diffuse correlation spectroscopy (DCS) to quantify regional cerebral blood volume, blood flow and oxygen metabolism ($CMRO_2$), is able to predict treatment and neurological outcomes. For this pilot study we enrolled 35 patients and performed FDNIRS-DCS measurements one day pre- and post- treatment to investigate the impact of PIH and surgical treatments on cerebral physiology and

correlates the NIRS results with the pre-surgery CT, and the six months treatment and CT outcomes.
CT pre-surgical scans revealed primary injuries from neonatal infection and severe hydrocephalus resulted in high compression and thinning of the cortical mantle. FDNIRS-DCS pre-surgical measurements on 4 brain locations demonstrated high accuracy in detecting these brain structural damages by quantifying the distortions of the light propagation through the tissue (ROC AUC = 0.93). Differences in tissue scattering one day post-surgery showed a high predictive value (ROC AUC = 0.93) in treatment failure within 6 months. We also found brain regions with higher $CMRO_2$ tend to recover better than regions with low $CMRO_2$ in agreement with the 6 months post -surgery CT scans.
We are the first report the potential of FDNIRS-DCS method to predict hydrocephalus treatment and brain outcomes. We plan to develop a larger and more comprehensive clinical trial to validate our results and test the clinical use of this novel method in predicting neurodevelopmental outcomes. Success in the larger trial would lead to immediate improvements of infant hydrocephalus care in both the developing and developed countries.

PS03-005

Poster Viewing Session III

Pediatric sleep apnea suppresses cerebral blood flow reactivity to hypercarbia

D.R. Busch[1,2], T. Ko[2], J. Lynch[1], M. Winters[1], J. Newland[1], K. Mensah-Brown[1], T. Boorady[1], M.A. Cornaglia[1], J. Radcliffe[1], J. McDonough[1], J. Samuel[1], E. Matthews[1], R. Xiao[1], A. Yodh[2], C. Marcus[1], D. Licht[1] and I. Tapia[1]

[1]Children's Hospital of Philadelphia, Philadelphia, United States
[2]University of Pennsylvania, Philadelphia, United States

Abstract

Objectives: Obstructive sleep apnea syndrome (OSAS) affects 2–3% of children. OSAS is characterized by episodes of repetitive upper airway collapse during sleep that result in intermittent hypercapnia, hypoxemia and arousal from sleep. Due to their chronic exposure to hypercapnia during sleep, children with OSAS may be habituated to hypercapnia during wakefulness: although OSAS occurs during sleep, children with untreated OSAS exhibit neurobehavioral deficits while awake. However, no polysomnographic measure has been shown to predict these outcomes. We have applied near-infrared (650–950nm) diffuse optical and diffuse correlation spectroscopy (DOS and DCS, respectively) to fill this gap by providing non-invasive measurement of cerebral blood oxygenation, volume, and flow.
Methods: We utilized carbogen rebreathing to induce a significant change in change in end tidal CO_2 ($\Delta EtCO_2$ $\sim$25 mmHg). We computed blood flow changes relative to a pre-hypercapnic baseline; OSAS subjects repeated this protocol six months after surgery. This combination of a significant hypercapnic challenge with a non-invasive continuous monitor of cerebral blood flow provides a unique window into the impact of pediatric OSAS on cerebral reactivity.
Results: We observed no significant differences in baseline cerebral blood oxygenation and tissue hemoglobin concentration between groups. However, the relative change in cerebral blood flow, normalized by $\Delta EtCO_2$, was significantly greater in controls compared to children with OSAS and snorers. No correlations between sleep architecture and $rCBF/\Delta EtCO_2$ were found in any group. Analysis of post-surgical data is ongoing.
Conclusions: We have demonstrated a blunted cerebral blood flow response to hypercapnia in children with OSAS and snorers compared to healthy control subjects during wakefulness. This finding suggests that OSAS in children is associated with impaired cerebrovascular reactivity even during wakefulness.

PS03-006

Poster Viewing Session III

Magnesium and verapamil after recanalization in ischemia of the cerebrum (MAVARIC) in the Kentucky regional population: a clinical and translational study. Study Design

J. Fraser[1,2,3], M. Dobbs[2], P. Kitzman[4], A. Cook[5], L. Parker[1], D. Lukins[6] and B. Gregory[1,2,3]

[1]University of Kentucky, Neurological Surgery, Lexington, United States
[2]University of Kentucky, Neurology, Lexington, United States
[3]University of Kentucky, Anatomy and Neurobiology, Lexington, United States
[4]University of Kentucky, Health Sciences, Lexington, United States
[5]University of Kentucky, Pharmacology, Lexington, United States
[6]University of Kentucky, Radiology, Lexington, United States

Abstract

Objectives: Ischemic stroke is a leading cause of death and morbidity. Randomized trials demonstrated clinical benefit from endovascular thrombectomy, but outcomes were not uniform. We hypothesize that superselective intra-arterial (IA) administration of a combination of neuroprotective compounds directly into the recanalized cerebral vessel immediately following thrombectomy will be safe and improve outcomes. Neuroprotective effects of the calcium channel blocker, verapamil, have been demonstrated in our published mouse model of large vessel occlusion/thrombectomy/IA drug delivery, which showed improved infarct volume, reduced apoptotic cell death, and improved functional outcome. Similarly, magnesium sulfate is a small compound that has gained significant interest as a neuroprotectant. Working as a physiological voltage-dependent blocker of the NMDA receptor, magnesium also reduces excitotoxic damage from ischemia. Given prior failures of neuroprotective trials in ischemic stroke, we designed a randomized controlled blinded-outcome study to evaluate dual-neuroprotective therapy as an adjunct to thrombectomy.

Methods: Adult patients with anterior circulation occlusion undergoing successful thrombectomy will be eligible for the study. Immediately following thrombectomy, subjects will receive superselective IA infusion of either control saline or the study drugs in a randomized fashion. The subjects will then receive usual care treatment after thrombectomy, including MRI (or CT if unable) within 48 hours of treatment. Primary outcome will be safety (significant intracranial hemorrhage at 24 hours). Secondary blinded radiographic outcomes will include stroke volume, presence of microhemorrhages, and cerebral edema. Clinical outcomes will include change in NIH Stroke Scale, inpatient cognitive assessment, length of stay, and follow-up blinded clinical/cognitive scales. Enrollment goal will be 15 patients in each group.

Results: We anticipate an 18-month enrollment period to complete this study.

Conclusions: This study will provide crucial initial clinical data on the safety and potential efficacy of dual-therapeutic superselective intra-arterial neuroprotective therapy as an adjunct to mechanical thrombectomy.

PS03-007

Poster Viewing Session III

Non-invasive cerebral autoregulation monitoring during cardiac surgery with cardiopulmonary bypass

V. Petkus[1], B. Kumpaitiene[2], R. Zakelis[1], S. Krakauskaite[1], R. Chomskis[1], M. Svagzdiene[3], E. Sirvinskas[3], R. Benetis[3] and A. Ragauskas[1]

[1]Kaunas University of Technology, Health Telematics Science Institute, Kaunas, Lithuania
[2]Kaunas Hospital of Lithuanian University of Health Sciences, Clinic of Cardiothoracic and Vascular Surgery, Kaunas, Lithuania
[3]Lithuanian University of Health Sciences, Institute of Cardiology, Kaunas, Lithuania

Abstract

Objectives: Post-operative cognitive dysfunction (POCD) following cardiac surgery with a cardiopulmonary bypass (CPB) can be related to a temporal cerebral hypoperfusion and impaired cerebrovascular autoregulation (CA). Objective is to validate prospectively the innovative non-invasive CA monitoring technology for patient-specific mean arterial blood pressure (MAP) management in order to prevent POCD.

Methods: The ongoing study included 59 patients undergoing the CPB surgery. All patients were ASA III class, NYHA III class. Their age limits were 47–87 years. The "Vittamed505" noninvasive CA monitor based on the

intracranial blood volume (IBV) slow wave monitoring was used during surgery. CA status was estimated continuously by calculating the pressure reactivity index vPRx(t) as a phase shift between the slow waves of MAP(t) and IBV(t). The neuropsychological tests of cognition were performed before and 10 days after CPB surgery for each patient in order to estimate changes of mental abilities and to detect POCD.

Results: Results of prospective clinical trial: 34 patients without post-operative deterioration, 14 patients with deteriorated mental abilities and 11 patients with POCD. Duration of longest cerebral autoregulation impairment (LCAI) event above critical 240 sec threshold when $vPRx > 0$ is statistically significantly associated with deteriorated mental abilities and POCD.

Conclusions: Prospective trial showed that the duration of LCAI event during CPB surgery is associated with deteriorated mental abilities and risk of POCD. The „Vittamed505" noninvasive CA monitor can be used for the patient-specific MAP management during cardiac CPB surgery in order to prevent cognitive dysfunctions.

Acknowledgement: This research has been funded by the grant MIP-022/2014 from the Research Council of Lithuania

PS03-008

Poster Viewing Session III

Evaluation of MRI tumor characteristics and quantitative FDG-PET assessments of cerebro-cerebellar diaschisis: Pathophysiologic implications for gliomas

E.A. Segtnan[1], J. Holm[1], J.H. Decker[2], C. Constantinescu[1], A. Gjedde[3,4], P.F. Høilund-Carlsen[1,5] and J. Ivanidze[2]

[1]Odense University Hospital, Department of Nuclear Medicine, Odense, Denmark
[2]Weill Cornell Medical College, NewYork-Presbyterian Hospital, Department of Diagnostic Radiology, New York, United States
[3]Panum Institute, Department of Neuroscience and Pharmacology, Copenhagen, Denmark
[4]University of Southern Denmark, Odense, Denmark
[5]University of Southern Denmark, Faculty of Health Sciences, Department of Clinical Research, Odense, Denmark

Abstract

Purpose: Using FDG-PET-based THGr methodology and MRI-based volume segmentation of key lesion characteristics, we sought to improve understanding of the implications of cerebral and cerebellar diaschisis in the diagnosis and management of supratentorial gliomas.

Methods: A prospective cohort of 14 glioma patients (5 men, 9 women; mean age 63 years, range 35–77) underwent baseline PET-CT and MRI. Tumor, edema, and necrosis volume were obtained based on volume segmentation of gadolinium-enhanced T1-weighted images using 3D Slicer Software, Version 4.5 (http://www.slicer.org). We obtained total hemispheric glucose metabolic ratios (THGr) by dividing total hemispheric FDG uptake in each hemisphere with the expected diaschisis site, i.e., the ipsilateral cerebral hemisphere (THGr(Ce)) and the contralateral cerebellar hemisphere (THGr(Cb)), to its respective contralateral side. THGr values were compared with qualitative assessment of diaschisis. Linear regression analysis was performed using GraphPad Prism 6 software.

Results: Volumetric segmentation yielded the following volumes in mL (mean followed by (standard deviation)): (enhancing) tumor 30.25 (23.50); edema 94.83 (62.65); necrosis 5.51 (5.23). Using the same notation, quantitative PET analysis yielded the following THGr values: THGr(Ce), 0.72 (0.24); THGr(Cb), 0.83 (0.22). Logistic regression analysis demonstrated the following R-square values (with p values in parentheses): THGr(Ce) versus edema volume, 0.2 (0.10); THGr(Ce) versus enhancing lesion volume, 0.03 (0.5); THGr(Ce) versus necrosis volume, 0.001 (0.9). THGr(Cb) versus edema volume, 0.47 (0.0065); THGr(Cb) versus enhancing lesion volume, 0.11 (0.2579); THGr(Cb) versus necrosis volume, 0.009 (0.74).

Conclusions: The THGr(Cb) and MRI segmentation analyses demonstrated an inverse correlation of cerebellar diaschisis with edema volumes. In contrast, there was no correlation of diaschisis to lesion volume or necrosis. Given the prognostic value of diaschisis in glioma assessment, our findings have important pathophysiologic and clinical implications, laying the foundation for future studies evaluating diaschisis and tumor-associated edema in a larger cohort.

PS03-009

Poster Viewing Session III

Using near-infrared spectroscopy to measure cerebral blood flow in neonatal brain injury

S. Mitra[1], G. Bale[2], A. Sudakou[2], J. Meek[1], N. Robertson[1] and I. Tachtsidis[2]

[1]University College London, Department of Neonatology, Institute for Women's Health, London, United Kingdom
[2]University College London, Medical Physics and Biomedical Engineering, London, United Kingdom

Abstract

Background: The aim of this work is to use the NIRS cerebral oxygenation data (HbD = oxyhaemoglobin-deoxyhaemoglobin) combined with arterial saturation (SpO_2) recorded using a pulse oximeter to calculate cerebral blood flow (CBF) in a group of hypoxic-ischaemic encephalopathy (HIE) infants, using a method based on spontaneous desaturation events and the Fick principle. Then assess the evolution of CBF between infants with mild and moderate/severe HIE over postnatal days 1–5 that includes the therapeutic hypothermia period.

Methods: The Fick principle states that when a substance is introduced into the arterial blood and the time of measurement is less than the transit time through an organ, the tracer will not appear in the venous blood. Therefore the flow can be measured as the ratio of tracer accumulated to the quantity of tracer introduced. We have used a change in HbD as a tracer; when a sudden change in SpO_2 occurs, the change in HbD represents a change in tracer concentration and thus we can calculate CBF.

Data analysed from 21 infants (mean gestational age:39 ± 1 weeks, mean birth weight 3.2 ± 0.6 kg, 11 female, 10 male). 9 infants had moderate/severe (Lac/NAA > 0.3) and 12 mild (Lac/NAA < 0.3) brain injury. In total 67 desaturation events were eligible for analysis (22 from infants with moderate/severe injury and 45 from mild).

Results: Fig.1 shows the evolution of CBF for infants with mild and moderate/severe HIE. We observed in the moderate/severe HIE an initial hypoperfusion (CBF≈5–10 ml/100 g/min) followed by hyperperfusion (CBF≈15–25 ml/100 g/min). In the infants with mild HIE the CBF was relative stable across days (CBF≈10–20 ml/100 g/min).

Conclusion: NIRS measured CBF from spontaneous desaturations can be an effective cot-side tool to monitor cerebral perfusion. We have observed a difference in CBF evolution between infants with mild and moderate/severe HIE over postnatal days 1–5.

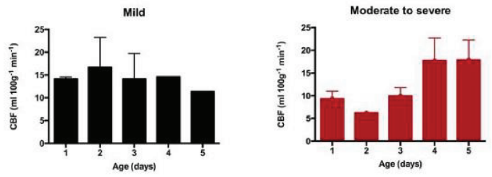

Figure 1. The evolution of CBF for infants with mild (Lac/NAA<=0.3) and moderate/severe (Lac/NAA>0.3) HIE over postnatal days 1-5.

PS03-010

Poster Viewing Session III

Interrogating changes in cerebral glucose availability, delivery, uptake and phosphorylation after traumatic brain injury; an ^{15}oxygen and ^{18}F-fluorodeoxyglucose positron emission tomography study

J. Hermanides[1], Y. Hong[2], M. Trivedi[1], J. Outtrim[1], F. Aigbirhio[2], P. Nestor[3], T. Fryer[2], D. Menon[1] and J. Coles[1]

[1]University of Cambridge, Division of Anaesthesia, Cambridge, United Kingdom
[2]Wolfson Brain Imaging Centre, Department of Neurosciences, Cambridge, United Kingdom
[3]German Center for Neurodegenerative Diseases, Magdeburg, Germany

Abstract

Objectives: Metabolic derangements are common after traumatic brain injury (TBI), but few studies have used multi-tracer positron emission tomography (PET) to interrogate underlying pathophysiology (1,2). We examined relationships between oxygen and glucose metabolism using ^{15}oxygen (^{15}O) and ^{18}F-fluorodeoxyglucose (FDG) PET.

Methods: Twenty-six TBI patients underwent combined ^{15}O and FDG-PET on 34 occasions; 10 and 18 healthy volunteers (controls) underwent ^{15}O and FDG-PET respectively. FDG rate constants were determined with an irreversible two-compartment model: transport across BBB (K_1,k_2), hexokinase activity (k_3), and influx rate (K_i). Regions of interest were defined for

haemorrhagic lesion (core), hypodense tissue (penumbra), 1 cm border zone of normal appearing tissue (peri-penumbra), and remote normal appearing tissue (normal). Plasma and microdialysis glucose were recorded.

Results: In patients, glucose delivery (K1) was dependent on supply with significantly lower values occurring below a threshold cerebral blood flow (CBF) of 25 ml/100 ml/min. K1 was particularly driven by CBF within lesion core ($R = 0.87, p < 0.001$) where CBF values were lower. Changes in hexokinase activity (k_3) were variable across the injured brain and not driven by CBF. While k_3 hotspots were found close to lesions they were often found within non-lesion brain with normal K1, and in the absence of OEF increases consistent with cerebral ischaemia. Increases in k_3 were associated with low microdialysis glucose ($R = -0.73$, $p = 0.016$).

Conclusions: These findings demonstrate that while glucose utilisation is reduced within the vicinity of lesions due to low CBF and impaired glucose delivery (K1), regional increases in utilisation occur across the injured brain and result from increases in hexokinase activity (k_3) associated with reduced glucose availability. Such evidence of non-ischaemic hyperglycolysis may relate to pathophysiological derangements such as inflammation, excitotoxicity or spreading depression. Future studies should address whether treatment guided by microdialysis glucose can ameliorate such findings and improve outcome.

References

1. Hattori, et al. J Nucl Med. 2004
2. Abate, et al. Neurocrit Care. 2008

PS03-011

Poster Viewing Session III

Cerebral hemodynamic response to head-of-bed manipulation can differentiate between brain hemispheres with and without severe internal carotid artery steno-occlusive lesions

C. Gregori-Pla[1], G. Cotta[1], P. Camps-Renom[2], J. Martí-Fàbregas[2], R. Delgado-Mederos[2] and T. Durduran[1,3]

[1]ICFO-Institut de Ciències Fotòniques, Castelldefels, Spain
[2]Hospital de la Santa Creu i Sant Pau, Barcelona, Spain
[3]Institució Catalana de Reserca i Estudis Avançats (ICREA), Barcelona, Spain

Abstract

Objectives: Cerebral microvascular hemodynamics during head-of-bed (HOB) manipulation are altered in patients with cerebrovascular disease [1]. We explored whether the response to HOB change is related to the degree of stenosis in the internal carotid artery (ICA).

Methods: We recruited patients with asymptomatic severe extracranial ICA stenosis and healthy controls. We used hybrid diffuse optics [2] to continuously monitor the microvascular cerebral blood flow (CBF) and total hemoglobin concentration (THC), as a surrogate of cerebral blood volume, in the frontal lobes. HOB challenge was performed from supine position to 30°. We categorized the hemispheres as <70% (non-severe) or ≥70% (severe) degree of ICA stenosis, and each hemisphere was considered as an independent result.

Results: We have studied ten patients with ICA stenosis (65 ± 6 y, 90% male) and five healthy controls (39 ± 10 y, 60% male). Results were the same whether using only controls or when also including the non-severe hemispheres, we report the mixed results. After HOB elevation, CBF and THC decreased in hemispheres without severe stenosis ($p = 0.0007$ and $p = 0.001$, respectively) (Figure 1), whereas no significant change occurred when severe ICA stenosis was present ($p = 0.06$ and $p = 0.2$, respectively). Relative CBF changes between non-severe and severe hemispheres were not significant ($p = 0.2$). THC changes differentiated between non-severe and severe ($p = 0.001$) hemispheres.

Conclusions: Cerebral hemodynamic response to HOB change is influenced by ICA steno-occlusive disease presence, probably due to damaged cerebrovascular autoregulation. More patients and controls are now recruited and future analysis will relate these results to clinical parameters, such as the status of the collateral circulation and the outcome.

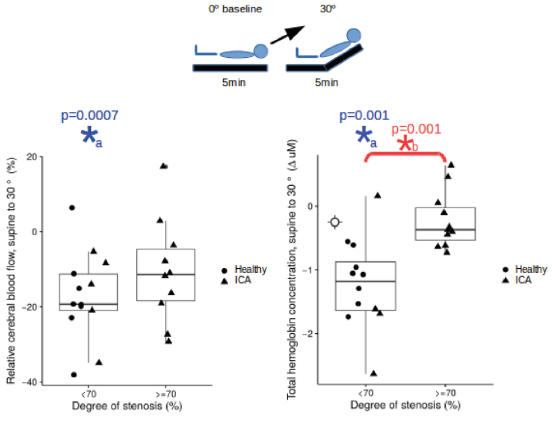

Figure 1: CBF and THC response to HOB challenge. $*_a/*_b$ statistically significant change from baseline/between groups ($p < 0.05$)

References

1- Favilla et al. Stroke (2014)
2- Durduran et al. NeuroImage (2014)

PS03-012

Poster Viewing Session III

Metabolic variability in a short status epilepticus model

Y. Wu[1], P. Pearce[2], A. Rapuano[3], K. Kelly[4], N. de Lanerolle[3] and J. Pan[5]

[1]Children's Hospital Pittsburgh, Developmental Biology, Pittsburgh, United States
[2]University of Pittsburgh School of Medicine, Pittsburgh, United States
[3]Yale University, School of Medicine, Neurosurgery, New Haven, United States
[4]Allegheny Singer Research Institute, Neurology, Pittsburgh, United States
[5]University of Pittsburgh School of Medicine, Neurology and Radiology, Pittsburgh, United States

Abstract

In rodent models of epilepsy, a lengthy period of status epilepticus of ~3 hrs is used to efficiently generate animals that will develop spontaneous recurrent seizures. However, the actual duration of status epilepticus is known to have an important effect on the outcome as shown with heat shock protein expression or fluoro-jade staining. We examined this temporal dependence using in vivo MR spectroscopic studies with a 45 min short status epilepticus (SE) kainate injection model.

Three days after a 45 min SE period, n = 21 male Sprague Dawley rats were studied using MRS measurements acquired from the dentate gyrus. All data were acquired on a Bruker Biospec 7T using a short echo single voxel PRESS acquisition (Fig. 1). LCM analysis was performed with metabolites reported as ratios to total creatine tCr (Fig. 1B).

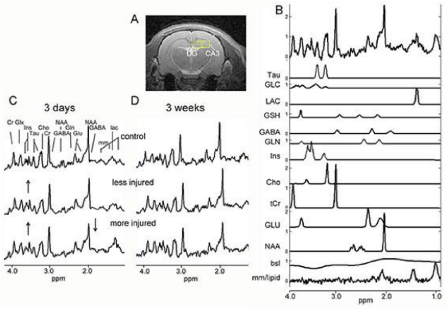

A hierarchical cluster analysis applied to 8 metabolites (NAA, glutamate, GABA, glutamine, lactate, inositol, glucose, glutathione) segregated the n = 21 animals into two groups: "kainate more injured" (KMI, n = 6) or "kainate less injured" (KLI, n = 15). The largest difference between them was seen in NAA/tCr although significant differences were seen in many metabolites. As survival studies, a repeat MRS performed 3weeks after SE showed that the KLI group largely returned to normal while the KMI group persisted with numerous abnormalities in neuronal and glial function (Fig. 1C, D). A subgroup of animals (n = 8) were sacrificed for semi-quantitative histologic Nissl analysis. As performed blinded to specific group, the KMI group showed increased neuronal loss and gliosis.

In this brief SE model, the results could have generated a single distribution of metabolic injury. However, the observed bimodal distribution of metabolic injury argues that this model generates at least two different pathophysiological paths such that the 3 days post-SE MRS evaluation identified the group with the persistent injury.

PS03-013

Poster Viewing Session III

Characterizing spontaneous cerebral vasculopathy in a murine model of sickle cell disease

H.I. Hyacinth[1], C.L. Sugihara[2], D.R. Archer[1] and A.Y. Shih[3]

[1]Emory University, Pediatrics: Hematology – Sickle Cell, Atlanta, United States
[2]Emory University, Neurosience and Behavioral Biology, Atlanta, United States
[3]Medical University of South Carolina, Neurosience, Charleston, United States

Abstract

Cerebrovascular disease is among the most dramatic complications seen among patients with sickle cell disease (SCD). Pathologies include; aneurysms, moya moya and ineffective collateral formation. Identification and characterization of spontaneous cerebral vasculopathy in the sickle cell mouse model is a necessary step for progress in the development of preventative strategies for stroke and other cerebrovascular complications of SCD. The focus of this study was to identify and characterize spontaneous cerebral vasculopathy and micro infarct in the

Townes mouse model of sickle cell disease. Our hypothesis was that spontaneously occurring cerebrovascular pathology is significantly more likely in the sickle cell mouse model compared to non-sickle cell controls.
One year old sickle cell mice and age and sex- matched controls (N = 3 each) were imaged using 9.4T MRI. Afterwards, stereotactic surgical procedures were used to create a cranial window (2–3 mm diameter) over the somatosensory cortex. The mouse cerebral vasculature was imaged using a two-photon laser scanning microscope (TPLSM) after intravenous injection of FITC-dextran. Following imaging, mice were injected with hypoxyprobe, sacrificed, and brains removed and sectioned for immunohistochemistry.
Our results show that the frequency of spontaneous cortical infarct was 2.5 fold higher ($p < 0.0001$) among sickle cell compared to control mice. Similarly, analysis of TPLSM images indicate that there were significantly more red blood cell (RBC) arrest ($p = 0.03$), frequency of blood flow stalls ($p < 0.0001$) and percent of vessel with thrombi ($p < 0.0001$) in sickle cell compared to control mice. Finally, sickle cell mice had significant evidence of cerebral hyperemia indicated by higher RBC volume flux ($p = 0.021$), capillary diameter ($p = 0.014$) and a marginally higher average RBC flow velocity ($p = 0.059$).
These pathologies have been described in humans with SCD; their spontaneous recapitulation in this mouse model represents new research opportunities to further our understanding of the underlying mechanism.

PS03-014

Poster Viewing Session III

Using multi-TI ASL to explore gray matter (GM) perfusion in multiple sclerosis (MS) patients

I. Lipp[1], C. Foster[1], R. Stickland[1], A. Davidson[1], R.G. Wise[1] and V. Tomassini[1,2]
[1]*Cardiff University, Cardiff, United Kingdom*
[2]*IRCCS Fondazione Santa Lucia, Rome, Italy*

Abstract
Objectives: Hypo-perfusion in GM and hyper-perfusion in white matter in MS have been demonstrated using various methods[1–3]. However, the spatial pattern of perfusion impairment and the reported relationship with disease characteristics are often inconsistent between studies, which might be due to measurement error in the perfusion estimation. Here, we first test the retest-reliability of GM perfusion measures obtained through multi-TI pulsed ASL in MS patients and healthy controls, and then relate perfusion to disease characteristics.
Methods: 75 right-handed MS patients (43 ± 10 years, 42 women) and 26 controls (38 ± 11 years, 15 women) underwent a T1-weighted structural and a pulsed ASL scan (10 Tis: 300–2000 ms). A subgroup (25 patients/19 controls) had a second scan four weeks later to assess reproducibility. Perfusion was estimated using *oxford_asl* with partial volume correction[4]. Global perfusion was calculated within T1-segmented GM. Perfusion maps were then registered to MNI space and values from various regions were obtained.
Results: Global perfusion had good repeatability (patients: $ICC = .72$, $p < .0001$, controls: $ICC = .79$, $p < .0001$) and local perfusion estimates were repeatable in most, but not all regions (Fig. 1). Global perfusion was lower in patients (55 ± 18 ml/100 g/min) than in controls (67 ± 18 ml/100 g/min; $Z = 2.6$, $p = .01$), but not correlated with age ($r = -.05$, $p = .62$), disease duration ($r = -.15$, $p = .21$), self-reported symptom severity ($r = -.06$, $p = .63$), PASAT score ($r = .04$, $p = .72$) or disease stage ($Z = -1$, $p = .3$). Women with MS had higher perfusion than men ($Z = 3.3$, $p = .001$). Local perfusion estimates showed widespread GM hypo-perfusion in cortical and sub-cortical structures (Fig. 1).
Conclusions: We demonstrate that it is possible to reliably measure GM hypo-perfusion in MS patients. Our results suggest that hypo-perfusion might a disease process prevalent in all stages and severities of MS.

References
[1]Rashid 2004, JNNP(75)
[2]Bester 2015, PlosONE(10(3))
[3]Inglese 2007, ArchNeurol(64)
[4]Chappel 2011, MRIM(65)

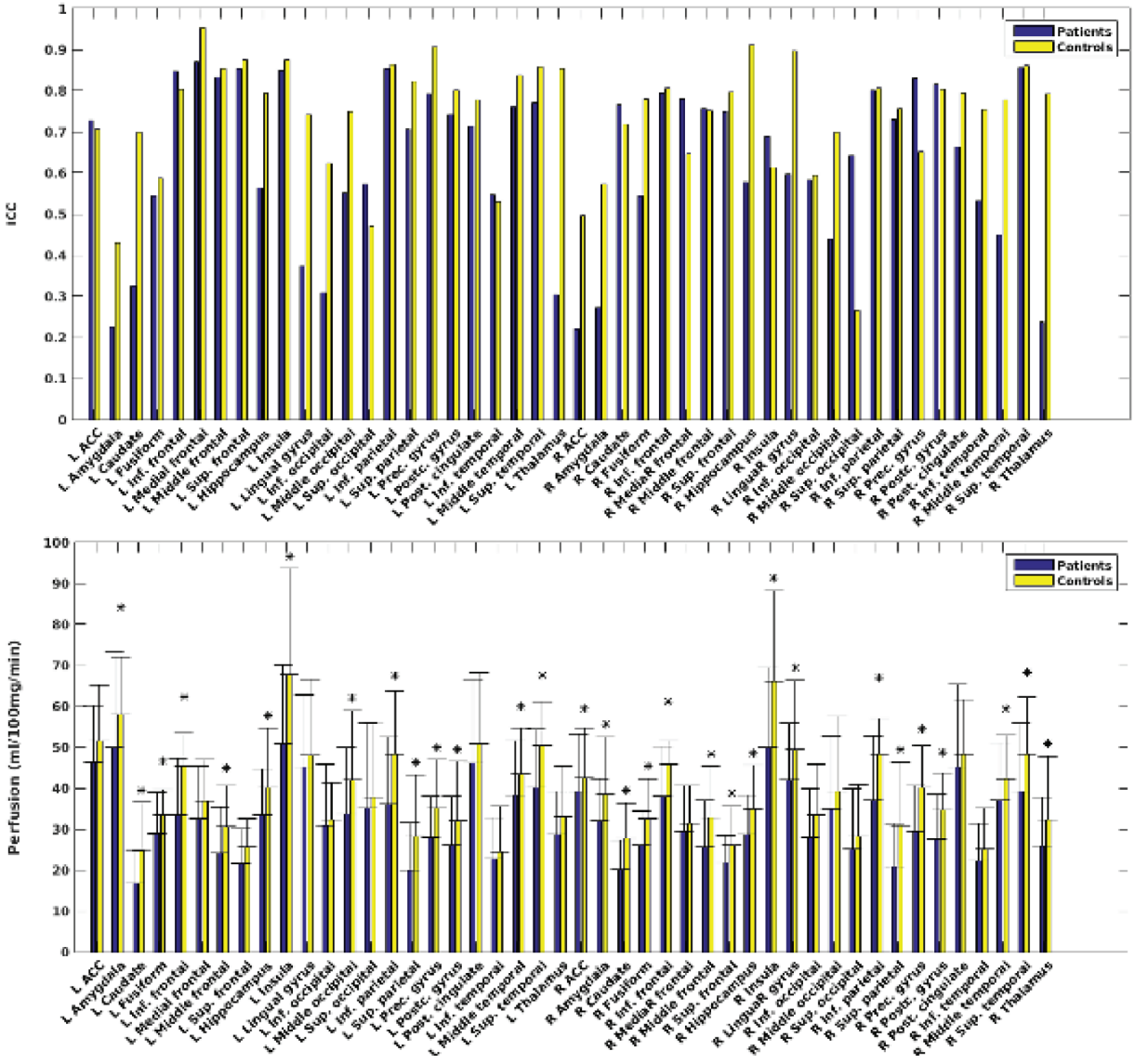

Fig 1: Regional perfusion estimates. Top: Repeatability of perfusion estimates: for each ROI the intraclass correlation coefficient (ICC) is plotted for patients (blue) and controls (yellow). Bottom: Regional perfusion estimates for patients and controls: for each ROI the median (+iqr) perfusion (in ml/100g/min) is shown for patients (blue) and controls (yellow). Significant differences (with $p < .05$, uncorrected for multiple comparisons) are indicated with a star.

PS03-015

Poster Viewing Session III

New insights into neuro-imaging changes in idiopathic intracranial hypertension

S. Lublinsky[1], A. Kesler[2], A. Friedman[1,3] and I. Shelef[1]

[1]*Ben-Gurion University of the Negev, Beer Sheva, Israel*
[2]*Sackler School of Medicine, Tel Aviv, Israel*
[3]*Dalhousie University, Halifax, Canada*

Abstract

Purpose: To investigate potential mechanisms underlying intracranial pressure normalization in idiopathic intracranial hypertension (IIH) patients and to test association between different neuroimaging signs of IIH and long-term disease outcomes for IIH patients followed lumbar puncture (LP) treatment.

Material and methods: Images from 18 IIH patients and 30 controls were analyzed. A novel approach for quantitative characterization of the intracranial venous system was described and implemented as a diagnostic tool for evaluation of the degree of occlusion in the cerebral sinus. A number of neuroimaging features associated with IIH disease were investigated before and after LP using a set of specially developed quantification techniques. A long-term follow-up investigation was performed to identify prognostic factors for the disease outcomes.

Results: As a result of LP, the following were found to be in good accordance with the opening pressure: restoration of obstructed sinuses, relative compression of cerebrospinal fluid and brain volumes, expansion in lateral ventricles and venous volume, reduction of Meckel's caves, enlargement of the pituitary, reduction in optic nerve tortuosity, and shrinkage of subarachnoid space and sulci. However, fast recovery following intracranial pressure normalization was not long-lasting for all patients. Neither the amount of immediate response nor the severity of conditions preceding LP predicted long-term outcomes. The presence of supplemental drainage pathways had a significant impact on long-term disease outcome.

Conclusion: We presented an approach for quantitative characterization of the intracranial venous system and its first implementation as a diagnostic assistance tool. Quantitative MRI analysis of arachnoid granulation, pituitary gland, Meckel's caves, optic nerve and supplemental drainage pathways may serve as clinical biomarkers for monitoring IIH disease and evaluation of treatment efficacy. We concluded that formation of adequate supplementary drainage veins might serve as a compensatory mechanism and can be used as an IIH disease long-term prognostic factor.

PS03-016

Poster Viewing Session III

Functional connectivity assessment in a mouse model of glioma growth

I. Orukari[1], A. Bauer[1], G. Baxter[1], J. Rubin[2] and J. Culver[1]

[1]*Washington University, Radiology, St Louis, United States*
[2]*Washington University, Pediatrics, St Louis, United States*

Abstract

Objectives: To assess the effects of tumor growth on functional connectivity in a glioma mouse model. The resting-state functional connectivity data was obtained using functional connectivity optical intrinsic signal (fcOIS).

Methods: 5.0×10^4–10^5 U87 gliomas cells that expressed firefly luciferase were stereotactically injected into the forepaw somatosensory cortex of adult nude mice. Tumor burden was monitored via MRIs and weekly bioluminescence imaging. For OIS imaging, illumination of the exposed cortex was provided by four LEDs and reflected light was captured by a CCD camera running at 120 Hz. The modified Beer-Lambert Law was used to interpret the reflected light intensity. Functional connectivity analysis was performed on the OIS images. We quantified changes in seed-based connectivity in homotopic regions. We also constructed maps of interhemispheric homotopic functional connectivity for all pixels within the field of view of OIS.

Results: The homotopic connectivity values at week 6 for the motor, somatosensory, and visual seeds were significantly (paired t-test, p-value < 0.05) reduced. Additionally, homotopic connectivity values for the motor, somatosensory, and visual seeds were significantly (p-value < 0.05) correlated with the log of bioluminescence values for all time points. Maps of interhemispheric homotopic functional connectivity revealed there is an early area of reduced connectivity near the injection site that decreased in size initially. The area of reduce connectivity began to grow in size starting at week 4. By week 6, there was a global reduction in connectivity.

Conclusions: We have shown fcOIS is capable of detecting alterations in functional connectivity due to glioma growth. Gliomas initially disrupts connectivity focally; however, as the gliomas grow, distant connections become affected. It has been hypothesized that network alterations underlie the cognitive deficits seen in glioma patients. A better understanding of the role gliomas growth plays in the development of cognitive deficits may lead to improved outcomes after neurorehabilitation.

PS03-017

Poster Viewing Session III

Anatomical and functional characterization of schizophrenia-linked genes

G.J. Thompson[1], K. Perez De Arce[2], E.T.C. Lippard[3], B.G. Sanganahalli[1,4], S.M. Strittmatter[5], F. Hyder[1,4,6] and T. Biederer[2]

[1]Yale University, Radiology and Biomedical Imaging, Magnetic Resonance Research Center (MRRC), New Haven, United States
[2]Tufts University School of Medicine, Neuroscience, Boston, United States
[3]University of Texas at Austin, Psychiatry, Austin, United States
[4]Yale University, Quantitative Neuroscience with Magnetic Resonance (QNMR) Core Center, New Haven, United States
[5]Yale University, School of Medicine, Cellular Neuroscience, Neurodegeneration, and Repair Program, and Departments of Neurology and Neurobiology, New Haven, United States
[6]Yale University, Biomedical Engineering, New Haven, United States

Abstract

Objectives: Schizophrenia is a debilitating disease that is partially heritable. How schizophrenia-linked genes produce changes at the cellular level to produce system level symptoms remains poorly understood. We studied the schizophrenia-linked gene LRRTM1 [1] alone and in combination with the synapse-organizing gene SynCAM1 [2] in an anesthetized mouse model using multimodal MRI.
Methods: Four groups of mice in a C57BL/6 background were imaged under urethane anesthesia: wild-type, SynCAM1 knockout, LRRTM1 knockout and a SynCAM1 and LRRTM1 double knockout. Imaging methods included functional MRI (fMRI) during whisker barrel activation, resting state fMRI of the bilateral whisker barrel, anatomical imaging of cortical thickness and DTI of fractional anisotropy of white matter tracts.
Results: Whisker barrel activation indicated that LRRTM1 knockout and double knockout reduced lateralization of activation (Figure 1A) and reduced cortical thickness. SynCAM1 knockout and double knockout increased activation in the whisker barrel cortex to stimulation, and had a similar (though non-significant) effect on functional connectivity (Figure 1B) with no change in cortical thickness. These results suggest that SynCAM1 may be influencing activity levels broadly while LRRTM1 may be affecting the larger scale morphology/lateralization. DTI results generally indicated in knockouts disrupted anatomical connectivity (reduced fractional anisotropy) in gray matter but greater anatomical connectivity near the gray-matter/white-matter boundary.

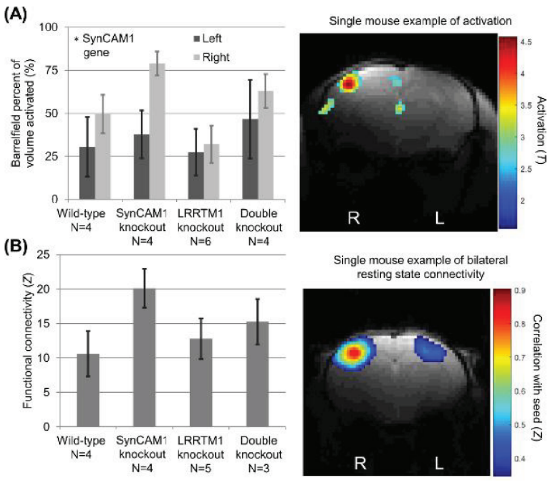

Conclusions: These results suggest interplay between synapse-organizing proteins may contribute to the functional and structural effects that create the schizophrenia phenotype. Our work illustrates the strengths of multimodal mouse imaging of genetic models to translate from the gene level to the systems level.

References

[1] Leach, et al., J Hum Genet, 2014. 59(6): p. 332–6.
[2] Park, et al., J Neurosci, 2016. 36(28): p. 7464–75.

PS03-018

Poster Viewing Session III

Cerebral venous sinuses thrombosis in Kyrgyzstan: a review of a series of clinical cases, clinical and imaging correlation

A. Shapovalova[1], I. Lutsenko[1,2,3] and S. Jumakeeva[1]

[1]Kyrgyz State Medical Academy, Neurology, Bishkek, Kyrgyzstan
[2]European Stroke Organisation, Kyrgyzstan, Bishkek, Kyrgyzstan
[3]SITS-Registry Kyrgyzstan, Bishkek, Kyrgyzstan

Abstract

We present an overview of 12 clinical cases of cerebral venous sinus thrombosis (CVST) and cerebral veins thrombosis (CVT). Etiology of thrombosis varies, and our observations often include cranial cavity infections (chronic otitis, etmoiditis, sinusitis, dental caries), gynecological diseases (vaginitis, endometritis), period of pregnancy, delivery and early postpartum period in women with disorders of hemostasis. Given the lack of opportunities of cerebral venography, we discuss the neuroimaging findings on MRI of the brain in different regimens in isolated sinus thrombosis, or in a combination of several sinuses and veins thrombosis. The tactics of these patients management is discussed according to etiology, caused thrombosis. In the period from 2009–2015 in Kyrgyzstan 12 patients with thrombosis of the cerebral veins and sinuses were examined. All of them were women, the average age was 34.3 years (22–57). 10 women were examined during acute cerebral accident in angionevrologic department of Bishkek City Clinic 1. Two patients with CVST were found in maternity hospitals (6 maternity ward and gynecological department of the Chui regional hospital). Important neurological symptoms included: headache (9 patients), hemiparesis (8), loss of consciousness (6), papilloedema (9), focal neurological deficit (9), convulsions (4). The most common site of thrombosis were: lower sagittal sinus (5 patients), the left transverse sinus (5 patients), thrombosis of two or more sinuses (7). Frequent etiologies were: pregnancy (3), the early postpartum period (2), the late postpartum period (2), ENT infections (2). Early administration of heparin in combination with antibiotics and corticosteroids showed a significant improvement in the condition observed in a sample of patients in the acute phase, if necessary. Our research shows that the disease may have a different outcome varying as a dramatic recovery from a coma to a normal state, as well as death in the early hours of pathology.

PS03-019

Poster Viewing Session III

Charcot-Marie-Tooth 2b associated Rab7 mutations dysregulate intra-axonal protein synthesis and mitochondrial function

A.V. Holtermann[1,2], J.-M. Cioni[2], J.Q. Lin[2], B. Turner-Bridger[2], M.A. Jakobs[2], A. Dwivedy[2] and C.E. Holt[2]

[1]University of Ulm, Medicine, Ulm, Germany
[2]University of Cambridge, Department of Physiology, Development and Neuroscience, Cambridge, United Kingdom

Abstract

Background: Charcot-Marie Tooth Type 2b is a hereditary axonal neurodegenerative disorder affecting the peripheral sensorimotor systems, leading to distal sensory loss, muscle weakness and atrophy. Several heterogeneous mutations in the Rab7 gene, a small GTPase involved in endosomal maturation and trafficking, have been identified to be associated with this disease but the exact pathological mechanisms resulting in axonal degeneration remain elusive. *Xenopus laevis* Rab7 is 96% identical to the human Rab7, including the four amino acids that are affected in CMT2b (L129F, K157N, N161T and V162M), making it a good vertebrate model to study this disease. Here, we investigated the cellular and molecular mechanisms underlying the Rab7 CMT2b associated axonopathy in the *Xenopus* retinal ganglion cells (RGCs).

Methods: *In vivo* expression of Rab7 CMT2b mutants (K157N, L129F, V162M, N161T) and phenotypic analysis, axonal mitochondria labelling and analysis, *puromycin assays* on RGC axon-only cultures to quantify local translation, live-imaging of *Xenopus leavis* RGC cultures visualizing Rab7a and RNA movements, proximity ligation assay to visualize local translation of specific proteins.

Results: In accordance with an autosomal-dominant effect, expression of the Rab7 CMT2b mutants was found to cause a severe reduction of the retinotectal axonal projections. Analysis of axonal mitochondria morphology showed a striking defect in presence of

CMT2b mutants, resulting in elongated mitochondria without affecting their total number. Intriguingly, we found that this phenotype was accompanied by a reduction of intra-axonal protein synthesis. Indeed, we characterized Rab7-positive endosomes as "hot spots" for local translation in RGC axons. Finally, we found a specific reduction of LaminB2 axonal synthesis, a protein reported to localize to axonal mitochondria and crucial to their function.
Conclusion: We suggest that local translation of proteins important for mitochondria maintenance is taking place on Rab7-positive endosomes, and dysregulation of this process by mutations of Rab7 can lead to axonal degeneration.

PS03-020

Poster Viewing Session III

Histomorphological spectrum of lesions of the central nervous system including the brain, spinal cord and vertebrae

P. Bista Roka[1]
[1]*NAMS,BIR Hospital, Pathology, Kathmandu, Nepal*

Abstract
Introduction: Lesions of the central nervous system including the brain, spinal cord and vertebrae cause profound morbidity and mortality as they occur within the tight confines of the rigid cranium and vertebral column. They constitute both primary tumors and secondary tumors spread from tumors outside the central nervous system and also many infective and parasitic infections that may simulate space occupying lesions.
Methods: All the slides of the central nervous system, spinal cord and vertebrae from the Department of Pathology, Bir Hospital, Kathmandu, Nepal of five years between 2007–2012 were retrieved and evaluated.
Result: A retrospective evaluation of slides of 357 representative biopsy samples of five years duration were conducted and it constituted 2.23% of the total specimens received for histopathology. Out of these, 338 were lesions, twelve cases were of normal glial tissue and seven cases were inadequate. In spite of suspicion of neoplasm in the brain it is not always possible to get the tumor tissue due to deep site of the lesion and poor general condition of the patient which allows only burr holing and minimal low yield of tmour mass. Neoplastic lesions comprised the majority of cases (82.0%) followed by non-neoplastic lesions (13.60%) and inflammatory lesions (4.43%). WHO grade I neoplasm comprised 127 cases (45.84%) followed by grade IV neoplasms 67 cases (24.18%), 48 cases (17.32%) of grade II, 13 cases (4.69%) of grade III neoplasms and 24 cases (8.66%) of all the neoplastic lesions comprised of neoplasms which were not categorized in any of the grades in the WHO classification. Out of the neoplasias, low-grade neoplasia and high-grade neoplasia comprised 42.58% and 20.60% respectively.
Conclusion: The lesions of the central nervous system including the brain, spine and vertebrae showed that neoplastic lesions comprised the majority of cases followed by non-neoplastic lesions and inflammatory lesions.

PS03-021

Poster Viewing Session III

Mapping and manipulating the fate of obstructed microvessels

P. Reeson[1] **and C.E. Brown**[1]
[1]*University of Victoria, Division of Medical Sciences, Victoria, Canada*

Abstract
The brain's high metabolic rate imposes unique demands and constraints on it's vascular system. The cerebral microvascular bed, the main site of exchange of oxygen and nutrients, is a low flow system prone to spontaneous stalls and occlusions. While previous studies have looked at larger arterioles, little is known about the microvascular response to temporary or prolonged loss of flow. We used 2 photon imaging through chronically implanted cranial window over the somatosensory cortex of Tie2-GFP mice to both acutely and longitudinally track the microvascular response to either natural obstructions or separately those induced with 4 μm fluorescent microspheres (injected i.v.). In healthy mice, the majority of occlusions were resolved within 12 hrs, while a small percentage were persistent, lasting for days. Microvessels with prolonged occlusions either eventually cleared the emboli or were pruned in a retraction reminiscent of developmental vessel pruning. A small portion of microvessels were able to recanalize by expelling the obstruction through the vascular wall, something previously described only in much larger vessels (Angiophagy). Surprisingly a significant portion of vessels that cleared an obstruction and restored flow, still underwent retraction at a later time point. Using parallel strategies of pharmacological inhibition and inducible genetic knock down we identified Vascular

Endothelial Growth Factor Receptor 2 (VEGF-R2) signalling as a critical component of microvessel recanalization following obstruction. Furthermore, in animals with a vascular disease, diabetes, the microvascular ability to clear obstructions was significantly compromised. Conceivably these occlusions and delayed pruning events could contribute to the decline in capillary density in dementia, particularly in diabetics.

PS03-022

Poster Viewing Session III

Effects of acute and chronic sleep deprivation on the resting-state activity of the human brain

J. Fronczek[1], D. Lange[2], E. Hennecke[2], D. Aeschbach[2], A. Bauer[1], E.-M. Elmenhorst[2] and D. Elmenhorst[1]
[1]Forschungszentrum Jülich, INM-2, Jülich, Germany
[2]Deutsches Zentrum für Luft- und Raumfahrt, Institut für Luft- und Raumfahrtmedizin – Flugphysiologie, Köln, Germany

Abstract
Sleep deprivation, both chronic and acute, has a detrimental effect on mental functions like memory, attention or reaction speed. Different amounts of total sleep deprivation reduced the activity of the resting-state default mode network (DMN). Others showed strengthening of the activity of interhemispheric connections as a putative compensatory mechanism. The objective of the current study was to investigate if chronic sleep restriction triggers comparable changes.
In an ongoing study we acquired resting-state MR data from 14 healthy volunteers (final study size: 36 volunteers) on three consecutive days under different states of sleep deprivation. The experimental group ($n = 9$) underwent chronic sleep restriction for 5 nights with 5 h time in bed (TIB) (control group: 8 h, $n = 5$) and were scanned on the last day of restriction. Both groups then had one recovery night with 8 h TIB followed by a night of acute sleep deprivation (0 h TIB) after each of which they were scanned again.
The resting-state patterns of brain activity were analyzed by an independent component analysis and subsequent dual regression comparing to an out-of-sample template of identified network components with FSL (FMRIB Software Library).
The preliminary dataset showed a significant increase of activity ($p < 0.05$) in the lateral visual area network in the experimental group on the last day of sleep restriction compared to the rested controls. Activity in this network increased ($p < 0.05$) within the experimental group between the recovery day and the day of acute sleep deprivation.
This study layout allows both the investigation of chronic sleep restriction and comparison of acute sleep deprivation following different sleep histories. The observed increase in activity in the resting-state might indicate that the preceding sleep restriction primes the brain for following acute sleep loss by increasing compensatory mechanisms.

PS03-023

Poster Viewing Session III

Endogenous recovery of impaired synaptic plasticity after juvenile global and focal ischemia

R. Dietz[1], J. Orfila[2], G. Deng[2], N. Chambers[2], H. Grewal[2], C. Schroeder[2], R. Traystman[2] and P. Herson[2]
[1]University of Colorado, Pediatrics, Aurora, United States
[2]University of Colorado, Anesthesia, Aurora, United States

Abstract
Cardiac arrest (CA) or stroke in children can be devastating, often leading to poor neurologic outcomes in children, including learning and memory deficits. Children tend to have improved outcomes compared to adults. An increase in synaptic efficiency, termed long-term potentiation (LTP), is a well-accepted cellular model for learning and memory. We have shown persistent impairment of synaptic function following CA and middle cerebral artery occlusion (MCAO) in adult mice. The goal of this study is to evaluate the effects of CA and MCAO on synaptic function in juvenile mice. Male juvenile mice (postnatal day 20–25) were subjected to 8 min CA and resuscitated or had transient occlusion of the MCA. Hippocampal CA1 function and synaptic plasticity were evaluated using acute brain slices 7 or 30 days after CA/MCAO or sham controls. Synaptic plasticity (LTP) was measured following a theta-burst stimulation (TBS, 40 pulses 100Hz). Increase in field excitatory post-synaptic potential (fEPSP) slope 60 min after TBS was analyzed as a measurement of LTP. In control

male mice, TBS resulted in LTP that increased fEPSP slope to 153% ($n = 8$) of baseline (100%). In contrast, 7 days after CA, there was significant impairment, in LTP (114%, $n = 6$, $p < 0.05$). By 30 days after CA, LTP recovered to control levels (155%, $n = 6$). Following MCAO, there was impairment in the ipsilateral (92%, $n = 5$, $p < 0.05$ compared to control) but not contralateral hippocampus (168%, $n = 6$, $p < 0.0.5$ compared to ipsilateral). Similar to CA, by 30 days after MCAO, both ipsilateral (175%, $n = 5$) and contralateral (166%, $n = 5$) LTP had recovered when compared to controls. This seminal discovery of endogenous recovery of LTP through development into adulthood may contribute to improved neurological outcome in children compared to adults.

PS03-024

Poster Viewing Session III

Using functional MRI to track neuroplasticity after cognitive rehabilitation post traumatic brain injury

S. Chopra[1], S. Kumaran[2], S. Sinha[3], H. Kaur[1] and A. Nehra[1]

[1]All India Institute of Medical Science, Clinical Neuropsychology, New Delhi, India

[2]All India Institute of Medical Science, Nuclear Magnetic Resonance, New Delhi, India

[3]All India Institute of Medical Science, Neurosurgery, New Delhi, India

Abstract

Introduction: Behavioural, environmental and cognitive stimuli can cause neuroplastic change, which have significant implications for recovery after brain injury. Functional Magnetic Resonance Imaging (fMRI) and connectivity data can give some information on the recovery from deficits after a Traumatic Brain Injury (TBI).

Methods: After ethics approval and informed consent, 27 patients between 18–45 years; 1 month post Mild or Moderate TBI were randomly assigned to control (CG) or intervention group (IG). fMRI using a 1.5T MRI was done at baseline, 6 weeks from baseline and 3 months post intervention using a paradigm for visual memory, verbal N-back and 2 Back. The 6-week indigenized literacy free cognitive intervention included retraining in areas of visual short term, long term memory; focussed and divided attention; planning and visuo-spatial ability and relaxation techniques.

Results: *Visual Memory*: Blood Oxygen Level Dependent (BOLD) revealed activations in culmen and precentral gyrus during visual recall of known objects and for unknown landscapes, in cuneus, parahippocampal gyrus, declive, cerebellar tonsil, fusiform gyrus, precuneus and lingual gyrus. Post intervention, right middle frontal gyrus was significantly active in comparison to the pre-therapy. The IG exhibited activation in left cerebral lingual gyrus in comparison to the CG.

Verbal N-Back: Pre, post intervention analysis showed significant improvements in the IG in working memory with activation in right hemispheric middle frontal gyrus, parahippocampal gyrus, medial frontal gyrus, bilateral precuneus and left cererbral thalamus, suggesting significant recovery. BOLD revealed more activation in the middle, medial frontal gyri, parahippocampal gyrus, caudate, pyramis in the intervention group as compared to the CG, suggesting better auditory working memory association.

Conclusions: These findings demonstrate retrieval of visual memory processing and significant working memory association post intervention. Functional imaging can not only provide the link between cognitive rehabilitation and plasticity in future, but also neuroplasticity after injury, in larger cohorts.

PS03-025

Poster Viewing Session III

Measuring cerebrovascular mechanisms of neuroplasticity using Arterial Spin Labelling (ASL) fMRI

C. Foster[1], J. Steventon[2], D. Helme[3], I. Driver[1], V. Tomassini[4] and R.G. Wise[1]

[1]Cardiff University, CUBRIC, School of Psychology, Cardiff, United Kingdom

[2]Cardiff University, Neurosciences and Mental Health Research Institute, Cardiff, United Kingdom

[3]Morriston Hospital, Department of Anaesthetics and Intensive Care, Swansea, United Kingdom

[4]Cardiff University, Institute of Psychological Medicine and Clinical Neurosciences, School of Medicine, Cardiff, United Kingdom

Abstract

Objectives: Functional recovery following neurological damage is dependent on adaptive brain plasticity. Neuroplasticity has been studied using BOLD fMRI[1] but, interpretation is limited by the complex physiological changes contributing to the BOLD signal. Here, we used calibrated fMRI to obtain additional direct quantification of cerebral blood flow (CBF) and the cerebral metabolic rate of oxygen consumption ($CMRO_2$) during motor learning.

Methods: BOLD and CBF data were acquired for 20 healthy subjects at 3T using PICORE QUIPSS II[2] dual-

1

BOLD, CBF and $CMRO_2$ Changes During SRT Performance vs. Rest

ROI	Voxels (n)	Task % ΔCBF	Task % ΔBOLD	% Δ$CMRO_2$	$CMRO_2$ change across the group
CBF Activity	24839	8.6 (4.1)	.15 (.1)	4.4 (3.9)	t = 6.04, p′ < 0.001
BOLD Activity	48110	4.7 (3.6)	.27 (.21)	1.6 (3.1)	t = 2.3, p = .034, 001 p′ = .1
BOLD-CBF Intersection	19406	6.9 (3.2)	0.25 (.2)	4.1 (2.1)	t = 4.39, p′ = .003

2

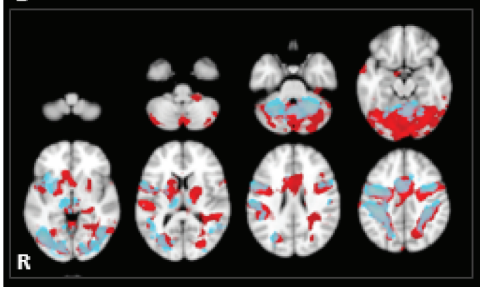

3

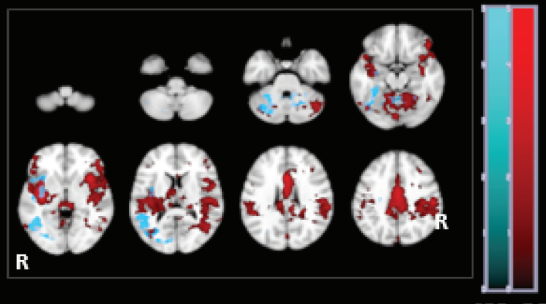

4

BOLD, CBF and $CMRO_2$ Changes in Regions with an Overall Signal Decrease over Time

ROI	Voxels (n)	Task % ΔCBF	Task % ΔBOLD	% ΔCMRO2	$CMRO_2$ change across the group
CBF Activity	4475	-22.1 (16)	-0.14 (0.13)	-15.6 (13.5)	t = 4.88, p′ < .001
BOLD Activity	39686	4.6 (32)	0.13 (.17)	10.3 (5.3)	t = 1.5, p = .148, p′ = .4
BOLD-CBF Intersection	1135	-21.5 (19.9)	-0.15 (.17)	-14.1 (14.3)	t = 4.05, p < .001

1. fMRI and $CMRO_2$ increases during SRT blocks. Average signal increases across all blocks and regions is shown. 2. BOLD and CBF signal increases during SRT blocks (z = 2.3, p < .05). 3. Average signal change across all blocks in regions showing an overall significant signal decrease over the course of the task. 4. Signal changes calculated over the average of all regions showing a linear signal decrease over consecutive SRT blocks.

echo pulsed ASL (14 slices, spiral gradient-echo, TE1/2 = 2.7/29 ms, TR = 2.4s, TI1/2 = 700/1500 ms) during a 12-minute serial reaction time task. Hypercapnic calibration to calculate cerebrovascular reactivity (CVR) to CO_2 was peformed[3]. Relative $CMRO_2$ changes for each ROI were obtained using the Davis model[3] with optimised values for $\alpha = 0.18$ and $\beta = 1.3$[5]. ROIs were created from the BOLD, CBF and BOLD-CBF intersection data averaged across all regions for task-related signal increases and task-related decreases over consecutive task blocks.

Results: BOLD and CBF task responses were observed in motor and supplementary motor cortex, insula, cerebellum, visual cortex and thalamus. CBF and intersection ROIs showed significant activity reductions in the same structures over time whereas only a decreasing trend was observed for the BOLD ROI (Figure 1). Changes reported are averaged over all regions and task blocks to maximise signal to noise (SNR).

Conclusions: The results demonstrate the feasibility of using calibrated fMRI to examine energetic changes during motor learning. However, the low SNR of ASL means that this method performs best where large ROIs are considered, further optimisation is required to investigate smaller ROIs.

PS03-026

Poster Viewing Session III

Murine microvascular pericytes promote recovery from an inflammatory mediated model of multiple sclerosis

P. Dore-Duffy[1], N. Esen[2], V. Katyshev[2,3] and S. Katysheva[1]

[1]Wayne State University School of Medicine, Neurology, Detroit, United States

[2]Wayne State University School of Medicine, Detroit, United States

[3]Cleveland Clinic, Cleveland, United States

Abstract

Stem Cell transplantation and replacement continues to be a promising therapeutic approach in the treatment of neurodegenerative diseases although with varying degrees of success. Studies have focused on adult stem cells, embryonic stem cell-derived progenitor populations, induced pluripotent stem cells (iPSC), and iPSC derive progenitor cells. In this study we show that intravenous injection of a novel adult stem cell population, the microvascular pericyte, results in clinical recovery in a murine model of the human degenerative disease multiple sclerosis (MS), myelin oligodendrocyte glycoprotein (MOG) 35–55 amino acid peptide-induced experimental autoimmune encephalomyelis (EAE). Primary murine platelet derived growth factor receptor (PDGFR) positive CNS pericytes were isolated and injected into normal animals. Small numbers of labeled pericytes were found in most organs as quantified by flow cytometry. Increased migration to injured tissue was seen. In MOG immunized mice primary pericytes were injected after mice exhibited a clinical score of 2.0. Pericytes migrated to the spinal cord in large numbers in the periventricular zone and resulted in improved clinical scores. Labeled pericytes were found for at least two weeks following injection. A small percentage of labeled pericytes became associated with newly formed microvessels. Improved clinical scores correlated with reduction in neuropathological evidence of disease. Clinical improvement also correlated with changes in the leukocyte populations within the spinal cord and with changes in leukocyte cytokine secreting phenotypes. Pericyte-leukocyte co-culture with activated splenic T cells resulted in reduced T cell proliferation in response to antigen. Our results indicate that pericytes have a major impact on disease activity in EAE and may have a potential therapeutic role in MS.

PS03-027

Poster Viewing Session III

Hypoxic preconditioning enhances neural stem cell transplantation therapy after intracerebral hemorrhage in mice

N. Fukuda[1], T. Wakai[1], H. Yoshioka[1], C. Pak[2] and H. Kinouchi[1]

[1]University of Yamanashi, Department of Neurosurgery, Interdisciplinary Graduate School of Medicine and Engineering, Yamanashi, Japan

[2]Stanford University, Department of Neurosurgery, California, United States

Abstract

Objective: Previous studies have shown that intraparenchymal transplantation of neural stem cells ameliorates neurological deficits in animals with intracerebral

hemorrhage. However, hemoglobin in the host brain environment causes massive grafted cell death and reduces the effectiveness of this approach. Several studies have shown that preconditioning induced by sublethal hypoxia can markedly improve the tolerance of treated subjects to more severe insults. Therefore, we investigated whether hypoxic preconditioning enhances neural stem cell resilience to the hemorrhagic stroke environment and improves therapeutic effects in mice.

Methods: Neuronal stem cells were isolated from the subventricular zones of postnatal day 1 green fluorescent protein (GFP) transgenic mice. Hypoxic preconditioning was induced by stimulation with 5% hypoxia for 24 hours before exposure to hemoglobin. To assess the protective effect of hypoxic preconditioning, neural stem cell viability 24 hours after hemoglobin exposure was assessed by WST-1 test. To study the effectiveness of hypoxic preconditioning on grafted-neural stem cell recovery, neural stem cells subjected to hypoxic preconditioning were grafted into the parenchyma 3 days after intracerebral hemorrhage. We also studied the effectiveness of the treatment on neural survival and functional recovery.

Results: Hypoxic preconditioning significantly enhanced viability of the neural stem cells exposed to hemoglobin ($n = 5$, $P < 0.05$) and increased grafted-cell survival in the brain 35 days after intracerebral hemorrhage ($n = 9$, $P < 0.05$). Transplanted neural stem cells with hypoxic preconditioning exhibited enhanced neuronal survival 35 days after intracerebral hemorrhage ($n = 9$, $P < 0.05$) that accelerated behavioral recovery assessed by corner turn test ($n = 9$, $P < 0.05$).

Conclusions: Our results suggest that hypoxic preconditioning in neural stem cells improves efficacy of stem cell therapy for intracerebral hemorrhage.

PS03-028

Poster Viewing Session III

Human amnion stem cell-derived exosomes improve stroke outcome

B. Broughton[1], A. Ghaly[1], M. Evans[1], R. Lim[2], G. Drummond[1], E. Wallace[2] and C. Sobey[1]

[1]Monash University, Pharmacology, Clayton, Australia
[2]Hudson Institute of Medical Research, The Ritchie Centre, Clayton, Australia

Abstract

Objectives: Human amnion epithelial cells (hAECs) are a placental stem cell that appear to exert neuroprotective effects following stroke, but little is known about the factors that these cells release to elicit neuroprotection. Like most cell types, hAECs are known to secrete extracellular microvesicles called exosomes, which are involved in cellular communication. As exosomes are much smaller than stem cells, they are more amenable to intravenous administration. The aim of this study was to test whether hAEC-derived exosomes exhibit neuroprotective effects comparable to those of hAECs following ischemic stroke.

Methods: Male mice (8–12 weeks old) were anaesthestised with intraperitoneal ketamine (80 mg/kg) and xylazine (10 mg/kg) and subjected to 30 min middle cerebral artery occlusion ($n = 22$) or sham surgery ($n = 6$). At 1 h following reperfusion, mice were injected intravenously with vehicle (saline; $n = 8$), 10^6 hAECs ($n = 8$) or 10 μg of hAEC-derived exosomes ($n = 6$). After 24 h, a neurological deficit score and hanging wire test were performed to assess functional deficit, and thionin staining was used to measure infarct volume. In addition, immune cell infiltration and glial scarring were analysed by immunohistochemistry.

Results: Mice treated with hAECs or exosomes had lower neurological deficit scores and longer hanging grip times than mice treated with vehicle. Furthermore, infarct volumes were reduced by 56% ($p = 0.05$) and 65% ($p < 0.05$) following administration of hAECs and exosomes, respectively, compared to vehicle. Consistent with the effects of hAEC treatment, exosomes prevented stroke-induced increases in neutrophils and T cells in the ischemic hemisphere. Exosomes also abolished stroke-induced glial scar formation, but this was not significantly altered by hAECs.

Conclusions: These data suggest that hAEC-derived exosomes may provide similar or superior neuroprotective benefits to those of hAECs following ischemic stroke, thus demonstrating the potential for exosomes as a future stroke therapy.

PS03-029

Poster Viewing Session III

Global glia replacement as a strategy for treatment of amyotrophic lateral sclerosis – a basic study on experimental mice model

L. Stanaszek[1], M. Majchrzak[1], J. Sanford[2], P. Walczak[3], B. Łukomska[1] and M. Janowski[1,3]

[1]Mossakowski Medical Research Centre, PAS, NeuroRepair Department, Warsaw, Poland
[2]Vetregen Laboratory and Stem Cell Bank for Animals, Warsaw, Poland
[3]The Johns Hopkins University School of Medicine, Russell H. Morgan Department of Radiology and Radiological Science, Division of Magnetic Resonance Research, Baltimore, United States

Abstract

Objectives: Glia plays a crucial role in proper function of the central nervous system (CNS). Previous studies showed that degeneration of neurons might result from a hostile microenvironment due to the glia failure. The experimental studies showed high efficacy of human glial restricted precursors (hGRPs) in immunodeficient small animal models of neurodevelopmental disorders. The overall goal of the study is to test the efficacy of GRPs transplanted in spontaneous degenerative myelopathy which is a progressive disease of the spinal cord in older dogs mimicking ALS. Due to lack of immunodeficient dogs and an applicable method of tolerance induction we restrained from humanGRP transplantation. Instead we decided to use allogeneic, canine GRPs. Thus, the aim of the study was to test the potency of canine GRPs (cGRPs) in a well-established double mutant shi/rag2-/- mice. The immunodeficiency (rag2-/-) of this dysmyelinated (shiverer) mouse model will facilitate full characterization of GRP potential without the interference of inflammation/immunosuppressive drugs.

Materials and Methods: GRPs were extracted from brain and spinal cord of second trimester dog foetuses and expanded in vitro over two passages. Then the cells were characterized immunocytochemically and 4×10^5 GRPs were transplanted intraventricularly into shi/rag2-/- 2 day-old mice. Myelination process was analysed with magnetic resonance imaging (MRI), electron microscopy and immunohistochemistry 18, 31 and 62 weeks after GRPs transplantation.

Results and Conclusions: cGRPs cultured in vitro were positive for the markers of glial progenitors but not mature oligodendrocytes. Additionally, the positive staining for proliferation marker and molecules involved in cell migration was observed. Shi/rag2-/- mice revealed prolonged lifespan after cGRPs transplantation (~270 days versus 200 days in nontransplanted mice). Furthermore, the myelin production has been detected using MRI, postmortem immunohistochemistry and electron microscopy analysis. It may prove the potential therapeutic effect of cGRPs.

Supported by a NCR&D grant for STRATEGMED project: "GRP&ALS"

PS03-030

Poster Viewing Session III

Cerebral decellularized extracellular matrix as in vitro model for neural development

D. Reginensi[1], S. Valerio[1,2], D. Ortiz[1], A. Pravia[1,3], C. Morgan[1,4] and R. Gittens[1]

[1]INDICASAT AIP, Center for Neuroscience, Panama, Panama
[2]Acharya Nagarjuna University, Guntur, India
[3]Universidad Latina de Panama, Panama, Panama
[4]University of Washington, Seattle, United States

Abstract

The extracellular matrix (ECM) serves as a scaffold that gives structural support to the tissue and helps maintain the tissue-specific cell phenotype. The high biochemical and structural potential to support cell biological functions have led to its use, after decellularization, as a biomaterial in clinical applications to promote tissue regeneration. However, its application for the regeneration of central nervous tissue has been less explored. Degenerative neurological disorders such as stroke, which is the fourth cause of death in Panama, would greatly benefit from therapies that could ameliorate the degenerative damage suffered in specific regions of the brain. In this study we optimized the decellularization protocol of ECM from porcine brain to study its ability to be used for neurological in vitro cell models. Our protocol combined physical, chemical and mechanical forces to remove

cell components and minimize immunogenicity while maintaining the highest integrity of the ECM possible. We characterized decellularization through DNA content, electrophoresis and histology (i.e., H&E, DAPI). The integrity of the decellularized ECM was evaluated before and after processing by measuring the protein content and performing mass spectrometry protein identification. We cultured the PC12 cell line as a uni-directional model of neuronal maturation. Cells grew on control surfaces (i.e., poly-D-lysine) or coverslips coated with native brain matrix or the decellularized biomaterial for up to 4 weeks and we evaluated their morphology and protein levels in their conditioned media. Our results show that PC12 cells were able to extend neurites when growing on the native brain and decellularized ECM coatings, similar to the positive control stimulated with neurotrophic growth factor (NGF). Cells developed and matured during the 4 weeks of culture on the biomaterial-coated surfaces without the need for any exogenous growth factors, suggesting that the decellularized ECM is able to mimic the neural microenvironment suitable for their development.

PS03-031

Poster Viewing Session III

Resting-state fMRI and behavioural indices of a human neural stem cell therapy for ischaemic stroke in rats

T. Hollyer[1], L. Gallagher[1], C. Hicks[2], R.P. Stroemer[2], K.W. Muir[3], J. Goense[4] and I.M. Macrae[1]

[1]University of Glasgow, Wellcome Surgical Institute, Glasgow, United Kingdom
[2]ReNeuron, Pencoed, United Kingdom
[3]University of Glasgow, Queen Elizabeth University Hospital, Glasgow, United Kingdom
[4]University of Glasgow, School of Psychology, Glasgow, United Kingdom

Abstract

Background: The human neural stem-cell line CTX0E03 has been reported to promote functional recovery in

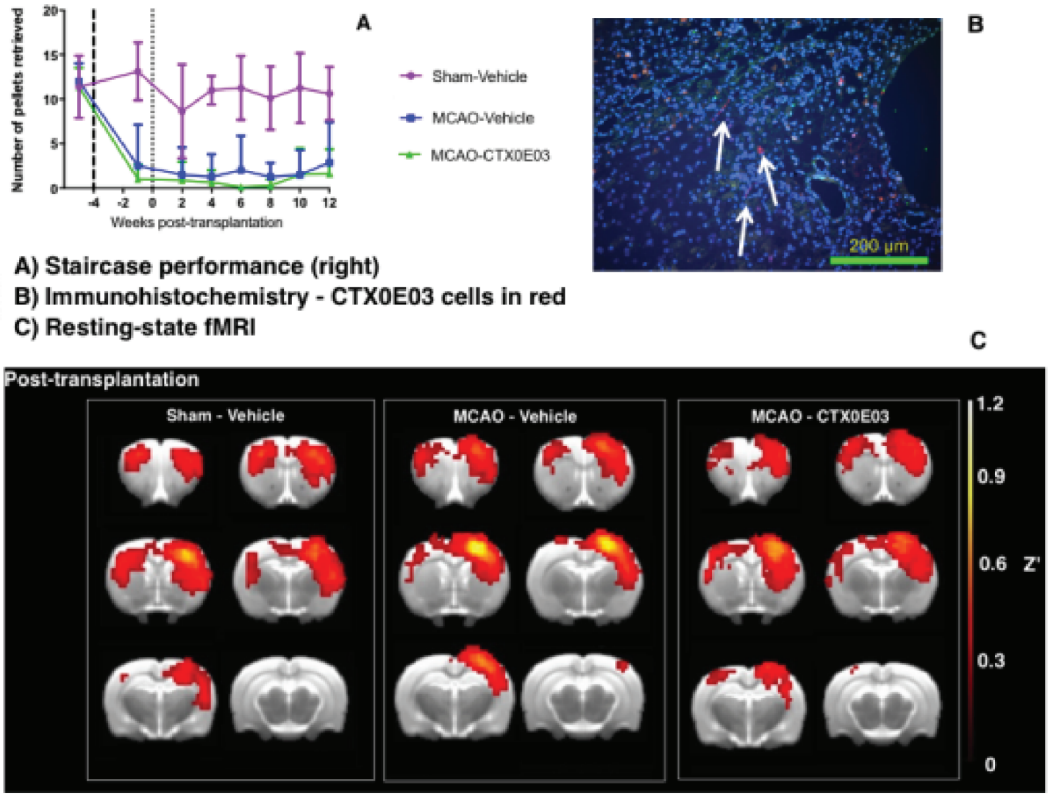

A) Staircase performance (right)
B) Immunohistochemistry - CTX0E03 cells in red
C) Resting-state fMRI

[Behavioural, histological, and functional outcomes]

rodents implanted 4 weeks after MCAO[1], and is currently in phase 2 clinical trials[2]. We evaluated measures of behavioural deficits along with resting-state fMRI to probe functional changes underlying post-treatment recovery in a longitudinal study.

Methods: Rats were randomised into three groups: Sham-Vehicle, MCAO-Vehicle, MCAO-CTX0E03 (n = 8/group). Blinding occured following stem cell/vehicle injection. The Staircase, Adjusting Steps, and Whiskers test were utilised to assess functional outcome. Resting-state fMRI was performed at 7T using GE-EPI. Seed-based correlation analysis was performed to identify changes in sensorimotor network using a seed in the contralesional S1 using the DPABI toolbox.

Timeline (weeks post-CTX0E03/vehicle transplant):

- *−5* Baseline behavioural testing
- *−4* MCAO/Sham
- *−1* Behavioural testing/MRI
- *0* Intrastriatal CTX0E03/HypoThermasol vehicle injection (2 × 4.5 μl)
- *Fortnightly* Behavioural testing
- *+6* Behavioural testing/MRI
- *+12* Perfusion fixation and paraffin embedding

Results: There was no difference in infarct volumes between the stem-cell and vehicle groups prior to transplant. MCAO caused permanent impairment on all functional assessments, with no evidence of functional recovery over 12 weeks following transplantation ($p > 0.05$, One-way ANOVA of AUC, Figure A). Ongoing histological studies suggest CTX cell survival (arrows Figure B) at similar rates as earlier studies[1]. Peri-infarct transplantation of CTX0E03 cells garnered no improvement in inter-/intra hemispheric connectivity of the resting sensorimotor network (Figure 1C).

[Behavioural, histological, and functional outcomes]

Conclusion: There were no differences in rs-fMRI and behaviour between the two groups, up to 12 weeks after MCAO.

References

1. Stroemer, P. *et al. Neurorehabil. Neural Repair* 23, 895–909 (2009).
2. Kalladka, D. *et al. Lancet* 388, 787–796 (2016).

Acknowledgements: T.Hollyer is grateful the financial and technical support for this project from SINAPSE, ReNeuron, and The University of Glasgow

PS03-032

Poster Viewing Session III

Microglia preconditioned by oxygen-glucose deprivation promote functional recovery in ischemic rats

M. Kanazawa[1], M. Miura[1], M. Toriyabe[1], M. Koyama[1], M. Hatakeyama[1], M. Ishikawa[1], T. Nakajima[2], O. Onodera[1], T. Takahashi[1], M. Nishizawa[1] and T. Shimohata[1]

[1]Niigata University/Brain Research Institute, Neurology, Niigata, Japan
[2]Niigata National Hospital, National Hospital Organization, Neurology, Kashiwazaki, Japan

Abstract

Objectives: Cell therapies that invoke pleiotropic mechanisms may facilitate functional recovery in stroke patients. We hypothesized that microglia preconditioned by oxygen-glucose deprivation (OGD) is a novel therapeutic strategy for ischemic stroke because optimal ischemia induces anti-inflammatory M2 microglia.

Methods: We performed confocal microscopic analyses to assess angiogenesis, axonal outgrowth, and the expression level of remodeling factors after ischemic stroke using the suture technique in rats. We prepared primary microglia from wild-type mice. We compared levels of cytokines and growth factors in microglial-conditioned media under normoxic and OGD conditions. Then, we examined the therapeutic benefits of intra-arterially administered primary microglia preconditioned by OGD (OGD microglia) at 7 days after focal cerebral ischemia.

Results: First, we found that angiogenesis was activated at the border area within ischemic core from 7 days after ischemia. Next, we demonstrated that administration of OGD microglia at 7 days after ischemia prompted functional recovery at 28 days after focal cerebral ischemia compared to control therapies. We also confirmed marked secretion of remodeling factors *in vitro*. In particular, expression of the anti-inflammatory cytokine, transforming growth factor-β (TGF-β), was 25 times higher after OGD compared with a normoxic condition ($P = 0.002$), and the ratio of TGF-β per tumor necrosis factor-α, which shows the polarization of M1 and M2 microglia, was six times higher after OGD, compared with a normoxic condition ($P = 0.009$). Finally, we found that intra-arterial administration of OGD microglia caused

increased expression of vascular endothelial growth factor, matrix metalloproteinase-9, and TGF-β in various cells around the injured brain parenchyma. This treatment promoted angiogenesis in the border area within the ischemic core as well as axonal outgrowth in the ischemic penumbra via decreasing levels of the axonal outgrowth inhibitor, chondroitin sulphate proteoglycan.
Conclusions: Intravascular administration of OGD microglia might be a novel therapeutic strategy against ischemic stroke.

PS03-033

Poster Viewing Session III

Distribution of bone marrow stromal cells after intravenous or intraventricular transplantation in experimental stroke

A. Lourbopoulos[1], U. Mamrak[1], C. Pan[1], R. Cai[1], A. Ghasemigharagoz[1], F.P. Quacquarelli[1], F. Hellal[1], A. Ertuerk[1] and N. Plesnila[1]
[1]Institute for Stroke and Dementia Research, Munich, Germany

Abstract
Objective: Bone marrow stromal cells (BMSCs) transplantation is promising for stroke. Although most BMSCs studies use intravenous (IV) infusion, it bears the trade-off of their peripheral entrapment (organs/vessels). We hypothesize that the cerebrospinal fluid compartment (CSFc) could be a safe/appealing route for direct delivery in the central nervous system (CNS).
Material and methods: We cultured syngenic BMSCs and labelled them in vitro with quantum dots (Qdots). Initially, we injected BMSCs into the CSFc (lateral ventricles, ICV infusion) of C57bl mice, naive (control) or subjected to filament middle cerebral artery occlusion (fMCAo). Distribution of the CSF was traced via a fluorescent 70kDa dextran, coinjected with the BMSCs. Analysis was done 30 minutes and 3 days post-injection. Secondly, mice (naive or 2 hours post-fMCAo) received BMSCs IV (tail vein) and were analyzed 3 hours post-injection. Imaging studies were done on cleared tissue (uDISCO method) or with Confocal microscopy.
Results: Within 30 minutes after ICV infusion, BMSCs are distributed in the entire CSFc (from the lateral brain ventricles down to the sacral subarachnoid space of the spinal cord) and remain unchanged by day 3. The CSF follows perivascular pathways of the penetrating arteries (30 minutes) and reaches deep parenchymal (brain and spinal cord) small vessels by day 3. The IV BMSCs'-infusion causes 40% mouse mortality. IV infused BMSCs were primarily trapped in the spleen, lungs and liver (>170 cells/mm^3). BMSCs were also found (<10 cells/mm^3) in previously unforeseen areas (the mediastinum, bone marrow, intestines and lymphnodes) plus as embolic BMSCs foci within the pulmonary arteries. BMSCs were absent from CNS after IV infusion.
Conclusion: ICV-injected BMSCs spread throughout the CNS, while CSF can carry secreted molecules deep and close to the injured areas. We show novel distribution sites and pulmonary embolism after IV-injected BMSCs, that warrants further studies and raises safety issues.

PS03-035

Poster Viewing Session III

Intra-arterial IL-1α is well tolerated and neuroprotective after experimental ischemic stroke

K. Salmeron[1], M. Maniskas[1], A. Trout[2], E. Pinteaux[3], J. Fraser[4] and G. Bix[5]
[1]University of Kentucky, Anatomy and Neurobiology, Lexington, United States
[2]University of Kentucky, Sanders Brown Center on Aging, Lexington, United States
[3]University of Manchester, Faculty of Life Science, Manchester, United Kingdom
[4]University of Kentucky, Neurosurgery, Lexington, United States
[5]University of Kentucky, Neurology, Lexington, United States

Abstract
Objectives: Endovascular thrombectomy combined with t-PA is the current standard of care for emergent large vessel occlusion (ELVO) stroke. Unfortunately, despite rising recanalization rates, stroke remains the leading cause of long-term disability worldwide suggesting that additional therapies are needed. Severe stroke morbidity may be due, in part, to the acute and sustained inflammatory stroke response. Preclinical research has shown some promise with anti-inflammatory agents in limiting brain injury and improving functional outcome; however, the post-stroke inflammatory cascade appears to have both beneficial and deleterious effects making the translation

of such anti-inflammatory approaches perilous. Indeed, we have recently demonstrated that delayed (3 day) post-stroke IV administration of the interleukin (IL)-1α (one of the two major isoforms of the pro-inflammatory family of cytokine IL-1), unexpectedly promoted, rather than suppressed, post-stroke angiogenesis in stroked mice (transient middle cerebral artery occlusion, MCAo).
Methods: In this study, we investigated the potential for IL-1α, administered acutely IV or IA ($n = 5$) after mouse MCAo, to also be neuroprotective. For the latter, our lab has recently developed a model of selective intra-arterial (IA) drug delivery in mice that can directly target stroke-affected brain with little to no systemic distribution.
Results: We noted that IV IL-1α (1 ng) is neuroprotective (as measured by cresyl violet stained infarct volumes) with mild, transient side effects (blunted hypertension and bradycardia) that were well tolerated, and with better functional recovery in free motion behavioral tests. IA IL-1α (0.1 ng) administration was even more neuroprotective without the systemic changes seen with IV treatment. Additionally, we noted that IL-1α is directly neuroprotective of primary mouse cortical neurons exposed to oxygen and glucose deprivation conditions *in vitro*.
Conclusions: Taken together, these results suggest that IL-1α could be therapeutic after stroke when administered IV or IA, and the latter may eliminate potentially harmful hemodynamic side effects.

PS03-036

Poster Viewing Session III

A1 adenosine receptor attenuates intracerebral hemorrhage-induced secondary brain injury in rats by activating the P38-MAPKAP2-Hsp27 pathway

W. Zhai[1], Z. Yu[1] and G. Chen[1]
[1]*The First Affiliated Hospital of Soochow University, Suzhou, China*

Abstract
Objectives: This study was designed to determine the role of adenosine receptors (ARs) in intracerebral hemorrhage (ICH)-induced secondary brain injury (SBI) and the underlying mechanisms.
Method: A collagenase-induced ICH model was established in Sprague-Dawley rats, and cultured primary rat cortical neurons were exposed to oxyhemoglobin at a concentration of 10 μM to mimic ICH *in vitro*. The A1 adenosine receptor (A1AR) agonist N(6)-cyclohexyladenosine (R-PIA) [1] and antagonist 8-phenyl-1,3-dipropylxanthine (8-PT) [2] were used to study the role of A1AR in ICH-induced SBI, and antagonists of P38 and Hsp27 were used to study the underlying mechanisms of A1AR actions.
Results: The protein level of A1AR was significantly increased by ICH, while there was no significant change in protein levels of the other 3 ARs. In addition, A1AR expression could be increased by R-PIA and decreased by 8-PT under ICH conditions. Activation of A1AR attenuated neuronal apoptosis in the subcortex, which was associated with increased phosphorylation of P38 MAPK, MAPKAP2, and Hsp27. Inhibition of A1AR resulted in opposite effects. Finally, the neuroprotective effect of A1AR agonist R-PIA was inhibited by antagonists of P38 and Hsp27.
Conclusions: This study demonstrates that activation of A1AR by R-PIA could prevent ICH-induced SBI via the P38-MAPKAP2-Hsp27 pathway.

References

1. Rosim FE, Persike DS, Nehlig A, Amorim RP, de Oliveira DM, Fernandes MJ. Differential neuroprotection by A(1) receptor activation and A(2A) receptor inhibition following pilocarpine-induced status epilepticus. Epilepsy Behav. 2011;22:207–213.
2. Nascimento FP, Figueredo SM, Marcon R, Martins DF, Macedo SJ, Jr., Lima DA, et al. Inosine reduces pain-related behavior in mice: involvement of adenosine A1 and A2A receptor subtypes and protein kinase C pathways. J Pharmacol Exp Ther. 2010;334:590–598.

PS03-037

Poster Viewing Session III

Differing image patterns in perfusion maps of Arterial Spin Labeling (ASL) perfusion in cerebral arterial stenosis: awareness of pitfalls is a must

S. Jaiswal[1] and S. Parida[2]
[1]*The Institute of Neurological Sciences, Care Hospitals, Dept. of Neurology, Hyderabad, India*
[2]*The Institute of Neurological Sciences, Care Hospitals, Dept. of Radiology, Hyderabad, India*

Abstract

Objectives: 1. Establish that ASL imaging can be included in the routine evaluation of a patient of suspected arterial stenosis.

2. Illustrate that unlike other perfusion studies ASL produces some varying and sometime spurious and puzzling findings that need to be considered while interpretation.

Methods: This is retrospective study in 20 patients evaluated for suspected cerebrovascular disease with a neurological deficit in an arterial territory of the anterior circulation or recurrent transient ischemic attacks. Only patients with a stenosis of >50% documented on vascular imaging were included.

The study was done in a 1.5 T SIEMENS Avanto scanner (SIEMENS, Erlangen, Germany) on the proprietary 3D ASL (pASL) sequence provided with the scanner.

ASL evaluation was done as a part of the routine stroke imaging work up in all these patients.

Color cerebral blood flow (CBF) maps generated by the evaluation software were analysed to infer about areas of reduced, normal or exaggerated cerebral blood flow.

Results: Majority of patients showed reduced cerebral blood flow in the arterial territories in question. Few patients showed spuriously increased CBF, This was due to an artefact called Arterial Transit Artefact that occurs due to slow flow within the arteries as a result of severe proximal stenosis, hence even though there is reduced blood flow, but there were apparent hyperperfsion.

Conclusions: ASL perfusion is a non contrast perfusion technique which without adding much time to the MRI evaluation of stroke has the potential of providing more functional information than the structural imaging alone.

In a majority of cases 3D ASL perfusion maps show images similar to other perfusion imaging techniques, but an artefact called Arterial transit artefact is a common phenomenon which needs to be considered in cases where there is apparent increase in CBF in the territory suspected.

PS03-038

Poster Viewing Session III

Dynamic changes in cortical cerebral blood flow following permanent MCAO: Influence of inhaled nitric oxide

I.J. Biose[1,2], I.M. Macrae[1] and C. McCabe[1]

[1]University of Glasgow, College of MVLS, Institute of Neuroscience & Psychology, Wellcome Surgical Institute, Glasgow, United Kingdom

[2]Cross River University of Technology, Department of Human Anatomy and Forensic Anthropology, Cross River, Nigeria

Abstract

Objective: Inhaled nitric oxide (iNO) is widely reported to have beneficial effects following ischaemic stroke; it has been shown to selectively vasodilate collateral arterioles [1]. We hypothesise that iNO will increase cortical collateral perfusion during permanent-middle-cerebral-artery-occlusion (pMCAo).

Method: pMCAo was induced in male Wistar rats (320–360 g). Laser-speckle-contrast-imaging (LSCI) provided dynamic changes in cortical CBF over the first 3 hrs following pMCAo and assessment of the influence of iNO. Rats were allocated to receive 20 mins doses (40, 50 and 60 ppm) of iNO ($n = 6$) or air inhalation ($n = 10$) during the 3 hr time-course. Naïve non-stroke rats ($n = 6$) were ventilated on medical air. Regions of interest (ROI) were determined at 30 min post-MCAo based on perfusion thresholds: Ischaemic core ($< 43\%$ of mean contralateral hemisphere), hypoperfused tissue (CBF between 43–75% of mean contralateral hemisphere) along with contralateral equivalent ROIs.

Results: A gradual recovery of perfusion via collaterals was observed in pMCAo groups with values reaching $185 \pm 144\%$ and $187 \pm 107\%$ (50 ppm of iNO and Air respectively) within the ischaemic core and $139 \pm 69\%$ and $141 \pm 20\%$ (50 ppm of iNO and Air, respectively) in hypoperfused ROI by 120mins post-pMCAo (Figure 1A-C). There was no significant change in perfusion in contralateral ROIs or in naïve rats over the time-course. Physiological variables (blood pressure, pH, $PaCO_2$ & PaO_2) remained stable throughout. Inhalation of NO resulted in no significant changes in perfusion when compared to air inhalation. Cortical spreading depolarisation frequency during pMCAo was equivalent in both MCAo-groups and absent in the Naïve-non-stroke-group.

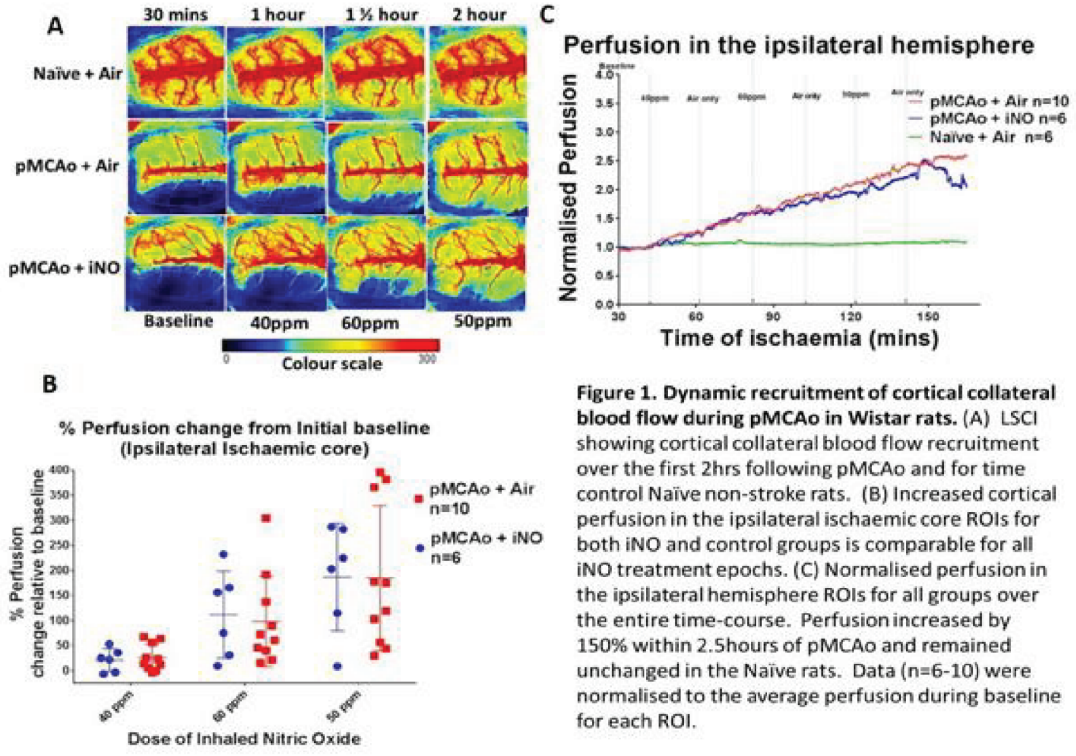

Figure 1. Dynamic recruitment of cortical collateral blood flow during pMCAo in Wistar rats. (A) LSCI showing cortical collateral blood flow recruitment over the first 2hrs following pMCAo and for time control Naïve non-stroke rats. (B) Increased cortical perfusion in the ipsilateral ischaemic core ROIs for both iNO and control groups is comparable for all iNO treatment epochs. (C) Normalised perfusion in the ipsilateral hemisphere ROIs for all groups over the entire time-course. Perfusion increased by 150% within 2.5hours of pMCAo and remained unchanged in the Naïve rats. Data (n=6-10) were normalised to the average perfusion during baseline for each ROI.

[Dynamic recruitment of cortical perfusion]

Conclusions: We have demonstrated for the first time dynamic recruitment of leptomeningeal anastomoses on the cortical surface following pMCAo. The inhalation of NO did not influence recruitment of collateral flow following pMCAo in normotensive rats.

[Dynamic recruitment of cortical perfusion]

Reference

1. Terpolilli NA et al., (2012). Circ. Res. 110: 727–738.

Funding: TETFund & Cross-River-University-of-Technology (CRUTECH).

PS03-039

Poster Viewing Session III

Evaluation of mechanical thrombectomy trends at University of Kentucky

S. Trott[1] and J. Fraser[2,3,4]

[1]*University of Kentucky, Neurosurgery, Lexington, United States*
[2]*University of Kentucky, Neurological Surgery, Lexington, United States*
[3]*University of Kentucky, Neurology, Lexington, United States*
[4]*University of Kentucky, Anatomy and Neurobiology, Lexington, United States*

Abstract

Introduction: Ischemic stroke is a devastating condition resulting in significant morbidity and mortality. The strong positive results of randomized trials have established mechanical thrombectomy as a mainstay for large vessel occlusive stroke, with significant improvements in functional outcomes. Our aim was to examine our thrombectomy procedures, and to evaluate relationships in practice

change and development that could inform the adoption and selection of techniques.

Methods: Retrospective review was conducted on mechanical thrombectomy cases from 07-2011 to 12-2015. Patients must have been 18 years old, diagnosed with ischemic stroke, and were treated with thrombectomy. Primary outcomes were final TICI score, procedural complications, NIHSS improvement, mortality, and incidence of single pass thrombectomy.

Results: 130 procedures were performed. 79.1% had a TICI score of at least 2b. 30% of thrombectomies were single pass. When evaluated by technique, single pass recanalization was achieved with reperfusion catheter alone in 52%, with stent-triever alone in 27%, and with combination techniques in 26% (Chi-squared 6.04, $p = 0.048$). In regards to technique used, 42.3% were a combination of reperfusion catheter and stent-triever, 19.2% were reperfusion catheter alone, and 31.5% were stent-triever alone. Median NIH stroke scale improvement with the procedure improved each year with a significant linear correlation (Pearson r -0.915, $p = 0.029$). Procedural mortality was 0.77% (one patient).

Conclusions: Preliminary data suggest that thrombectomy is a safe procedure that results in extremely low mortality and significant decreases NIH score over time, which may point to better functional outcome. Overall, there was an improvement in NIHSS reduction with time. There was a significant difference in the ability of different techniques to achieve first-pass recanalization, though this may reflect clinical judgments about when to use each technique.

PS03-040

Poster Viewing Session III

White matter hyperintensity segmentation in large scale clinical acute ischemic stroke cohort using a fully automated pipeline

M.D. Schirmer[1], A.V. Dalca[2], R. Sridharan[2], A.K. Giese[1,3], J. Broderick[4], J. Jimenez Conde[5], L. Holmegaard[6], B. Kissela[4], D. Kleindorfer[4], R. Lemmens[7], A. Lindgren[8], J. Meschia[8], T. Rundek[9], R. Sacco[9], R. Schmidt[10], P. Sharma[11], A. Slowik[12], V. Thijs[13], D. Woo[4], B. Worrall[14], S. Kittner[15], J. Rosand[1,3], O. Wu[16], P. Golland[2] and N.S. Rost[1]

[1]MGH and Harvard Medical School, Boston, United States
[2]Massachusetts Institute of Technology, Cambridge, United States
[3]Broad Institute of MIT and Harvard, Cambridge, United States
[4]University of Cincinnati, Cincinnati, United States
[5]Universitat Autonoma de Barcelona, Barelona, Spain
[6]Sahlgrenska Academy at University of Gothenburg, Gothenburg, Sweden
[7]KU Leuven – University of Leuven, Leuven, Belgium
[8]Skane University Hospital, Lund, Sweden
[9]University of Miami, Miami, United States
[10]Medical University Graz, Graz, Austria
[11]University of London, London, United Kingdom
[12]Jagiellonian University Medical College, Krakow, Poland
[13]Florey Institute of Neuroscience and Mental Health, Heidelberg, Australia
[14]University of Virginia, Charlottesville, United States
[15]University of Maryland, School of Medicine and Veterans Affairs, Maryland Health Care System, Baltimore, United States
[16]MGH Martinos Center for Biomedical Imaging, Boston, United States

Abstract

Objectives: To develop a fully automated, high-throughput white matter hyperintensity (WMH) analysis pipeline for clinical fluid-attenuated inversion recovery (FLAIR) images.

Background: WMH volume (WMHv) is an important and highly heritable phenotype, which is closely linked to risk and outcomes of acute ischemic stroke (AIS). Genetics

can aid the understanding of WMH biology; however, large scale genetic studies of WMH in AIS patients are hindered by manual or semi-automated approaches for clinically acquired MRI scans, necessitating a high-throughput, fully automated WMHv analysis pipeline.

Methods: Each FLAIR image is first upsampled using bi-cubic interpolation to reduce the effect of anisotropic voxel sizes. Subsequently, parameter-free brain extraction is performed using RObust Brain EXtraction. All images are then registered to an in-house FLAIR template using Advanced Normalization Tools. Automated WMH identification and outlining of leukoaraiosis is performed using principal component analysis modes, learned from 100 manual segmentations. WMHv are calculated for each subject from non-interpolated slices only. Inter-rater variations in manual segmentations are assessed by calculating the standard deviation (SD) of WMHv (9 subjects; 6 raters each). Good agreement between automated and manual outlines is assessed in 358 subjects (automated WMHv within 3SD of manual WMHv).

Results: WMHv are calculated on a set of 2703 FLAIR images of patients from 12 independent AIS cohorts (sites), as part of the MRI-Genetics Interface Exploration (MRI-GENIE) study. Distributions are shown in Figure 1. Agreement between manual and automated segmentations shows that 88% of the automated WMHv fall within 3SD from the manual WMHv, suggesting good agreement.

Conclusion: Using a fully-automated WMHv analysis pipeline for clinical MRIs is feasible and shows good agreement to manual outlines. Further analysis of the extracted WMHv has the potential to advance current knowledge of risks and outcomes in AIS.

PS03-041

Poster Viewing Session III

Time-Domain NIRS oxygenation parameters in healthy volunteers compared to ischemic stroke patients

G. Giacalone[1], M. Zanoletti[2], D. Contini[2], R. Re[2], L. Spinelli[3], B. Germinario[4], A. Torricelli[2,3] and L. Roveri[1]

[1] *San Raffaele Scientific Institute, Neurology Department, Milan, Italy*

[2] *Politecnico di Milano, Dipartimento di Fisica, Milan, Italy*

[3] *Istituto di Fotonica e Nanotecnologie, Consiglio Nazionale delle Ricerche, Milan, Italy*

[4] *'Vita-Salute' San Raffaele University, Milan, Italy*

Abstract

Time-Domain Near-Infrared Spectroscopy (TD-NIRS) is an optical technology able to non-invasively measure the absolute concentrations of deoxy-haemoglobin (HHB), oxy-haemoglobin (OHB), total haemoglobin (tHB) and to calculate tissue oxygen saturation ($SO_2 = OHB/tHB$) in the outer layers of brain tissue. The aim of our study was to measure ranges of normal values of HHB, OHB, tHB, SO_2 in controls and to evaluate changes of SO_2 in acute ischemic stroke patients.

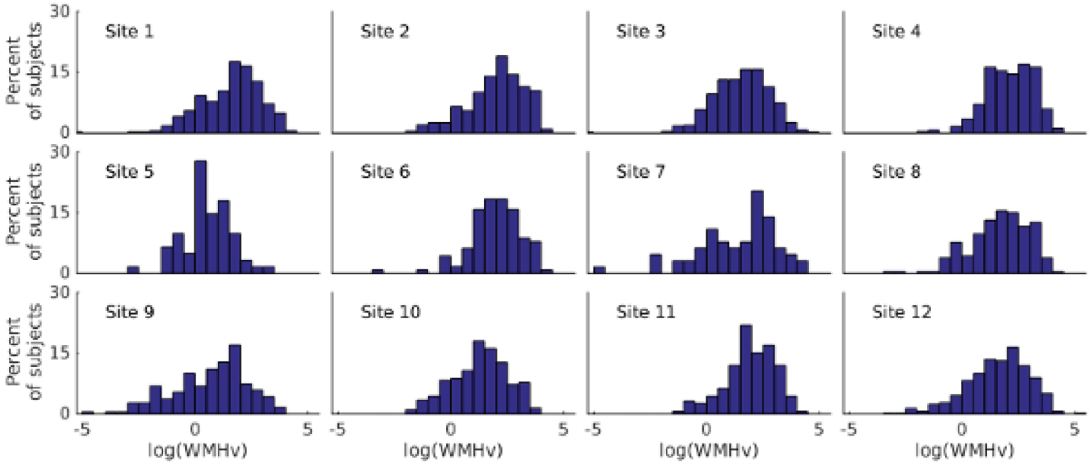

[Figure 1: Distributions of WMHv for MRI-GENIE.]

Figure 1. Distributions of WMHv for MRI-GENIE.

We enrolled 33 controls (mean age:71.6 ± 8.4), and 4 ischemic stroke patients (mean age:81.2 ± 5.4) (< 24h from stroke onset). TD-NIRS measurements of at least 3 brain regions per hemisphere were performed using 3 wavelengths (690, 785, 830 nm). Data were fitted with the diffusion model for semi-infinite homogenous media. TD-NIRS optodes were placed on corresponding ischemic brain tissue according to the orthogonal projection of fiducial markers in CT- MRI-scans. Ischemic stroke involved deep brain tissue in 3 patients without evidence of arterial occlusion and cortical-subcortical brain tissue in 1 patient due to middle-cerebral artery occlusion treated with rTPA and thrombectomy.

Mean (CI 95%) concentrations (uM) in controls were: HHB = 23.5 (23.1–23.9), OHB = 44.6 (43.6–45.6), tHB = 68.1 (66.8–69.4), SO_2 = 65.1% (64.1–65.5). In both controls and ischemic stroke patients, not-significant SO_2 inter-hemispheric differences were detected for positions above normal tissue ($p_{controls} = 0.34$; $p_{deep\text{-}stroke\ patients} = 0.59$; $p_{cortical\text{-}subcortical\ patient} = 0.13$). The patient with cortical-subcortical stroke had significantly reduced SO_2 in optodes above subcortical core compared to normal tissue (51.3% vs 60.5%; $p < 0.001$) and to control subjects ($p < 0.001$). Functional outcome at discharge was favorable: delta NIHSS = 19, mRS = 2. Patients with deep core stroke had SO_2 of brain areas above the deep core similar to normal brain regions (respectively SO_2 = 64.9% vs. SO_2 = 66%; $p = 0.44$) and to control subjects ($p = 0.87$).

According to these preliminary data, SO_2 is reduced in cortical brain regions rescued by recanalization. SO_2 may represent a surrogate marker of increased oxygen extraction and favorable outcome.

PS03-042

Poster Viewing Session III

Inhibition of α5β1 integrin with ATN-161 is neuroprotective and stabilizes the blood-brain barrier after experimental ischemic stroke

D. Edwards[1], K. Salmeron[1], J. Fraser[2] and G.J. Bix[3]

[1]*University of Kentucky, Anatomy and Neurobiology, Lexington, United States*

[2]*University of Kentucky, Neurosurgery, Lexington, United States*

[3]*University of Kentucky, Neurology, Lexington, United States*

Abstract

Stroke is a leading cause of death and disability with limited therapeutic options. The β1 integrin extracellular matrix receptor family has been linked to changes in BBB permeability via changes to tight junction (TJ) protein expression and function. We hypothesized that one particular β1 integrin subtype, α5β1, a pro-angiogenic fibronectin receptor that is expressed in developing brain vasculature but downregulated in the adult brain, contributes to BBB breakdown via effects on the localization and expression of the TJ protein claudin-5.

Objectives: Our aim was to determine the spatiotemporal expression of α5β1 integrin as well as the potential therapeutic and BBB stabilizing effect of inhibiting it with the small peptide ATN-161 following experimental stroke.

Methods: *In vivo:* Male wildtype mice underwent transient middle cerebral artery occlusion for 1 hour. Mice were treated intravenously with ATN-161 (1 mg/kg) upon, 24 and 48 hours after reperfusion. Stroke volume was assessed on post-stroke day 3 using cresyl violet. Immunohistochemical analysis of α5β1, claudin-5, NeuN, GFAP, and IgG expression was performed. *In vitro:* Mouse brain endothelial cell monolayers underwent oxygen-glucose deprivation or TNFα treatment f followed byATN-161 treatment. Permeability was assessed using FITC-dextran migration. Claudin-5 and α5β1 expression was also analyzed by immunocytochemistry.

Results: α5β1 was acutely (PSD2) upregulated away from the vascular extracellular matrix basement membrane. Post-stroke administration of ATN-161 decreased infarct volume and reduced BBB breakdown. *In vitro*, ATN-161 decreased permeability of endothelial cell monolayers following OGD or TNFα and re-localized claudin-5 to the extracellular surface.

Conclusion: Endothelial cell α5β1 integrin expression is increased acutely after stroke, is expressed luminally (suggesting a non-basement membrane novel interaction and availability to intravascular therapeutics) upon upregulation, and may contribute to BBB breakdown and worsening brain injury. Furthermore, blocking α5β1 with ATN-161 could represent a promising novel therapeutic approach for ischemic stroke.

PS03-043

Poster Viewing Session III

Investigation of effective reserve as a protective mechanism for stroke outcome

M.D. Schirmer[1], M.R. Etherton[2], A.V. Dalca[3], A.K. Giese[2,4], L. Cloonan[2], O. Wu[5], P. Golland[3] and N.S. Rost[2]

[1]MGH/HMS, Neurology, Boston, United States
[2]MGH and Harvard Medical School, Boston, United States
[3]Massachusetts Institute of Technology, Cambridge, United States
[4]Broad Institute of MIT and Harvard, Cambridge, United States
[5]MGH Martinos Center for Biomedical Imaging, Boston, United States

Abstract

Objectives: To determine if effective reserve (eR) is a protective mechanism that improves functional outcome after acute ischemic stroke (AIS).

Background: Stroke is a leading cause of disability worldwide. However, mechanisms of post-stroke recovery are complex, and conventional outcome prediction models are limited. "Brain reserve" has been proposed as a construct to model the brain's capacity to withstand insults. BR has been shown to co-vary with white matter hyperintensity volume (WMHv) using structural equation modeling (SEM), a technique to test models with latent variables.

Methods: Using SEM, we define an effective reserve (eR), the remaining brain reserve after other influences have been accounted for. We characterize eR using intra-cranial volume (ICV), age and systolic blood pressure (SBP). Our model incorporates known relationships between age, SBP, WMHv, acute infarct volume on diffusion-weighted imaging (DWIv) and 90-day functional post-stroke outcome (modified Rankin Scale; mRS), as shown in Figure 1. Path analysis was performed (R; package lavaan) to estimate the relations within the model in a dataset of 451 AIS patients (*: $p < 0.05$; **: $p < 0.01$; ***: $p < 0.001$). No priors were used for the path coefficients.

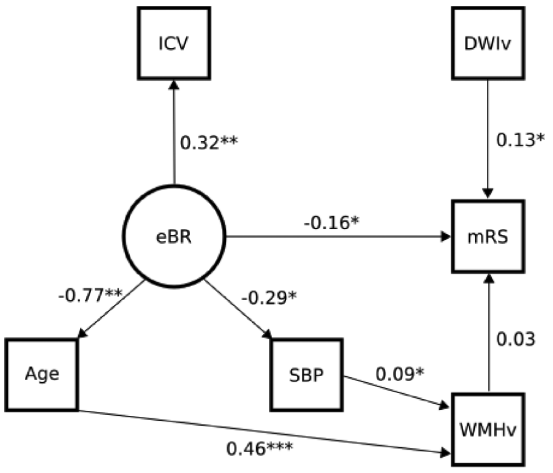

[Figure 1: eR model estimated using path analysis.]

Results: The estimated model coefficients (Figure 1) show that eR is negatively associated with age and SBP, but positively with ICV. Association between age, SBP and WMHv are positive. Outcome is positively associated with WMHv and DWIv and negatively with eR, suggesting that eR acts as a protective mechanism. All path coefficients are statistically significant, except for WMHv and mRS.

Conclusion: Our analysis shows that eR is negatively associated with post-stroke outcome (the higher eBR, the lower mRS), suggesting that eR acts as a protective mechanism. Additionally we reproduced known relationships between WMHv, SBP, age, DWIv and mRS.

PS03-044

Poster Viewing Session III

Peroxisomal turnover in ischemic brain

W. Zhu[1], W. Zhang[1], J. Young[1], A. Barnes[1] and N. Alkayed[1]

[1]Knight Cardiovascular Institute, Oregon Health & Science University, Portland, United States

Abstract

Objectives: We have previously demonstrated that increasing peroxisomal biogenesis serves a protective function in neurons experiencing ischemic injury, in part by increasing their antioxidant capacity (1). The role of autophagy in adult cerebral ischemia has been studied, yet the specific role for the targeted destruction of damaged peroxisomes (pexophagy) in ischemic stroke

has not yet been explored. We used a combination of pharmacologic and genetic strategies to determine if perturbation of autophagy in general and pexophagy in particular alters ischemic brain injury by targeting mammalian Target Of Rapamycin (mTOR) and its upstream regulator Tuberous Sclerosis Complex 1 (TSC1).

Methods: Transient middle cerebral artery occlusion (MCAO, 60 min) was performed in adult male mice treated with mTOR rapamycin (1.25 mg/kg, IP) or vehicle at the beginning of reperfusion. Similarly, TSC1 knock-out and wild-type mice underwent 60-min MCAO, and brains were harvested and analyzed for infarct size at 24 hrs of reperfusion. Separate brains were analyzed for peroxisomal membrane protein co-localization with autophagic markers, and for autophagic activity based on microtubule-associated protein 1A/1B-light chain 3 (LC3) turnover.

Results: Activation of autophagy using rapamycin reduced infarct in the cerebral cortex from $37.3 \pm 1.8\%$ ($n = 9$) in vehicle- to $27.2 \pm 2.8\%$ ($n = 10$) in rapamycin-treated mice ($p = 0.01$), whereas TSC1 knockout mice, which have reduced pexophagy, sustained larger infarcts than WT mice ($48.5 \pm 4.5\%$ ($n = 4$) vs. $33.0 \pm 5.8\%$ ($n = 5$), respectively, $p = 0.007$).

Conclusions: We conclude that organelle autophagy, including pexophagy, is an endogenous mechanism of neuroprotection after stroke, and that both biogenesis and pexophagy of peroxisomes are protective by promoting peroxisomal turnover.

References

1. Antioxid Redox Signal. 2015 Jan 10;22(2):109–20

PS03-045

Poster Viewing Session III

Expression of leukemia inhibitory factor receptor in the brain and immune system after permanent stroke

S. Davis[1], L. Collier[1], J. Fazal[2], C. Leonardo[2], C. Ajmo[2] and K. Pennypacker[1]

[1]University of Kentucky, Neurology, Lexington, United States
[2]University of South Florida, Molecular Pharmacology and Physiology, Tampa, United States

Abstract

Objective: The leukemia inhibitory factor (LIF), an anti-inflammatory cytokine, regulates neuroprotective signaling through the activation of the LIF receptor (LIFR). The regulation of LIFR expression was examined in neural cells and splenocytes after MCAO and with LIF treatment.

Methods: Male Sprague-Dawley rats underwent middle cerebral artery occlusion or sham surgery and injected with PBS or LIF (125 μg/kg) ($n = 8$ per group). Levels of LIFR and LIF-dependent transcription factors MZF-1, and Sp1, were measured using western blotting. Immunohistochemistry was used to determine localization of Sp1, LIF receptor, MZF-1, and superoxide dismutase 3, a LIF-inducible enzyme.

Results: LIF (1.494 OD $\pm$ 0.161) significantly increased brain LIFR levels in ipsilateral tissue at 72 h after stroke compared to sham surgery (0.299 OD $\pm$ 0.060) and PBS treatment (0.399 OD $\pm$ 0.154) (0.0281 OD $\pm$ 0.011, $p < 0.01$). LIFR expression was localized to the nucleus of cortical neurons in culture and in the intact brain. Regardless of treatment, ischemic injury caused the LIFR to translocate to the cell membrane in cortical neurons in the ipsilateral hemisphere, but not contralateral. After LIF treatment, MZF-1 and Sp1 co-localized with superoxide dismutase 3 in cortical neurons. Splenic LIFR levels decreased significantly after LIF (0.170 OD $\pm$ 0.010) treatment compared to PBS (0.228 OD $\pm$ 0.285, $p < 0.05$) and sham rats (0.329 OD $\pm$ 0.031, $P < 0.001$). LIF significantly increased MZF-1, but not Sp1, in spleen tissue (0.158 OD $\pm$ 0.038) compared to PBS (0.109 OD $\pm$ 0.044) and sham (0.090 OD $\pm$ 0.018).

Conclusions: LIF administration increases LIFR expression, which will enhance neuroprotective signaling after MCAO. Injury alone increased LIFR trafficking from the nucleus to membrane in neurons. In contrast, LIF causes downregulation of LIFR perhaps through MZF-1 in the spleen after stroke to downregulate its inflammatory response.

PS03-046

Poster Viewing Session III

Membrane trafficking dysfunction leads to Cathepsin B release and ischemia-reperfusion brain injury

D. Yuan[1], C. Liu[1] and B. Hu[1]

[1]University of Maryland School of Medicine, Shock Trauma and Anesthesiology Research Center, Baltimore, United States

Abstract

Objectives: The objective of this study is to investigate the cascade of events of membrane trafficking dysfunction, massive buildup of late endosome (LE), release of cathepsin B (CTSB), and brain ischemia-reperfusion injury. Membrane trafficking encompasses 3 major types: (i) to assemble or deliver newly synthesized polypeptides to organelles, (ii) the endocytic pathway; and (iii) the autophagy pathway. N-ethylmaleimide sensitive factor (NSF) is the sole ATPase for controlling membrane trafficking from Golgi apparatus to the endosome-lysosome system.

Methods: Rats were subjected to 20 min of global ischemia followed by 0.5, 4, 24 and 72 h of reperfusion. New NSF deficient and overexpression transgenic mice were generated. Neuronal ultrastructure was examined by electron microscopy. NSF, cathepsins, and endosomal and lysosomal proteins were analyzed by Western blotting and confocal microscopy in brain sections.

Results: NSF ATPase is progressively trapped as inactive protein aggregates within hippocampal CA1 neurons that undergo delayed neuronal death after ischemia. EM shows extensive buildup of Golgi/transport vesicles (***Vs***) and late endosomes (***LEs***) in *postischemic CA1 neurons*. Confocal microcopy and Western blotting demonstrates massive CTSB accumulation in and release from ***Golgi/Vs/LEs*** structures, which is followed by delayed neuronal death after brain ischemia. To study whether NSF inactivation after brain ischemia leads to buildup of ***Golgi/Vs/LEs*** and ***CTSB*** release, we generated a new neuron-specific NSF activity-deficient transgenic (***tg***) mouse line. The most prominent pathological phenotype of this NSF activity-deficient tg mouse line is massive buildup of ***Golgi/Vs/LEs*** and ***CTSB*** release, followed by delayed neuronal death, virtually identical to events observed in CA1 neurons of wildtype mice after brain ischemia. Furthermore, overexpression of NSF in tg mice significantly protects neurons from brain ischemia.

Conclusions: Brain ischemia leads to NSF inactivation, massive buildup of Golgi/Vs/LEs and fetal CTSB release, resulting in delayed neuronal death.

PS03-047

Poster Viewing Session III

Post-stroke induction of alpha-synuclein mediates ischemic brain damage

T. Kim[1,2], S. Mehta[1], B. Kaimal[1], K. Lyons[1] and R. Vemuganti[1,2]

[1]University of Wisconsin – Madison, Neurological Surgery, Madison, United States

[2]University of Wisconsin – Madison, Neuroscience Training Program, Madison, United States

Abstract

Objectives: α-synuclein (α-syn) is one of the most abundant proteins in mammalian brain implicated in the several neurodegenerative processes. In particular, abnormal α-syn aggregation by post-translational modifications (e.g. S129 phosphorylation) has been shown to cause Parkinson's disease. However, even though α-syn is linked to pathophysiological mechanisms similar to those that produce acute neurodegenerative disorders, such as stroke, the role of α-syn in such disorder is not clear. Therefore, we examined whether α-syn contributes to post-stroke neuronal death and neurological dysfunction.

Methods: Rodents were subjected to intraluminal transient middle cerebral artery occlusion. α-syn induction was silenced with Silencer Select α-syn siRNA via intracerebral injection. Total and phospho-α-syn levels were measured with either qPCR or Western Blots. The post-ischemic motor deficit was evaluated with Rotarod, beam walk and adhesive removal test 1 to 7 days after ischemia, and brain damage was measured on cresyl violet stained brain sections. Cellular changes after ischemia were examined using immunofluorescence staining.

Results: We found transient focal ischemia upregulates α-syn protein expression and nuclear translocation in neurons of the adult rodent brain. We further showed that knockdown or knockout of α-syn significantly decreases the infarction and promotes better neurological recovery in rodents subjected to focal ischemia. Furthermore, α-syn knockdown significantly reduced post-ischemic induction of phospho-Drp1, 3-Nitrotyrosine, cleaved caspase-3, and LC-3 II/I, indicating its role in modulating mitochondrial fragmentation, oxidative stress, apoptosis, and autophagy, which are known to mediate post-stroke neuronal death. Transient focal ischemia also significantly upregulated S129 phosphorylation of α-syn and nuclear translocation of phospho-α-syn. Furthermore, knockout mice that lack

PLK2 (predominant kinase that mediates S129 phosphorylation) showed better functional recovery and smaller infarcts when subjected to transient focal ischemia, indicating a detrimental role of S129 phosphorylation of α-syn.
Conclusions: Therefore our studies indicate that α-syn is a potential therapeutic target to minimize post-stroke brain damage.

PS03-048

Poster Viewing Session III

Impaired assembly of HTRA1 oligomers as a pathogenic mechanism in cerebral small vessel disease

N. Beaufort[1], K. Bravo-Rodriguez[2], J. Nelles[3], E. Sanchez-Garcia[2], C. Haffner[1], E. Tournier-Lasserve[4,5], M. Ehrmann[3,6] and M. Dichgans[1,7]

[1]Institute for Stroke and Dementia Research, Hospital of the Ludwig-Maximilians-University Munich, Munich, Germany
[2]Max-Planck-Institut für Kohlenforschung, Mülheim an der Ruhr, Germany
[3]Centre for Medical Biotechnology, Faculty of Biology, University Duisburg-Essen, Essen, Germany
[4]Génétique et Physiopathologie des Maladies Cérébro-Vasculaires, UMR 1161, University Paris-Diderot, Paris, France
[5]Hôpital Lariboisière, Assistance Publique des Hôpitaux de Paris, Paris, France
[6]School of Biosciences, Cardiff University, Cardiff, United Kingdom
[7]Munich Cluster for Systems Neurology (SyNergy), Munich, Germany

Abstract
Objectives: Homozygous loss-of-function mutations in the high temperature requirement A1 (HTRA1) protease cause CARASIL, a recessively inherited cerebral small vessel disease (SVD) manifesting with lacunar infarcts, white matter ischemia, stroke, and dementia. In addition, heterozygous HTRA1 mutations have recently been identified as a major cause of autosomal dominant SVD. Moreover, there is evidence suggesting that altered HTRA1 expression might be involved in the more common sporadic forms of SVD. In the current study, we set up to elucidate the mechanisms by which pathogenic HTRA1 mutations confer loss of enzymatic activity.
Methods: To investigate the conformation and enzymatic activity of disease-related HTRA1 variants, we combined protein overexpression and purification, size exclusion chromatography, crosslinking, protease activity measurements and computational modelling.
Results: HTRA1 assembles as trimers and higher order oligomers to form a mature and proteolytically active complex. We show that a subset of pathogenic mutations interfere with HTRA1 oligomeric assembly. We further engineered an enzymatically inactive HTRA1 variant able to selectively restore the assembly and enzymatic activity of one of the pathogenic mutants in biochemical and cell based assays.
Conclusions: Our data identify impaired oligomeric assembly as a major mechanism by which pathogenic HTRA1 mutations abrogate enzymatic activity. We further provide proof of concept it is possible to rescue the function of individual disease-causing mutants, thus opening avenues for therapeutic intervention.

References

Hara K et al., Association of HTRA1 mutations and familial ischemic cerebral small-vessel disease, N Engl J Med, 2009.
Verdura E et al., Heterozygous HTRA1 mutations are associated with autosomal dominant cerebral small vessel disease, Brain, 2015.
Truebestein L et al., Substrate-induced remodeling of the active site regulates human HTRA1 activity, Nat Struct Mol Biol, 2011.

PS03-049

Poster Viewing Session III

Growth differentiation factor-11 causes neurotoxicity during oxygen and glucose deprivation *in vitro*

B.A. Sutherland[1,2], G. Hadley[1], Z. Alexopoulou[3], T. Lodge[4], A.A. Neuhaus[1], Y. Couch[1], N. Kalajian[1], K.J. Morten[4] and A.M. Buchan[1]

[1]University of Oxford, Acute Stroke Programme, Radcliffe Department of Medicine, Oxford, United Kingdom
[2]University of Tasmania, School of Medicine, Hobart, Australia
[3]University of Oxford, Nuffield Department of Clinical Neurosciences, Oxford, United Kingdom
[4]University of Oxford, Nuffield Department of Obstetrics and Gynaecology, Oxford, United Kingdom

Abstract

Age-related neuronal dysfunction can be overcome by circulating factors present in young blood[1]. Growth differentiation factor-11 (GDF-11), a systemic factor that declines with age, can reverse age-related dysfunction in brain[2], heart[3] and skeletal muscle[4]. Given that age increases susceptibility to stroke, we hypothesised that GDF-11 may be neuroprotective following ischaemia. Primary cortical neurons were isolated from E18 Wistar rat embryos and cultured for 7–10 days. Neurons were deprived of oxygen and glucose (OGD) to simulate stroke. Neuronal death was assessed by lactate dehydrogenase or CellTox™ green cytotoxicity assay. Results are from at least 3 experiments. 40ng/mL GDF-11 administration during 2h OGD significantly increased neuronal death (vehicle: 19.3% ± 1.9% cell death, GDF-11: 33.9% ± 2.3%; $p = 0.0005$). However, 7 day GDF-11 pre-treatment did not affect neuronal death during 2h OGD (vehicle: 11.0% ± 3.3%, GDF-11: 11.1% ± 1.7%; $p = 1.000$). GDF-11 treatment during the 24h recovery period after 2h OGD also did not alter death (vehicle: 17.9% ± 1.7%, GDF-11: 17.2% ± 1.6%; $p = 0.988$). Real-time monitoring for 24 h revealed that by 2h OGD, GDF-11 treatment had increased neuronal death (1.11 ± 0.03 fold over vehicle; $p = 0.0437$) which remained raised at 24 h (1.23 ± 0.08 fold over vehicle; $p = 0.0024$). Co-treatment of 1 μM SB431542 (TGFβI/ALK5 receptor antagonist) with GDF-11 prevented GDF-11 neurotoxicity after 2 h OGD (0.89 ± 0.03 fold over vehicle; $p < 0.0001$) and 24 h OGD (0.90 ± 0.04 fold over vehicle, $p < 0.0001$). These results reveal for the first time that GDF-11 is neurotoxic to primary neurons in the acute phase of simulated stroke through TGFβI/ALK5 receptor signaling. Blockers of neuronal TGFβ signaling could provide a novel therapeutic strategy for ischaemic stroke.

References

1. Villeda et al. (2014) Nat Med 20:659–63.
2. Katsimpardi et al. (2014) Science 344:630–4.
3. Loffredo et al. (2013) Cell 153:828–39.
4. Sinha et al. (2014) Science 344:649–52.

PS03-050

Poster Viewing Session III

Exosomes shed from M2 microglia protect neuron from hypoxia

Y. Song[1], Y. Feng[1], M. Qu[1], T. He[1], F. Yuan[1], W. Li[1], Z. Li[1], L. Jiang[1], Y. Wang[1], Z. Zhang[1] and G. Yang[1]

[1] *Shanghai Jiaotong University, Shanghai, China*

Abstract

Objective: Exosome released into the brain microenvironment acts as a novel way of intercellular transmission [2,3]. M2 microglia shows a critical role in modulating cell death and neuronal recovery in response to the brain injury [1]. While the regulatory mechanism of exosome from microglia mediating neuronal recovery is obscure. Here we explore whether microglia M2 benefits neuroprotection via transferring exosomes carrying critical information.

Methods: We isolate exosomes from M2 microglia induced by IL-4 (M2-EXO) and co-cultured M2-EXO with injured neuron induced by oxygen-glucose deprivation (OGD). The experimental group include neurons without treatment, neurons underwent OGD with no treatment, M2-conditioned-media treatment, M2-EXO treatment, and M2-conditioned-media deprived exosomes. We also tracked the route of exosomes entering neuron by time-lapse.

Results: We found inflammatory factors and neuron apoptosis were inhibited, anti-inflammatory factors were up-regulated in the group with M2-EXO treatment ($P < 0.05$). Neurotrophic factors increased both in neuron and neuronal conditioned-media treated with M2-EXO ($P < 0.05$). The increase of neurotrophic factors in injured neurons were blocked when neuron co-cultured with M2 conditioned media which deprived exosome. Exosomes derived from M2 microglia cells were up taken by injured neurons, and exosome mediated horizontally transference of intercellular information between neuron and microglia.

Conclusion: This study highlighted exosomes released from M2 microglia attenuated neuronal apoptosis in hypoxic injury, which indicates exosomes play a critical role in transferring information between neuron-microglia communications.

Reference
1. Lee J H, Wei Z Z, Cao W, et al. Neurobiology of Disease, 2016, 96: 248-260.
2. Budnik V, Ruiz-Cañada C, Wendler F. Nature Reviews Neuroscience, 2016, 17(3): 160-172.
3. Alvarez-Erviti L, Seow Y, Yin H F, et al. Nature biotechnology, 2011, 29(4): 341-345.

PS03-051

Poster Viewing Session III

Blockade of acid sensitive ion channels attenuate recurrent hypoglycemia-induced potentiation of post-ischemic hypoperfusion and ischemic brain damage in treated diabetic rats

A.K. Rehni[1], V. Shukla[1] and K.R. Dave[1,2]
[1]*University of Miami Miller School of Medicine, Neurology, Miami, United States*
[2]*University of Miami Miller School of Medicine, Neuroscience Program, Miami, United States*

Abstract
Objectives: Diabetes is one of the major risk factors for cerebral ischemia[1]. Recurrent hypoglycemia (RH) is a side-effect of anti-diabetic therapy. Previously, we observed increased ischemic brain damage[2] and increased intra-ischemic acidosis (lactate and pH drop) in RH-exposed insulin-treated diabetic (ITD) rats. The present study tested the hypothesis that increased intra-ischemic acidosis in RH-exposed ITD rats leads to post-ischemic hypoperfusion via activation of acid sensitive ion channels (ASICs).
Methods: Diabetes was induced in rats using streptozotocin and treated with insulin. Groups employed were: ITD+vehicle, ITD+RH+vehicle, ITD+RH+PcTx1 (ASIC1a inhibitor, 0.75 ng/ventricle over 5 min), and ITD+RH+APETx2 (ASIC3 inhibitor, 75 ng/ventricle over 5 min-repeated every 20 min). RH was induced for three hours/day for five days. Transient cerebral ischemia was induced overnight after completion of RH by bilateral carotid artery occlusion with hypotension. Inhibitor treatment was started 10 min before ischemia. Laser Doppler flowmetry was used to measure cerebral blood flow. Neuronal death was quantified in CA1 hippocampus.
Results: Ischemia-induced hypoperfusion in RH-exposed ITD rats was significantly higher than in ITD rats from 23 to 62 min of reperfusion (difference 25–50%). Treatment with PcTx1 (3–7 and 22–80 min of reperfusion) and APETx2 (2–4 and 25–66 min of reperfusion) prevented RH-induced increase in post-ischemia hypoperfusion. Moreover, PcTx1 as well as APETx2 treatments prevented RH-induced increased ischemic damage in CA1 hippocampus (difference 56–62% decrease in neuronal count) (Fig.1).
Conclusions: Our results suggest a role of ASIC activation in observed increased ischemic damage in RH-exposed ITD rats. Better understanding of mechanisms involved in exacerbated cerebral ischemic damage in RH-exposed ITD rats may help lower the severity of ischemic damage in diabetic patients.

References
1) Diabetes Care. 2005;28(2):355–9.
2) Stroke. 2011;42(5):1404–11.

Acknowledgement: This study was supported by NIH (NS073779).

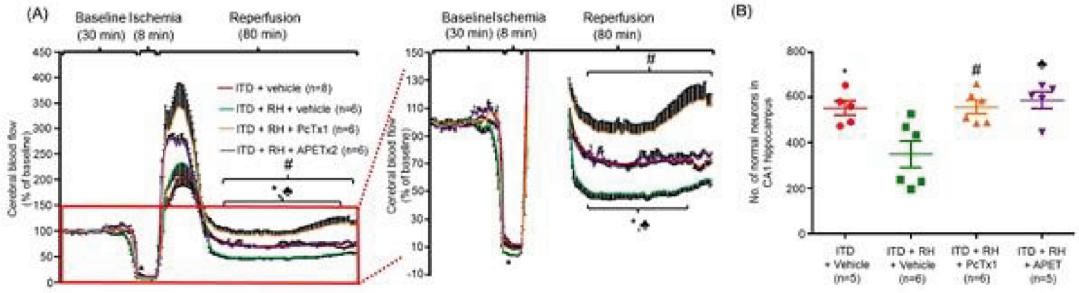

Figure 1 : The role of ASIC 1 and 3 in RH-induced increase in (A) post-ischemic cerebral hypoperfusion and; (B) ischemic damage in hippocampus of ITD rats. (A) Percent change in cerebral blood flow versus time curve and (B) number of normal neurons in CA1 hippocampus per field of rats belonging to 1) ITD + vehicle, 2) ITD + RH + vehicle, 3) ITD + RH + PcTx1 and, 4) ITD + RH + APETx2 groups. The results are presented as mean ± SEM. * p<0.05, ITD + vehicle vs ITD + RH + vehicle, # p<0.05, ITD + RH + PcTx1 vs ITD + RH + vehicle and, ♣ p<0.05, ITD + RH + APETx2 vs ITD + RH + vehicle.

PS03-052

Poster Viewing Session III

Nur77 ameliorate brain ischemic injury through polarize microglia from M1 to M2 phenotype

Y. Chen[1], H. Zhan[1], Y. Jin[1], L. Han[1] and Y. Xu[1]

[1]Affiliated Drum Tower Hospital of Nanjing University Medical School, Nanjing, China

Abstract

Introduction: The immune response to cerebral ischemia is a major contributor to stroke pathobiology in which microglia play a crucial role. Microglia are present in the classical M1 pro-inflammatory and the alternative M2 anti-inflammatory microglia. The Nur77 has been implicated in the regulation of macrophage M1/M2 polarization. However, the function of Nur77 in microglia and stroke pathology has not been studied yet. We investigated the role of Nur77 in modulating microglial M1/M2 polarization and improve brain injury.

Methods: Wild type and Nur77$^{-/-}$ mice were subjected to right middle cerebral artery occlusion (MCAO). Behavior test, infarction volume, inflammation factors, and microglial phenotypes were determined at 1 d, 3 d, 7 d after MCAO. *In vitro*, wild type and Nur77$^{-/-}$ microglia were simulated with conditional medium of oxygen glucose deprivation neuron. M1/M2 markers were measured at different time points. To explore mechanisms, proteomics analysis was conducted. Then we induced a lentivirus into the microglial cells for abrogation of Nur77 downstream protein in Nur77$^{-/-}$ microglia.

Results: Nur77 expression in ipsilateral peri-infarction is markedly decreased. Nur77 deficiency enlarged infarction size, exacerbated sensorimotor and cognitive function, increased the expression of pro-inflammatory mediators (COX-2, TNFα), and decreased anti-inflammatory mediators (IL-4, IL-10) at 3d and 7d after MCAO. Nur77$^{-/-}$ mice present more CD16^{+}Iba-1^{+} and CD86^{+}Iba-1^{+} M1 microglia and less CD206^{+}Iba-1^{+} M2 microglia than wild type mice. *In vitro* conditional medium treated Nur77$^{-/-}$ primary microglia express more pro-inflammation mediators and less anti-inflammation factors. LPS-treated Nur77$^{-/-}$ and wild type microglia was used for mass spectrometry and we found that Nur77 down-regulate the expression of dedicator of cytokinesis 2 (DOCK2), which promote release of proinflammation mediators in microglia. After knockdown of DOCK2 in Nur77$^{-/-}$ microglia, up-regulated pro-inflammation mediators in Nur77$^{-/-}$ microglia have been reversed.

Conclusions: Nur77 protects against ischemic brain injury by promoting M2 polarization, which probably be mediated by DOCK2-dependent pathway.

PS03-053

Poster Viewing Session III

Proteomic analysis of HDAC3 selective inhibitor in the regulation of inflammatory response of primary microglia

M. Zhang[1], M. Xia[2], Q. Zhao[1] and Y. Xu[3]

[1]Nanjing Drum Tower Hospital of Nanjing University, Nanjing, China

[2]Nanjing Drum Tower Hospital of Nanjing Medical University, Nanjing, China

[3]Nanjing University, Nanjing, China

Abstract

Histone deacetylases (HDACs) regulate acetylation states of histone and non-histone proteins and could be a potential regulator of inflammatory process. However, individual subtypes of HDACs remain largely unknown. RGFP966 is a newly discovered selective HDAC3 inhibitor. In this study, we aimed to profile molecular alternations in LPS-treated primary microglia with the application of RGFP966. We used protein mass spectrometry to analyze protein discrepancies in LPS group and LPS+RGFP966 group. RT-PCR and western blot were involved to detect mRNA and protein level of Toll like receptor 2 (TLR2), TLR3, TLR6, CD36, spleen tyrosine kinase (SYK). Supernatant tumor necrosis factor (TNF)-α, Interleukin 6 (IL-6) of various time points were collected and detected by CBA kit. We also stained microglia with CD16 in different groups by immunofluorescence to observe microglia activation. Phosphorylation and total level of STAT3 and STAT5 were measured by western blotting. Generally, about 2000 proteins were studied. 168 of 444 (37.8%) LPS-induced proteins were significantly reduced with the treatment of RGFP966, which mainly concentrated on Toll-like receptor signaling pathway. In this regard, we selected TLR2, TLR3, TLR6, CD36 and SYK for further validation, and found that they were all significantly up-regulated after LPS stimulation and down-regulated in the presence of

RGFP966. Additionally, RGFP966 inhibited supernatant TNF-α, IL-6 concentrations. Activation of STAT3, STAT5 was partially blocked by RGFP966 at 2 h post LPS-stimulation. The fluorescence intensity of CD16/32 was significantly decreased in LPS-treated group. In conclusion, our data provided a hint that RGFP966 may be a potential therapeutic medication combating microglia activation and inflammatory response in central nervous system, which was probably related to its repressive impacts on TLR signaling pathways and STAT3/STAT5 pathways.

PS03-053a

Poster Viewing Session III

The neuroprotective compound P7C3-A20 improves behavioral and histopathological outcomes after transient focal cerebral ischemia in rats

Z.B. Loris[1], A.A. Pieper[2] and W.D. Dietrich[3]

[1]University of Miami, Neurology, Miami, United States
[2]University of Iowa, Psychiatry, Neurology, and Free Radical and Radiation Biology Program, Iowa City, United States
[3]University of Miami Miller School of Medicine, Neurology, Miami, United States

Abstract

Objectives: Ischemic stroke is a devastating condition with few therapeutic interventions available. The neuroprotective compound P7C3-A20 inhibits mature neuronal apoptosis while increasing the net magnitude of postnatal neurogenesis in models of neurodegeneration and acute injury. The effectiveness of P7C3-A20 treatment on chronic histopathological and behavioral outcomes and neurogenesis after ischemic stroke has not been established.

Methods: Here, a transient middle cerebral artery occlusion in rats was followed in a randomized fashion by immediate injection of P7C3-A20 or vehicle which then continued for 7 days. The therapeutic window was also investigated by treating animals immediately or 6hrs after reperfusion. Blinded behavioral and histopathological assessments were conducted both acutely and chronically over 6 weeks.

Results: Immediate P7C3-A20 (iA20) treated rats performed significantly better than vehicle-treated controls in sensorimotor cylinder (A; $p < 0.001$) and grid-walk tasks at 7 days post injury (dpi), and in a chronic test (28 dpi) of spatial learning and memory ($p < 0.05$). These behavioral improvements with iA20 treatment were associated with significantly decreased cortical (B; $p < 0.05$) and hippocampal ($p < 0.05$) atrophy, as well as increased neurogenesis in the hippocampal dentate gyrus subgranular zone (C; $p < 0.05$) and subventricular zone (D; $p < 0.01$) and . Delayed P7C3-A20 (dA20) treated animals also performed significantly better on both the cylinder ($p < 0.01$) and grid-walk (E; $p < 0.05$) task. On the final day of learning and memory testing, dA20 rats performed significantly better than vehicle treated animals on the water maze task ($p < 0.05$).

Conclusions: Our current findings indicate that P7C3-A20 treatment mitigates neurodegeneration and augments repair in the brain after focal ischemia, which translates into chronic behavioral improvement. This suggests a new therapeutic approach of using P7C3 compounds to safely treat stroke patients.

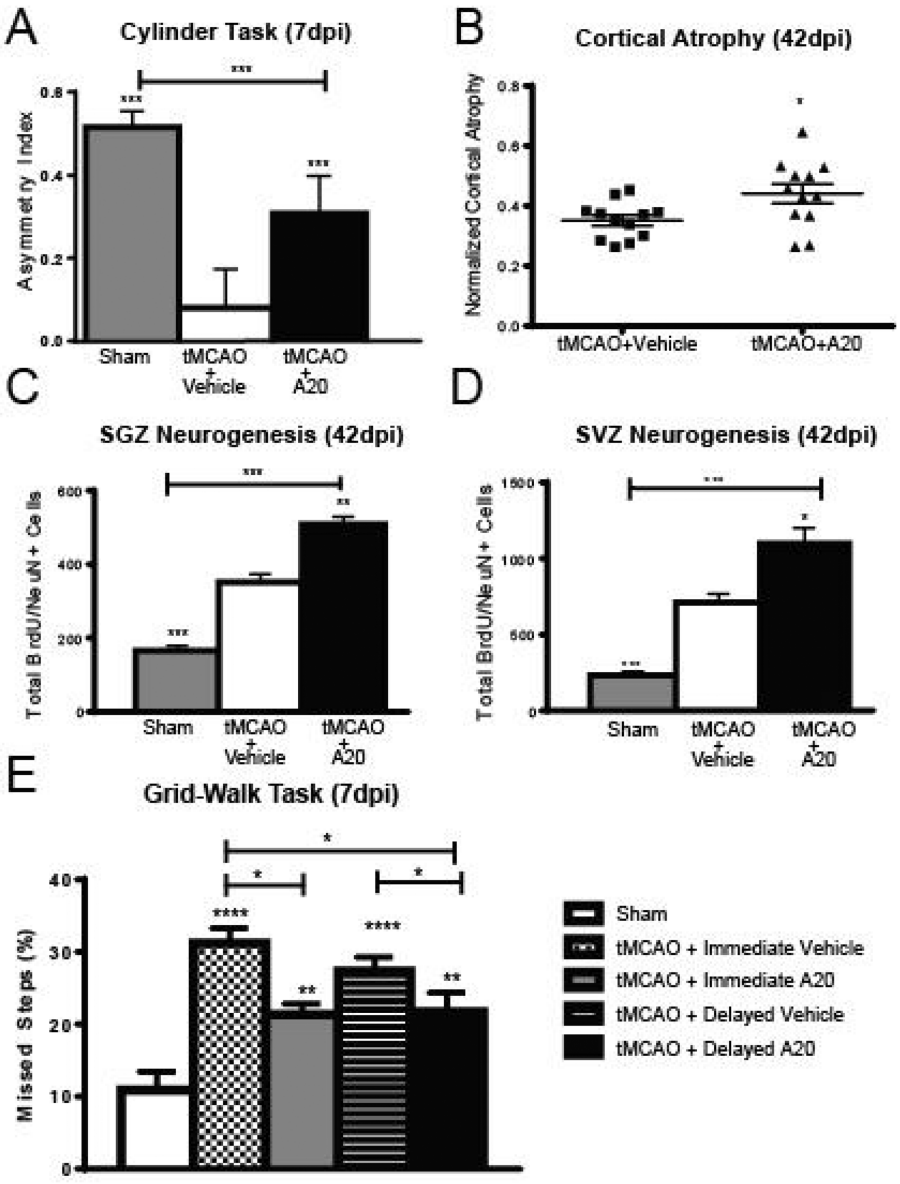
A
Cylinder Task (7dpi)
Asymmetry Index
Sham
tMCAO + Vehicle
tMCAO + A20
B
Cortical Atrophy (42dpi)
Normalized Cortical Atrophy
tMCAO+Vehicle
tMCAO+A20
C
SGZ Neurogenesis (42dpi)
Total BrdU/NeuN+ Cells
D
SVZ Neurogenesis (42dpi)
E
Grid-Walk Task (7dpi)
Missed Steps (%)
Sham
tMCAO + Immediate Vehicle
tMCAO + Immediate A20
tMCAO + Delayed Vehicle
tMCAO + Delayed A20

PS03-054

Poster Viewing Session III

Hemorrhagic transformation in rodents: different models, similar mechanism?

Y. Zheng[1], Y. Liu[1,2], K. Yigitkanli[1,3], H. Karatas[1,4], J.E. Jung[1], J. Carr[5], O. Bruns[5], M. Bawendi[5] and K. van Leyen[1]

[1]Massachusetts General Hospital & Harvard Medical School, Radiology & Neurology, Charlestown, United States
[2]The Second Affiliated Hospital of Harbin Medical University, Neurology, Harbin, China
[3]Polatli Government Hospital, Neurosurgery, Ankara, Turkey
[4]Hacettepe University, Institute of Neurological Sciences and Psychiatry, Ankara, Turkey
[5]Massachusetts Institute of Technology, Chemistry, Cambridge, United States

Abstract

Objectives: Neurovascular failure leading to increased hemorrhage is a major complication of ischemic stroke. Perhaps best known as a major side effect of thrombolytic therapy with tissue plasminogen activator (tPA), hemorrhagic transformation (HT) also occurs frequently in severe strokes, and in stroke patients on oral anticoagulants. Focusing on 12/15-lipoxygenase (12/15-LOX), we investigated the hypothesis that key mediators of neurovascular injury are common to different triggers.

Methods: Ischemia was induced in mice using a filament 24h after warfarin exposure, or through thrombosis by ferric chloride. tPA was infused 3h after onset of ischemia, with or without 12/15-LOX inhibitor. Hemoglobin was determined photometrically in brain homogenates, and by measuring hemorrhage areas in brain sections. 12/15-LOX expression oxidized lipids were detected by immunohistochemistry. Early hemorrhage was detected by intravenous injection of fluorescent quantum nanodots and whole body infrared imaging. Brain endothelial cells were grown on transwell filters and subjected to oxygen/glucose deprivation.

Results: 12/15-LOX was increased in all HT models. Warfarin pretreatment resulted in reproducible anticoagulation and significant HT, which occurred early after reperfusion following 3h MCAO. Lipoxygenase inhibition protected against HT even after normalization to infarct size, and 12/15-LOX knockout mice suffered less HT than wild-type mice. HT following tPA was similarly reduced by 12/15-LOX inhibition. Endothelial cell barrier function was protected against OGD by lipoxygenase inhibition.

Conclusions: Despite different triggers – in the presence or absence of anticoagulant, with or without tPA treatment – 12/15-LOX is activated in all models of HT studied. In addition to its benefits in infarct size reduction, 12/15-LOX inhibition may independently reduce HT by protecting the vasculature.

References

1. Yigitkanli et al., Inhibition of 12/15-lipoxygenase as therapeutic strategy to treat stroke. Ann Neurol. 2013 Jan;73(1):129–35.
2. Franke et al., Continuous Injection Synthesis of Indium Arsenide Quantum Dots for Short-Wavelength Infrared Imaging. Nature Commun. in Press

PS03-055

Poster Viewing Session III

Endothelial TRPV1 channels modulate cerebral blood flow during reperfusion phase following ischemic stroke

S.-H. Hong[1] and S. Marrelli[1]

[1]Baylor College of Medicine, Anesthesiology, Houston, United States

Abstract

The transient receptor potential vanilloid 1 (TRPV1) channel is a non-specific cation channel that possesses high conductance for Ca^{2+}. The channel is activated by heat ($>43^{\circ}C$), protons, certain metabolites of arachidonic acid, and exogenously-derived capsaicinoids – such as capsaicin (CAP) and dihydrocapsaicin (DHC). Recent studies have further demonstrated that oxidative stress can modify the channel and significantly potentiate the responsiveness to capsaicinoid agonists. The role of TRPV1 in the brain vasculature and control of cerebral blood flow (CBF) is largely undefined. We hypothesized that the *TRPV1 channel is expressed in cerebrovascular endothelium and contributes to endothelial-mediated vasodilation and increased CBF, particularly in the reperfusion phase following ischemic stroke*.

Experiments were performed with male WT and TRPV1 KO mice of a C57BL/6 background in accordance with BCM IACUC approved protocols. Functional expression of TRPV1 was demonstrated in the cerebral microvasculature by immunofluorescence and endothelial whole cell patch clamp. Isolated pressurized cerebral arteries were used to evaluate CAP-mediated vasodilation. CAP (10–

30 μM) application produced weak transient vasodilation. However, after brief intraluminal treatment with H_2O_2 (modeling oxidative stress), CAP produced significantly potentiated and prolonged vasodilation. This vasodilation was abolished by endothelial denudation. Laser speckle and laser Doppler were used to evaluate cerebral perfusion following stroke. Following stroke (60 min MCAO), cerebral perfusion in WT mice was marked by an initial hyperemia, followed by a transient hypoperfusion period (~30% reduction). In TRPV1 KO mice, the hyperemia was absent and the delayed hypoperfusion was more severe (>60% reduction) and prolonged (>2 hrs). Using a closed cranial window preparation, pial arteriolar diameter in TRPV1 KO mice exhibited vasoconstriction (compared to WT) during ischemia and the reperfusion period.
Together, these data demonstrate the presence and functional role of TRPV1 channels in promoting vasodilation and increased cerebral perfusion, particularly in environments of oxidative stress or stroke.

PS03-057

Poster Viewing Session III

Simulating arteriolar smooth muscle mediated cerebral blood flow regulation and oxygenation in response to optogenetic activation and ischaemia

P. Sweeney[1], R. Hill[2], J. Grutzendler[2], S. Walker-Samuel[3] and R. Shipley[1]

[1]*University College London, Mechanical Engineering, London, United Kingdom*
[2]*Yale University, School of Medicine, Department of Neurology, New Haven, United States*
[3]*University College London, Centre for Advanced Biomedical Imaging, London, United Kingdom*

Abstract

The manner in which blood vessels tightly regulate cerebral blood flow remains controversial. Pericyte covered capillaries have been reported to control cerebral blood flow and constrict capillaries in response to transient ischaemia. However, a recent study indicates that cerebral pericytes lack contractile properties *in vivo* and it is in fact arteriolar covered smooth muscle which have the functionality to mediate vasomotion within the cortex[1].
Genetically encoded microvascular mural cell labelling of the protein α-SMA, is used to identify the locations of vascular smooth muscle within mouse cortical microvasculature whilst simultaneously measuring diameter and velocity changes in individual blood vessels *in vivo*. These data parametrise a discrete-network model which simulates Poiseuille flow through individual vessels whereby network-dependent boundary conditions are assigned to meet target physiological parameters[2]. Data on mural cell locations enables us to model perfusion changes in response to network-wide or single-cell vasomotion, enabling us to gain further insight than *in vivo* experiments in isolation. This novel approach provides insight into mural cell contribution to network-wide perfusion which may not be obtain *in vivo*. This method is also applied to model cerebral ischaemia using an oxygen transport model which incorporates oxygen-bound erythrocytes, dissolved within blood plasma, diffusion through the tissue and uptake by the cellular population[3]. Quantitative predictions have been made around tissue oxygen distributions during health and disease, informing mural cell contribution to hypoxia as a result of the "no-reflow" phenomenon.

References

1. Hill, RA et al. 2015, 'Regional Blood Flow in the Normal and Ischemic Brain Is Controlled by Arteriolar Smooth Muscle Cell Contractility and Not by Capillary Pericytes', Neuron 87(1), 95–110.
2. Fry, BC et al. 2012, 'Estimation of Blood Flow Rates in Large Microvascular Networks', Microcirculation 19, 530–538.
3. Secomb, TW et al. 2004, 'Green's Function Methods for Analysis of Oxygen Delivery to Tissue by Microvascular Networks', Annals of biomedical engineering 32(11), 1519–1529.

PS03-058

Poster Viewing Session III

Omega-3 fatty acid supplement prevents progression of Intracranial Atherosclerosis (ICAS)

X. Geng[1], J. Shen[2], J. Stevenson[2] and Y. Ding[2]

[1]*Capital Medical University, Neurology, Beijing, China*
[2]*Wayne State University, Neurosurgery, Detroit, United States*

Abstract

ICAS is a disease state that has been implicated as a leading cause of recurrent ischemic stroke. Popular media has

promoted the use of omega-3 fatty acid (OFA) supplementation for its purported health benefits. We adapted a rat model for atherosclerosis and applied it to brain for the first time to investigate whether OFA attenuated ICAS development.

Adult male Sprague-Dawly rats were divided into control normal- or high-cholesterol diet groups with or without O3FA for up to 6 weeks. During the first 2 weeks, NG-nitro-L-arginine methyl ester (L-NAME, 3mg/mL) was added to the drinking water of the high-cholesterol groups. The rats received O3FA (5mg/kg/day) by gavage. Blood lipids including low density lipoprotein (LDL), cholesterol (CHO), triglycerides (TG) and high density lipoprotein (HDL) were measured at 3 and 6 weeks. The lumen of middle cerebral artery (MCA) and the thickness of the vessel wall were assessed histologically. Inflammatory molecules were assessed by Western blot.

High-cholesterol diet exhibited significant increase in the classic blood markers (LDL, CHO and TG), and decrease in HDL, which became more severe in time. Increased lumen stenosis and intimal thickening were observed in MCA. O3FA significantly attenuated blood lipids with an absence of morphological changes, the inflammatory marker CD68 in MCA, and prevented monocyte chemotactic protein (MCP-1) and interferon-γ (IFN-γ) expression. O3FA decreased Inducible nitric oxide synthase (iNOS), tumor necrosis factor alpha (TNF- α), and Interleukin 6 (IL-6), markers affiliated with monocyte activity in atherosclerosis. O3FA inhibited vascular cell adhesion molecule-1(VCAM-1), a marker for endothelial activation. O3FA increased ATP-binding cassette transporter A1 (ABCA1) protein expression via silent information regulator 1 (SIRT1) activation, thus increasing cholesterol efflux from macrophages to HDL.

O3FA prevents the development of ICAS. This appears to be mediated by its prevention of macrophage infiltration into the vessel wall, therefore reducing inflammation and intimal thickening.

PS03-059

Poster Viewing Session III

A novel mouse model of cerebellar stroke with motor and non-motor deficit

M. Moreno-Garcia[1], C. Mehos[1], M. Kubesh[1], R. Schmidt[2] and N. Quillinan[1]

[1]*University of Colorado, Denver, Anesthesiology, Aurora, United States*

[2]*University of Colorado, Denver, Cell and Developmental Biology, Aurora, United States*

Abstract

Objective: Each year in the U.S. there are an estimated 20,000 strokes resulting in cerebellar infarction. The neurological impairments observed in these patients include motor coordination and motor learning impairments. Surprisingly, cerebellar stroke patients also exhibit executive and emotional dysfunction. Establishing a model of cerebellar stroke that recapitulates aspects of human cerebellar infarction will allow for us to perform mechanistic studies of brain injury and identify therapeutic targets to improve recovery in stroke patients. The goal of this study was to develop and characterize a photo-thrombotic mouse model of focal cerebellar stroke.

Methods: Adult male and female mice were head-fixed in a stereotaxic frame, were administered Rose Bengal (150 ug/g) and the superior cerebellar artery was illuminated for 15 minutes with a cold white LED light source. Behavioral testing of motor and memory function was performed in mice subjected to sham procedure or photo-thrombosis at 7 days following surgery. Stereological analysis of lesion volume was performed at 1 and 7 days after surgery.

Results: Cerebellar stroke volumes were larger at 1 day ($1.92 \pm 0.42\,mm^3$) than 7 days ($1.034 \pm 0.30\,mm^3$), likely due to edema at the earlier time point. Lesion volumes were similar between males and females at both time points. Increased blood brain barrier permeability at 1 day (ovalbumin leakage) and glial reactivity (microglia and astrocyte) at 7 days were observed in the infarct region. Cerebellar infarction resulted in sensorimotor complications, observed as gait abnormality, motor coordination deficits and ipsilateral limb impairments. Spatial memory impairments (contextual fear conditioning) were also present at 7 days after cerebellar stroke. Thus, we have developed a reproducible model of cerebellar stroke that

results in cerebellar infarction and associated motor impairments. This will be a valuable tool for understanding how alterations in the cerebellar network resulting from cerebellar infarction produce motor and non-motor deficits.

PS03-060

Poster Viewing Session III

A "Crowdsourced' method to incorporate variability in experimental stroke to better mimic the biology and diversity of human stroke

T.A. Kent[1], H.C. Rea[1], W. Dalmeida[1], R.H. Fabian[1], C. Ayata[2] and P. Mandava[1]
[1]*Baylor College of Medicine, Neurology, Houston, United States*
[2]*Harvard Medical School, Neurology, Boston, United States*

Abstract
Objectives: Failures to translate pre-clinical results have resulted in efforts to improve their relevance and validity. Less attention has been paid to data analysis. We have contended that stroke is too heterogeneous for standard statistical methodologies to adjust for biological and methodological variance, while efforts to improve biological homogeneity renders results less applicable to humans. Here, we report an approach we developed to capture clinical variability adapted to experimental stroke, incorporating baseline variability and generating statistical thresholds so that treatment effects can be screened against a broader population.
Methods: Using transient MCA occlusion in 32 unfasted rats, we created variability by varying occlusion times from 90–120 min and driving glucose with streptozotocin. Bederson Score was assessed 3 days later (BS; 0–6 functional measure, 7 death). Statistical surfaces were generated flanking the model to provide a screening threshold (±1 SD) for comparing therapies against this model.
Results: These 2 factors explained 70% of outcome variance ($r^2 = .49$, $p = .0003$; middle surface is the function surrounded by ± 1 SD surfaces). Outcome was sensitive to change in glucose and time, suggesting small imbalances in these factors between treatment groups or labs may influence the perceived efficacy of a new therapeutic. Lower surface at normoglycemia and 90 minutes occlusion approached no deficit, indicating any finding of benefit under these conditions would be difficult to replicate.

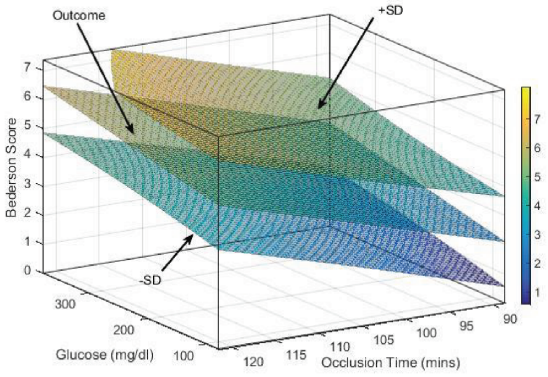

Conclusions: We demonstrated the feasibility of a single lab to incorporate biological variability in controls. We have asked other labs to contribute additional variables, such as stroke severity and other occlusion models to ultimately develop a generalized "crowdsourced" method to screen for therapies worthy of further study.

Reference

Kent TA, Shah SD, Mandava P. Improving early clinical trial phase identification of promising therapeutics. Neurology 2015;85:274–283.

PS03-061

Poster Viewing Session III

Aged and sex influence the neutrophil response after ischemic stroke in mice and humans

M. Roy-O'Reilly[1], J. Bravo Alegria[1], H. Ahnstedt[1], M. Spychala[1] and L. McCullough[1]
[1]*University of Texas Health Science Center, Houston, United States*

Abstract
Background: Ischemic stroke is a leading cause of mortality worldwide. Importantly, age and sex have important effects on stroke outcome. Infiltration of neutrophils into the brain after stroke worsens tissue damage and impairs recovery. We tested the hypothesis that there are sex differences in neutrophil function and neutrophil-mediated damage after ischemic stroke.
Methods: Blood was obtained from stroke patients 24 hours after stroke onset. Absolute neutrophil count was quantified ($n = 604$), with RNA sequencing of whole blood performed on a small subset of age and severity matched

patients (n = 24). Results were analyzed by multivariate regression analysis or differential expression analysis with correction for multiple comparisons (RNA-sequencing). For animal experiments, aged (18–20 month) and young (8–10 week) old male and female mice were subjected to 60-minute middle cerebral artery occlusion and sacrificed at 24 hours, with mice undergoing surgery without occlusion serving as "sham" control. Neutrophils from blood, bone marrow, lung, brain and spleen were identified by flow cytometry.

Results: Neutrophil counts from human patients revealed that neutrophils account significantly 24 hours after stroke in both male and female patients (n = .01). Interestingly, female stroke patients had more differentially expressed genes after stroke than males, including matrix metalloprotease 9 (MMP9) and TNFa, two genes associated with detrimental neutrophil functions. In animal experiments, aged animals were found to be more neutrophilic 24 hours after stroke than young animals. In addition, aged females a more activated neutrophil phenotype 24 hours after stroke than aged males ($p = < 0.05$).

Conclusion: These results suggest that the immune response to ischemic stroke differs with age and sex. Understanding the influence of aging and sex on the acute inflammatory response is crucial to developing future immunomodulatory drugs for the safe and effective treatment of ischemic stroke in both sexes.

PS03-062

Poster Viewing Session III

Increased infarction and hemorrhagic transformation in aged apontaneous hypertensive rats: role of collateral CBF

S.L. Chan[1] and M.J. Cipolla[1,2]

[1]*University of Vermont, Neurological Sciences, Burlington, United States*

[2]*University of Vermont, Pharmacology, Burlington, United States*

Abstract

Objectives: Collateral perfusion is an important predictor of stroke outcome. Both hypertension and aging negatively impact collateral status that may promote greater infarction and hemorrhagic transformation (HT). We hypothesized that compared to young spontaneously hypertensive rats (~18 weeks; SHR-young; n = 12), aged SHR (~50 weeks; SHR-aged; n = 8), would have poor collateral status during ischemia that is associated with incomplete reperfusion, greater infarction and increased incidence of HT.

Methods: Collateral openings (number, duration (min), magnitude (area under the curve)) were identified from dual laser Doppler and blood pressure tracings during 2 hours proximal middle cerebral artery occlusion (MCAO). Probe 1 (core MCA) was placed +4mm lateral of midline and −2mm posterior of Bregma and probe 2 (collateral) was placed +3mm lateral of midline and +2mm anterior of Bregma. Collateral openings were defined as increases in probe 2 CBF independent of changes in blood pressure. Infarct volume was determined by 2,3,5-Triphenyltetrazolium chloride (TTC) and edema by ipsilateral vs. contralateral hemisphere area. HT was assessed by pink coloration within the infarct area.

Results: CBF reduction from baseline during ischemia was similar between groups that was sustained during 2 hours (-84 ± 3 vs. $-81 \pm 3\%$; $p > 0.05$). There was no difference between SHR-young vs. SHR-aged in collateral number (0.5 ± 0.3 vs. 1.3 ± 0.4; $p > 0.05$), duration (4.5 ± 2.8 vs. 7.4 ± 3.2 min; $p > 0.05$) or magnitude (8.0 ± 6.3 vs. 7.3 ± 3.9 AUx1000; $p > 0.05$). Reperfusion CBF was incomplete and below baseline in both groups of SHR (-42 ± 7 vs. $-45 \pm 7\%$ at 90 min reperfusion; $p > 0.05$). Infarct volume was significantly increased in SHR-aged vs. SHR-young (48.9 ± 2.6 vs. $30.3 \pm 2.2\%$; $p < 0.05$). Edema was similar between groups (9.5 ± 1.0 vs. $11.9 \pm 2.1\%$; $p > 0.05$). HT was only observed in SHR-aged (4 of 8) and not SHR-young (0 of 12).

Conclusions: Aging in the setting of hypertension worsened infarct and increased the incidence of HT that was unrelated to collateral openings and reperfusion CBF that was poor in both groups of SHR.

PS03-063

Poster Viewing Session III

Degeneration of muscles supplied by the external carotid artery in the intraluminal filament mouse model of middle cerebral artery occlusion

M. Vaas[1], R. Ni[1], M. Rudin[1,2], A. Kipar[3] and J. Klohs[1]

[1]University of Zurich & ETH, Institute for Biomedical Engineering, Zürich, Switzerland
[2]University of Zurich, Institute of Pharmacology and Toxicology, Zürich, Switzerland
[3]University of Zurich, Institute of Veterinary Pathology, Zürich, Switzerland

Abstract

Objectives: Transient or permanent middle cerebral artery occlusion (MCAO) in mice is the most common form of focal cerebral ischemia, to study pathophysiological mechanisms and interventions. In the surgical procedure the external carotid artery (ECA) is ligated, and restricts the blood flow to the ECA territory. Yet the consequences for the underlying musculature including chewing and swallowing have not been described. Therefore, we studied the effects of restricted blood flow in the ECA territory with multi-spectral optoacoustic tomography (MSOT) on the oxygenation and long-term pathophysiological changes with magnetic resonance imaging (MRI) and histology on the temporal muscle.

Methods: C57BL/6 mice underwent 1h of transient MCAO (tMCAO) or sham surgery with ligation of the ECA. MSOT was employed at 30min after surgery to assess acute changes in tissue oxygenation in the temporal muscles. Time-of-flight angiograms were acquired to examine blood flow in large arteries and in T_2 maps region-of-interest were drawn over the temporal muscles to observe microstructural changes after 24h and 48h. Histology of the whole mouse head was used to assess pathological changes in the entire ECA territory.

Results: Ligation of the ECA resulted in an acute decrease in tissue oxygenation in the left temporal muscle in around 70% of sham and tMCAO animals, while time-of-flight angiogram showed an arrest of the blood flow in the ECA. Susceptible mice of both groups exhibited increased T_2-relaxation times at 24 and 48h in the affected muscle with similar values. Histopathology revealed myofibre degeneration and interstitial edema in the temporal muscle and other tissues underlying the ligated ECA. Also the histopathological changes correspond to increased T_2-relaxation times, whereas the contralateral side was unaltered.

Conclusions: ECA ligation leads to degenerative changes in the muscles of the ECA territory, while a potential impact on outcome needs to be considered in this stroke model.

PS03-064

Poster Viewing Session III

Substrain and sex differences in infarct size after permanent focal ischemia in C57BL/6 mice

L. Zhao[1], M.K. Mulligan[2] and T.S. Nowak[1]

[1]University of Tennessee Health Science Center, Department of Neurology, Memphis, United States
[2]University of Tennessee Health Science Center, Department of Genetics, Genomics and Informatics, Memphis, United States

Abstract

Objectives: The C57BL/6 (B6) mouse strain is widely used in experimental stroke. Commonly available B6J and B6N substrains have been separately maintained since 1951 and differ in a number of phenotypes and at thousands of genetic loci (1). Importantly, the B6N line provides the background strain for the Knockout Mouse Project. This study examined the impact of substrain and sex on stroke vulnerability.

Methods: Male and female mice of B6 substrains ($n = 118$) were obtained from commercial vendors (J, NJ and NCrl) or in-house breeding colonies (J, ByJ, NJ) maintained <5 generations from original Jackson Laboratory stock. Focal ischemia was produced by tandem permanent occlusion of the right middle cerebral artery and ipsilateral common carotid artery under isoflurane anesthesia. Estrous status was assessed in females using vaginal washes collected during occlusion surgery. Infarct size at 24 hours was determined by triphenyltetrazolium staining.

Results: Infarct volumes ($mm^3 \pm SD$) in male and female mice were: J: 12.2 ± 3.9, 10.1 ± 7.4; ByJ: 13.7 ± 3.2, 7.2 ± 5.6; NCrl: 19.1 ± 2.6, 18.1 ± 5.5; NJ: 21.5 ± 4.7, 18.8 ± 8.4. Infarcts were comparable in J and ByJ, and in NJ and NCrl, but these pairs of strains differed significantly from each other (Kruskal-Wallis and Dunn's Multiple Comparison tests). Mean infarct size was comparable for

male and female mice but females showed markedly greater variability (Figure), which was independent of the estrous cycle (not shown).

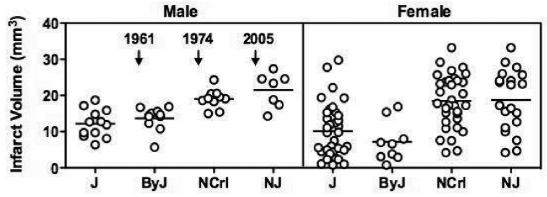

[Substrain and sex differences]

Conclusions: C57BL/6N mice exhibit two-fold larger infarcts than C57BL/6J, establishing the critical importance of control strain selection in experimental stroke. Since the ByJ, Crl and NJ substrains were split from the N lineage in 1961, 1974 and 2005, respectively, the responsible mutation(s) appeared between 1961 and 1974 (Figure). Female variability presents an under-appreciated practical challenge in designing adequately powered studies.

References

(1) Simon et al., Genome Biology 14:R82 (2013)

PS03-066

Poster Viewing Session III

cGMP-dependent protein kinase I in smooth muscle cells improves cerebral reperfusion and stroke outcome

D. Atochin[1], T. Suzuki[2], M. Litvak[3], E. Buys[4], S. Wong[1], N. Kurlyandchik[1], D. Fukumura[5], J. Roberts Jr[1,4], C. Ayata[2], R. Feil[6] and P.L. Huang[1]

[1]Harvard Medical School, Department of Medicine, Division of Cardiology, Cardiovascular Research Center, Massachusetts General Hospital, Charlestown, United States

[2]Massachusetts General Hospital, Department of Radiology, Neurovascular Research Laboratory, Charlestown, United States

[3]Tomsk Polytechnic University, RASA Center, Tomsk, Russian Federation

[4]Massachusetts General Hospital, Department of Anesthesia, Critical Care, and Pain Medicine, Anesthesia Center for Critical Care Research, Boston, United States

[5]Massachusetts General Hospital, Department of Radiation Oncology, Edwin L. Steele Laboratory, Boston, United States

[6]University of Tübingen, Interfaculty Institute of Biochemistry, Tübingen, Germany

Abstract

Objective: Although cGMP-dependent protein kinase I (cGKI) is a key mediator of cGMP signaling in vascular smooth muscle cells (SMC), its role in mediating the protective effect of nitric oxide (NO) during stroke is unknown. Accordingly, we tested the hypothesis that vascular SMC cGKI has a protective role in maintaining cerebrovascular reperfusion during stroke injury.

Animals: We utilized tamoxifen-inducible SMC-specific cGKI knockout mice (cGKI KO), which express CreERT2 recombinase under control of the smooth muscle alpha-actin promoter. Littermate mice (no Cre gene) receiving the same tamoxifen treatment were used as control (cGKI WT) mice.

Methods and Results: A specific COOH-terminal cGKI antibody and immunohistochemistry revealed specific ablation of cerebrovascular SMC cGKI protein expression in the cGKI KO but not sGKI WT mice.

Stroke experiments, conducted under 30% oxygen/70% nitrous oxide/1.5% isoflurane anesthesia, using 30 minutes of middle cerebral artery filament-mediated occlusion (MCAO) and 47 hours of reperfusion, revealed greater cerebral infarct volume (TTC staining, indirect calculation) in cGKI KO ($75 \pm 10\,mm^3$, Mean $\pm$ SD) than in cGKI WT (50 ± 12) mice ($n = 5$/group, $p < 0.05$). Neurological deficit (5 point severity scale) was more pronounced in cGKI KO (2.5 points) than in cGKI WT (1.7 points) mice.

High spatial resolution cerebral laser speckle flowmetry was then employed during distal MCAO to test whether regional cerebral blood flow (CBF) differences correlated with stroke outcome.

Although intraischemic core CBF did not differ among groups, after 5 minutes of reperfusion, the CBF was greater in cGKI WT ($58 \pm 23\%$) and C57black6 (WT) mice ($67 \pm 22\%$) than in cGKI KO mice ($40 \pm 20\%$, $n = 8$–9/group, $p < 0.05$, Two-way Anova, Newman-Keuls multiple comparison test).

In conclusion, these studies suggest that cGKI plays a protective role in regulating CBF during reperfusion and improving stroke outcome. These results suggest that cGKI and downstream pathways should be targeted in studies designed to protect brain tissue during stroke.

PS03-067

Poster Viewing Session III

Inadequate food and water intake determine mortality following severe stroke in mice

A. Lourbopoulos[1], U. Mamrak[1], J. Shrouder[1], S. Roth[1], M. Balbi[1], A. Liesz[1], F. Hellal[1] and N. Plesnila[1]
[1]Institute for Stroke and Dementia Research, Munich, Germany

Abstract
Objectives: Long-term mouse stroke studies with the clinically relevant 60 minute filament MCA occlusion (fMCAo) are biased due to high mortality-driven exclusion of animals with large strokes. We aim to overcome this mortality-bias without ameliorating stroke outcomes.
Methods: We adapted principles from human post-stroke care (feeding/fluid support: mouse post-stroke care protocol, mPSC) to the 60′ fMCAo model (bedside-to-bench approach). We subjected C57Bl/6 mice (8–10 weeks old, $n = 88$) to fMCAo, we supported them from day 2 onwards with the mPSC or standard laboratory practices (control), and followed them for 14 days (randomized, blinded study). We evaluated mortality, body weight/temperature, neurological/behavioural deficits, food/water consumption (% from baseline), infarct volume, brain atrophy, post-stroke immune depression (blood) and pneumonia (lung bacterial rtPCR). We verified our approach with a 2-month long-term study ($n = 46$ mice). Data are reported as mean ± s.e.
Results: The mPSC reduced mortality from 59% (control) to 15% ($p = 0.001$). Bias was removed by mPSC because the majority of animals with large infarcts survived. Thus, infarct volumes and cortical atrophy at day 14 (% of the contralateral hemisphere) were found double in mPSC vs control group ($32 \pm 4\%$ vs. $16 \pm 4\%$ and $-20 \pm 3\%$ vs. $-10 \pm 2\%$, respectively, $p < 0.05$). Removal of bias revealed significant post-ischemic body weight loss, hypothermia and immune depression, all as inherent model characteristics unaffected by mPSC. The mPSC prevented mortality by counterbalancing the preceding -on day 3- reduced food ($-39 \pm 13\%$ vs. $-70 \pm 7\%$) and water ($-41 \pm 10\%$ vs. $-87 \pm 5\%$) consumption of controls (for mPSC vs. control respectively, $p < 0.05$). Pneumonia was ruled out as cause of mortality (negative lung rtPCR for bacteria). Evidently, our long-term (2 months) study verified the primary mPSC results.
Conclusion: Mortality in the 60' fMCAo model is caused by reduced food and water intake, which is successfully counterbalanced by the mPSC. The mPSC allows for unbiased, translational, cost-effective, large-stroke, long-term studies in mice.

PS03-068

Poster Viewing Session III

The effect of 20-HETE inhibition by HET0016 on the cerebral microvascular circulation after asphyxial cardiac arrest in pediatric rats

L. Li[1], S. Poloyac[1], S. Waltkins[2], C. St Croix[2], H. Alexander[3], G. Gibson[2], P. Loughran[4], R. Clark[3,5,6], P. Kochanek[3,5,6], L. Kirisci[1], A. Vazquez[7] and M. Manole[3,5,6]
[1]University of Pittsburgh, School of Pharmacy, Pittsburgh, United States
[2]University of Pittsburgh, Center for Biologic Imaging, Pittsburgh, United States
[3]University of Pittsburgh, Safar Center for Resuscitation Research, Pittsburgh, United States
[4]University of Pittsburgh, Pittsburgh, United States
[5]University of Pittsburgh, Department of Critical Care Medicine, Pittsburgh, United States
[6]University of Pittsburgh, Department of Pediatrics, Pittsburgh, United States
[7]University of Pittsburgh, Department of Radiology, Pittsburgh, United States

Abstract
Objectives: Previously cerebral blood flow disturbances, especially cortical hypoperfusion and hypoxia has been observed in animals post cardiac arrest (CA). No-reflow phenomenon and increased mean transit time (MTT) were also found post-CA. We propose to evaluate the effect of 20-HETE inhibition on the cerebral microvasculature and microvascular blood flow in a clinical relevant pediatric CA rat model.
Methods: Postnatal 17 day old rats underwent tracheal intubation, arterial and venous cannulation, and were equipped with a cranial window. Asphyxial CA of 12 min was induced by cessation of mechanical ventilation after neuromuscular blockade. Rats were resuscitated with chest compressions, epinephrine, sodium bicarbonate and HET0016 (or vehicle). We utilized in vivo multiphoton

microscopy to measure microvascular diameter change, no-reflow capillary branches and mean transit time (MTT) at baseline and post-CA at 5, 30, and 60 minutes post-resuscitation.
Results: Pial arterioles were significant dilated in HET0016 group at 5 min post-CA compared with vehicle ($n = 6$/group, $p = 0.043$). Venules were dilated at 5min post-CA but were not affected by HET0016 treatment. No-reflow phenomenon was observed in both groups (29% in HET0016 compared with 21% in vehicle group). MTT significantly increased post-CA at 30 and 60min ($128.7 \pm 11.7\%$ and $162.7 \pm 21.0\%$, $p = 0.004$) regardless of HET0016 treatment ($153.1 \pm 19.2\%$ and $146.8 \pm 17.6\%$).
Conclusions: HET0016 treatment can dilate pial arterioles early post-CA in pediatric rats without effect on no-reflow phenomenon and capillary mean transit time. These data suggests that inhibition of 20-HETE can prevent arteriolar constriction early post-CA which could be beneficial in mitigating cortical hypoperfusion and hypoxia post-CA.

Reference

Manole, M.D., et al., Magnetic resonance imaging assessment of regional cerebral blood flow after asphyxial cardiac arrest in immature rats. J Cereb Blood Flow Metab, 2009. 29(1): p. 197–205.

PS03-069

Poster Viewing Session III

Validation of noninvasive measurements of cerebral blood flow and oxygenation in a pediatric swine model of cardiac arrest and cardiopulmonary resuscitation

T. Ko[1,2], C. Mavroudis[3], T. Boorady[2], K. Mensah-Brown[2], R. Morgan[4], A. Lautz[4], M. Karlsson[4], G. Bratinov[4], R. Berg[4], A. Yodh[5], R. Sutton[4], D. Licht[2] and T. Kilbaugh[4]

[1]University of Pennsylvania, Bioengineering, Philadelphia, United States
[2]Children's Hospital of Philadelphia, Neurology, Philadelphia, United States
[3]Children's Hospital of Philadelphia, Cardiothoracic Surgery, Philadelphia, United States
[4]Children's Hospital of Philadelphia, Anesthesiology and Critical Care Medicine, Philadelphia, United States
[5]University of Pennsylvania, Physics and Astronomy, Philadelphia, United States

Abstract

Objective: Pediatric in-hospital cardiac arrest (p-IHCA) is a predominantly respiratory-mediated cardiac arrest and affects thousands of children each year in the United States. Half of these children will not survive to discharge after such an event, and most survivors have significant neurological injury. The lack of standardized neuromonitoring during resuscitation has precluded the use of cerebral diagnostics to guide CPR and optimize neurological outcomes. The purpose of this study is to validate a novel, noninvasive method of assessing cerebral blood flow and oxygenation against invasive methods in a swine model of p-IHCA.
Methods: One-month old female swine ($n = 7$) underwent a simulated respiratory-induced cardiac arrest with randomization to one of three different CPR strategies: conventional depth-guided chest compressions, compressions targeting a systolic aortic blood pressure (BP) of 90mmHg, or targeting a BP of 110mmHg. Invasive cerebral blood flow (CBF; Bowman Perfusion Monitor, Hemedex, Cambridge, MA, USA), invasive cerebral oxygen content ($PbtO_2$, Licox, Integra, Plainsboro NJ, USA) and noninvasive near-infrared diffuse correlation spectroscopy (DCS)

and frequency-domain diffuse optical spectroscopy (FD-DOS; Imagent, ISS Inc., Champaign, IL) were used to monitor cerebral hemodynamics. A Pearson correlation coefficient was calculated between non-invasive DCS measurements of blood flow index (BFI) and invasive Bowman CBF measurements.

Results: Invasive measures of CBF and non-invasive measures of BFI exhibited significant correlation ($R^2 = 0.789$, $p < 0.001$). BFI may be used to approximate absolute CBF using the relationship: CBF (ml/100 g/min) = $0.010 \times$ BFI (10^{-8} cm^2/s). Non-invasive optical measurements of relative CBF and blood volume showed discriminant trends across CPR strategies.

Conclusions: These results are an important feasibility study for use of non-invasive diffuse optical measurements of cerebral blood flow and oxygenation to optimize CPR strategies and provide real-time guidance of CPR administration in high-risk children. Further studies are needed to translate this potentially paradigm-shifting technology into the clinical realm.

PS03-070

Poster Viewing Session III

Physical exercise promotes cognitive recovery after cardiac arrest in Sprague-Dawley rats

H. Stradecki-Cohan[1], C. Cohan[1], M. Youbi[1], E. Perez[1] and M. Perez-Pinzon[1]

[1]University of Miami Miller School of Medicine, Neurology, Miami, United States

Abstract

Objectives: Half a million people experience a cardiac arrest in the US annually and 50% of the survivors endure long term cognitive deficits. Physical exercise can reduce cognitive deficits after cerebral ischemia by augmenting plasticity and this is thought to be most beneficial when initiated early[1]. The ability of exercise to restore cognition after cardiac arrest has not been examined. The goal of this study was to examine cognitive recovery in rats subject to cardiac arrest after subacute treadmill exercise at different speeds.

Methods: Experimental timeline is depicted below (**A**). Male Sprague-Dawley rats were acclimated to treadmill walking then underwent cardiac arrest or sham surgery and allowed to recover for 3 full days. Rats were randomized to exercise at 0, 6, 10, or 15 meters/minute for 30 minutes daily over the next 5 days. Cognition was tested with the Barnes Circular Platform Maze (BCPM, 9–17 days post-surgery) then contextual fear conditioning (18–19 days post-surgery).

Results: After cardiac arrest, rats exercised at 10 or 15 m/min used a random search strategy on the BCPM less often than cardiac arrest rats exercised at 0 or 6 m/min (**B**; χ^2, $p = 0.0011$). The cardiac arrest groups exercised at 10 or 15 m/min also had enhanced contextual fear memory as compared to the 0 or 6 m/min exercised groups (**C**; 1 Way ANOVA, $p = 0.0230$, $n = 4$–8/group; $^*p < 0.05$, Bonferroni's Multiple Comparison test).

Conclusions: These results suggest that a 5 day, subacute bout of treadmill exercise at 10 or 15 meters/minute after cardiac arrest can result in lasting enhancement of cognition in Sprague-Dawley rats.

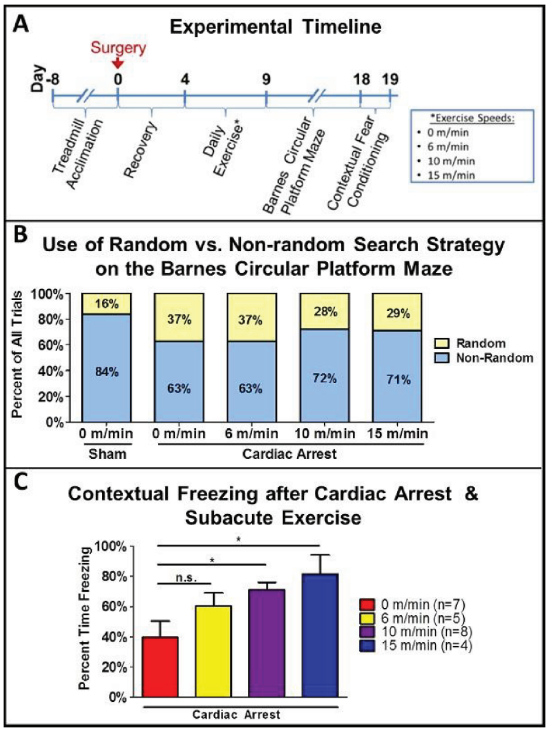

[behavior w/o electrophys]

Reference

1. Schmidt *et al.* (2014) *Stroke* (1)239–247

Funding:

1. American Heart Association Predoctoral Fellowship 15PRE2236000 (PI: Stradecki-Cohan)
2. American Heart Association/ASA-Bugher Foundation 14BFSC17690007 (PI: Sacco)
3. NIH/NINDS R01 NS45676-08 (PI: Perez-Pinzon)

PS03-071

Poster Viewing Session III

Perfusion-related changes in the temporal dynamics of the blood-oxygen-level-dependent signal in a mouse model of focal cerebral ischemia

A. Khalil[1,2,3], S. Mueller[2,4], M. Foddis[2], U. Dirnagl[2], J. Fiebach[1], A. Villringer[3,5] and P. Boehm-Sturm[2,4]

[1]*Charité – Universitätsmedizin Berlin, Center for Stroke Research Berlin, Berlin, Germany*
[2]*Charité – Universitätsmedizin Berlin, Department of Experimental Neurology, Berlin, Germany*
[3]*Max Planck Institute for Human Cognitive and Brain Sciences, Department of Neurology, Leipzig, Germany*
[4]*Charité – Universitätsmedizin Berlin, Charité Core Facility 7T Experimental MRIs, Berlin, Germany*
[5]*Berlin School of Mind & Brain, Berlin, Germany*

Abstract

Objectives: Delayed blood-oxygen-level-dependent (BOLD) signal oscillations reflect low blood flow and provide a non-invasive measure of perfusion in cerebrovascular diseases (1). We identified and characterized BOLD signal delay in a mouse model of stroke.

Methods: C57/BL6 mice underwent 90-minute middle cerebral artery occlusion (MCAO) (2). Anesthesia was induced with 2.5% isoflurane and adjusted to maintain normal physiological parameters (1–1.25%). Using a 7T Bruker BioSpec scanner and a cryogenically cooled RF coil, a single-slice echo planar imaging (EPI) sequence (repetition time = 0.1 s, echo time = 20 ms, flip angle = 20, voxel size $0.15 \times 0.15 \times 1$ mm, 3400 timepoints) was acquired during MCAO. Several temporal bandpass filters were applied to assess the contribution of different physiological processes to BOLD delay (see Figure 1). Each voxel's time series was cross-correlated with that of the venous sinus (1) to produce maps of time shift at maximum correlation (BOLD delay).

Results: A temporal delay in low frequency oscillations relative to the venous sinus was seen in ischemic tissue but not in healthy tissue. High correlations between the time courses in the ischemic tissue and venous sinus were found in the low frequency range (0.01 to 0.1 Hz), accompanied by temporal delays in the ischemic hemisphere's BOLD signal. This was not present at higher frequency bands (see figure).

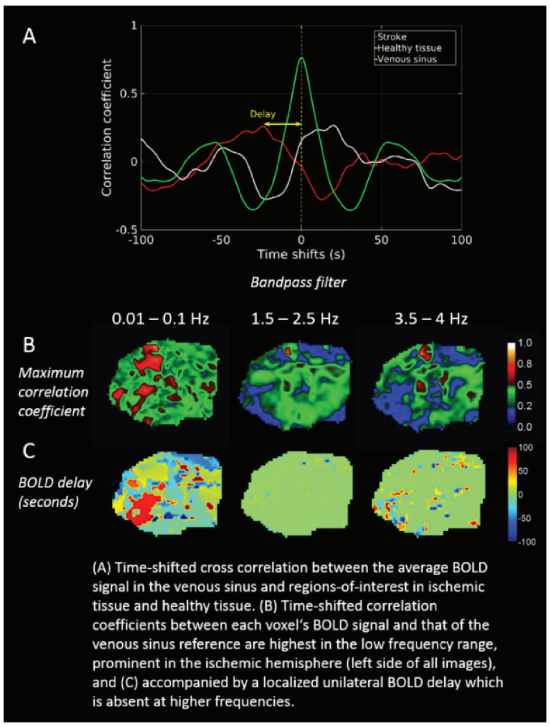

Conclusions: Temporal delays in BOLD signal in ischemic tissue are driven by low frequency oscillations and not directly by the cardiac and respiratory cycles. Variations in heart and breathing rates, which produce oscillations in the low frequency range, are the likely cause of these delays (3).

References

[1] Lv et al, Ann Neurol, 2013
[2] Engel et al, J Vis Exp, 2011
[3] Tong and Frederick, Front Hum Neurosci, 2014

PS03-072

Poster Viewing Session III

Connection between paravascular spaces and the cerebrospinal fluid compartment in the rat brain

B. Bedussi[1], N.N. van der Wel[2], J. de Vos[1], H. van Veen[2], M. Siebes[1], E. VanBavel[1] and E.N.T.P. Bakker[1]

[1]Academic Medical Center (AMC), Biomedical Engineering and Physics, Amsterdam, Netherlands
[2]Academic Medical Center (AMC), Electron Microscopy Centre Amsterdam, Department of Cell Biology and Histology, Amsterdam, Netherlands

Abstract

The clearance of waste and potentially toxic compounds such as amyloid beta is important for preservation of brain health and cognitive functions. As the brain parenchyma lacks a proper lymphatic system, the removal of fluid and solutes takes place via different paths. One of these pathways involves specific transporters at the blood-brain barrier. In addition to this, bulk flow of extracellular fluids as a clearance mechanism recently received more attention. However, the anatomical base and physiological mechanisms of bulk fluid transport are under debate. Thus, in the present study we investigated the anatomical relations between cerebrospinal fluid compartments, brain vasculature, and paravascular spaces in male Wistar Kyoto rats. To reveal the CSF compartment and its connections, we infused a fluorescent tracer in the cisterna magna. We then analyzed tracer distribution using a 3D imaging cryomicrotome, confocal microscopy, and correlative light and electron microscopy (CLEM). In the 3D reconstruction we found a strong co-localization of tracer and the major vessels in the subarachnoid space (SAS) and cerebral cisterns. This result was confirmed by confocal imaging. Confocal imaging also revealed a novel cisternal connection between the ventricular system and the SAS. The CLEM technique indicated that in the parenchyma, the tracer is confined outside of the endothelial layer in capillaries and just outside of the smooth muscle cells in arteries. To conclude, the SAS, cisterns, ventricles, and para-arteriolar spaces all together form a continuous CSF compartment. This compartment deeply penetrates the brain, allowing for exchange with interstitial fluid.

PS03-073

Poster Viewing Session III

Clinical mapping of cerebrovascular reactivity using MRI: a framework for reaching consensus

M.G. Bright[1], E.L. Mazerolle[2], O. Sobczyk[3], A.P. Fan[4], M.J.P. van Osch[5], C.I. Mark[6], L. Huber[7], A.J.L. Berman[2,8], D.P. Bulte[9], B.G. Pike[2], C.J. Gauthier[10] and N.P. Blockley[11]

[1]University of Nottingham, Sir Peter Mansfield Imaging Centre, School of Medicine, Nottingham, United Kingdom
[2]University of Calgary, Hotchkiss Brain Institute, Department of Radiology, Calgary, Canada
[3]University of Toronto, Institute of Medical Science, Toronto, Canada
[4]Stanford University, Radiological Sciences Laboratory, Stanford, United States
[5]Leiden University Medical Center, C.J. Gorter Center for High Field MRI, Radiology, Leiden, Netherlands
[6]Queen's University, Centre for Neuroscience Studies, Kingston, Canada
[7]National Institutes of Health, Section on Functional Imaging Methods, National Institute for Mental Health, Bethesda, United States
[8]McGill University, Montreal Neurological Institute, Montreal, Canada
[9]University of Oxford, Institute of Biomedical Engineering, Oxford, United Kingdom
[10]Concordia University, PERFORM Centre, Montreal, Canada
[11]University of Oxford, FMRIB Centre, Nuffield Department of Clinical Neurosciences, Oxford, United Kingdom

Abstract

Objectives: Cerebrovascular reactivity (CVR) mapping using a CO_2 stimulus assesses the ability of cerebral vessels to satisfy the demand for an increase in cerebral blood flow. In recent years the number of clinical CVR exams has greatly increased[1]. However, so far the application of CVR mapping across the world has been variable[2] due to a lack of standardisation[3]. Here we identify a process by which convergence and interoperability may be attained, enabling more widespread adoption of CVR in the clinic.

Methods: To build consensus across the field, we established the Imaging Cerebral Physiology Network, now consisting of 100 members representing 10 countries. An open-ended questionnaire was circulated to

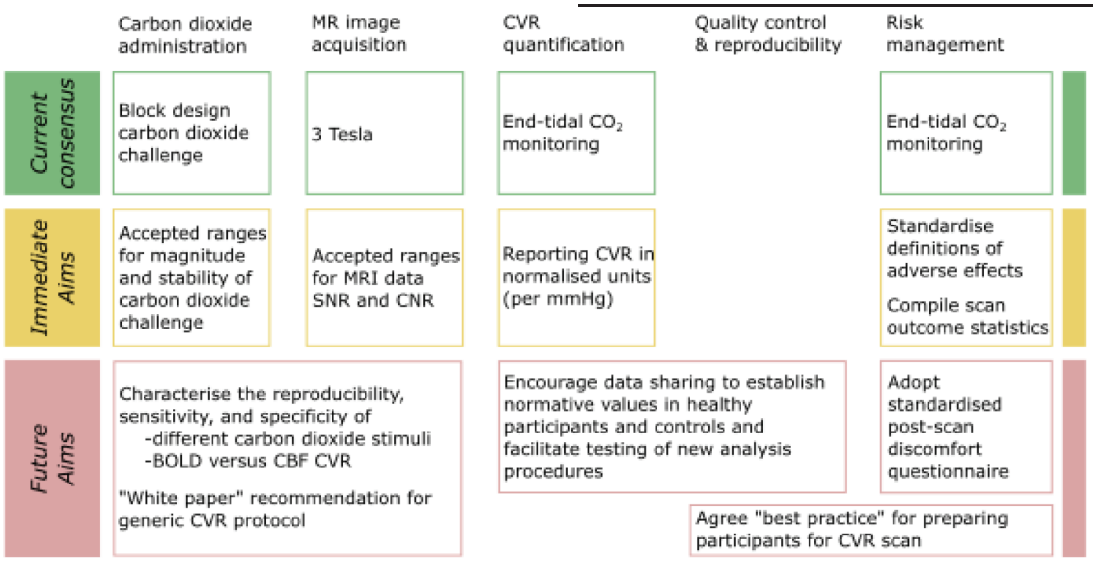

characterise current practice, pool experiences in ethics/safety, and identify areas where the network could build methodological consensus. Taking inspiration from the Quantitative Imaging Biomarkers Alliance and Uniform Protocol for Imaging in Clinical Trials, we used the responses to frame a discussion of how consensus in CVR mapping may be reached within the following areas:

- The clinical motivation for CVR
- Carbon dioxide administration
- MR imaging procedure
- CVR quantification
- Quality control and reproducibility
- Risk management

Results: Responses were received from researchers at 10 institutions. Some consensus already exists: all sites monitored end-tidal gas levels and utilized block-design hypercapnia paradigms, and 90% of sites focus on 3T scanning. However, understanding current variation in gas delivery equipment, MRI acquisition parameters, quantification of CVR, and participant safety/discomfort reporting facilitated the identification of immediate and long-term targets for future agreement (Figure).

Conclusions: We present a framework towards CVR consensus to initiate larger discussion amongst the community and accelerate the wider clinical adoption of CVR mapping.

References

1. Spano et.al. Radiology. 2012(266):592–598.
2. Blair et.al. JCBFM. 2016:1–9.
3. Moreton et.al. Neuroimage Clinical. 2016(11)667-677.

PS03-075

Poster Viewing Session III

Novel non-invasive method for monitoring intracranial pressure with diffusion correlation spectroscopy

K.C. Wu[1,2], J. Sutin[1], B. Zimmerman[1], P. Farzam[1], B. Fu[1], D. Boas[1] and M.A. Franceschini[1]

[1]Massachusetts General Hospital, Martinos Center for Biomedical Imaging, Charlestown, United States
[2]National Cheng Kung University, Institute of Biomedical Engineering, Tainan, Taiwan, Republic of China

Abstract

Monitoring of intracranial pressure (ICP) is essential for managing traumatic brain injury and other neurological conditions. ICP is measured invasively with insertion of a pressure sensor into the brain. Its invasiveness limits its use to monitoring only patients in critical conditions. The development of a non-invasive ICP monitoring method would allow extension of ICP diagnostics to more patients and avoid complications arising from an invasive procedure. The critical closing pressure (CrCP), the arterial blood pressure (ABP) at which cerebral blood flow (CBF) approaches zero, has been proposed as a surrogate measure of ICP. CrCP is currently estimated with transcranial Doppler ultrasound (TCD) measurements of pulsatile

CBF velocity in large, intracranial arteries. However, the accuracy of TCD-measured CrCP has been insufficient for clinical acceptance. We propose to use diffuse correlation spectroscopy (DCS) to measure pulsatile CBF in small cortical vessels and, from that, to monitor CrCP and ICP. Traditionally, DCS has rather low temporal resolution. In order to derive pulsatile blood flow, we developed a fast DCS device based on a custom FPGA-based photon counting board. In addition, to maintain SNR despite the fast acquisition rate, we developed a new algorithm that gates the photon arrivals with the ABP signal and allows us to resolve 400 points along an arterial pulse by overlapping measurements from 50 pulses.

To demonstrate our method, we performed measurements on 10 rats. ABP and ICP were measured invasively with a commercial fiber-optic pressure sensor. Pulsatile CBF was measured transcranially with our DCS system. In each animal we performed CO_2 and hyperoxia challenges, increasing ICP with subdural saline infusions. We found good correlation between the invasive ICP and the non-invasive DCS based CrCP measures.

We believe that this novel approach has the potential to be translated into the first clinically viable non-invasive ICP monitoring method.

PS03-076

Poster Viewing Session III

New pattern of cerebral autoregulation in response to intrathoracic pressure changes

Z. Zhang[1,2], N. Bolz[1], M. Laures[1], C. Schmidt[1], M. Oremek[1], M. Qi[1] and R. Khatami[1]

[1]*Clinic Barmelweid, Barmelweid, Switzerland*
[2]*University Bern, Bern, Switzerland*

Abstract

Cerebral autoregulation (CA) is vital to maintain appropriate cerebral perfusion and oxygenation despite changes of systemic influences including blood pressure and intrathoracic pressure (ITP). However, the responses of CA to different directions and degrees of ITP changes are still less well-known.

Using advanced frequency-domain multi-distance near-infrared spectroscopy (FDMD- NIRS) and echocardiography, we measured changes in cerebral and muscular hemodynamics, and cardiac hemodynamics in 11 healthy people in five respiratory maneuvers (breath holding, moderate and strong Valsalva maneuvers with +15 mmHg and +30 mmHg increments in ITP, and moderate and strong Mueller maneuvers with −15 mmHg and −30 mmHg decrements in ITP) controlled by esophageal manometry.

We found cerebral blood volume (CBV) maintains relative constant during the strains indicating intact CA, and it increases during the recovery period in every respiratory maneuver associated with increased oxygen supply. By contrast changes in muscular blood volume (MBV) are mainly dominated by systemic changes. Our results suggest a new pattern of CA, i.e., cerebral perfusion commonly increases following various ITP strains.

We propose local brain mechanisms allowing to increase cerebral oxygen supply independent of changes in systematic hemodynamics and ITP. These local cerebral hemodynamic changes may represent active overcompensation of cerebral oxygen supply induced by local neuronal activities or facilitate the washout of the accumulated brain metabolites during the strains driven by the restored inspiration. To increase cerebral perfusion by changing ITP may have clinical implications in cardiovascular diseases like stroke and hypertension in the future. Our results also suggest FDMD-NIRS is a useful tool in assessing dynamic CA.

PS03-077

Poster Viewing Session III

A diffuse optical method and a compact device for measuring cerebral blood flow in adult human brain

J. Hollmann[1], T. Dragojević[1], D. Tamborini[2], D. Portaluppi[3], M. Buttafava[3], F. Zappa[3], J. Culver[4] and T. Durduran[1,5]

[1]*ICFO – The Institute of Photonic Sciences, Castelldefels, Spain*
[2]*Harvard University Massachusetts General Hospital, Boston, United States*
[3]*Politenico di Milano, Milano, Italy*
[4]*Washington University in St Louis, St Louis, United States*
[5]*Institució Catalana de Recerca i Estudis Avançats (ICREA), Castelldefels, Spain*

Abstract

Objectives: We introduce a novel and compact diffuse optical method [1] and a device for monitoring cerebral blood flow (CBF) non-invasively. The device uses a 64 element single-photon avalanche photo diode (SPAD) array to quantify speckle statistics using a combination of SCOS and single-shot multiple exposure speckle contrast (sMESI) measurements. The device then processes the data in real-time using a field programmable gate array (FPGA) and returns the speckle contrast.

Methods: The device, shown in Figure 1a, is mounted in a standard 1 inch optical tube (Thorlabs) with cooling vents machined along the side. A camera objective matches the speckle to the detector active-area. The source, a 785 nm laser, is coupled to the skin using an optical fiber optic at a source-detector distance of 2 cm. The system is mounted on subjects' heads using a custom-made holder. Subjects were asked hold their breath for 30 s followed by two minutes of recovery. This challenge was repeated three times on three healthy subjects (2 males, 1 female, 24 to 36) and compared to diffuse correlation spectroscopy (DCS).

Results: Figure 1b demonstrates the average CBF response over three subjects as measured by the device. The error bars represent the standard-error-of-the-mean across the subjects. This is in agreement with previously reported results [2]. We will present statistical results and findings from more subjects and different challenges.

Conclusions: We have introduced a novel method and a compact device for measuring cerebral blood flow in adult human brain.

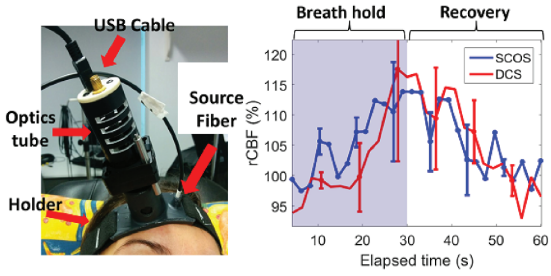

Figure 1 (a) Device shown on a subject's head (b) Resulting change in the cerebral blood flow due to a breath hold challenge for three subjects.

References

1. Valdes C., et.al., BOE (2014).
2. Rodgers, ZB, et.al., JCBFM (2013).

PS03-078

Poster Viewing Session III

Mapping extracellular pH of gliomas in presence of superparamagnetic nanoparticles

S. Maritim[1], D. Coman[2], Y. Huang[2], J. Rao[2], J. Walsh[1] and F. Hyder[1,2]

[1]*Yale University, Biomedical Engineering, New Haven, United States*
[2]*Yale School of Medicine, Radiology & Biomedical Imaging, New Haven, United States*

Abstract

Objectives: Brain's microvasculature is disrupted in several pathologies, including cancer. Breakthroughs in glioma imaging and therapy exploit the fact that nanoparticles enter the interstitial space by extravasation. Thus co-injection of tumor-targeted nanoparticles containing drugs (D-NPs) and superparamagnetic iron oxide nanoparticles (SPIO-NPs) can enable safe delivery of chemotherapy to the tumor (via D-NPs) and imaging of drug biodistribution (via SPIO-NPs). However, molecular readout beyond the generated contrast is inhibited by the large magnetic field gradients created by SPIO-NPs. Because

lower extracellular pH (pHe) is a hallmark of cancer pathogenesis that promotes invasion and resistance to therapy, a particular need exists for non-invasive methods to report on tumor pHe quantitatively.

Methods: We measured brain pH_e in 9L and RG2 glioma-bearing rats at 9.4 T before and after SPIO infusion with biosensor imaging of redundant deviation in shifts (BIRDS), which utilizes paramagnetically-shifted resonances of non-exchangeable protons on shift agents (e.g., $TmDOTP^{5-}$). Since proton relaxation is significantly enhanced by pseudo-contact interactions with unpaired electrons of Tm^{3+}, we hypothesized that BIRDS-based pH_e readout from $TmDOTP^{5-}$ remains uncompromised by the presence of SPIO-NPs.

Results: While superior MRI contrast of the tumor core was revealed upon SPIO-NPs in 9L and RG2 gliomas, the pH_e measured in absence and presence SPIO-NPs were very similar. Acidic pHe was restricted to the tumor-core in 9L but spreads beyond tumor boundary in RG2 tumors

Conclusions: We envisage co-injection of $TmDOTP^{5-}$ and nanoparticles, containing drugs and SPIO, as a new protocol that can track delivery of therapeutic agents to tumors, concurrently map tumor location and size (by MRI), and at the same time measure changes in tumor pH_e in response to therapy (by BIRDS).

References

1. Coman, D et. al., *NMR Biomed* (2016).
2. Maritim, S et. al., *J Biol Inorg Chem* (2014).

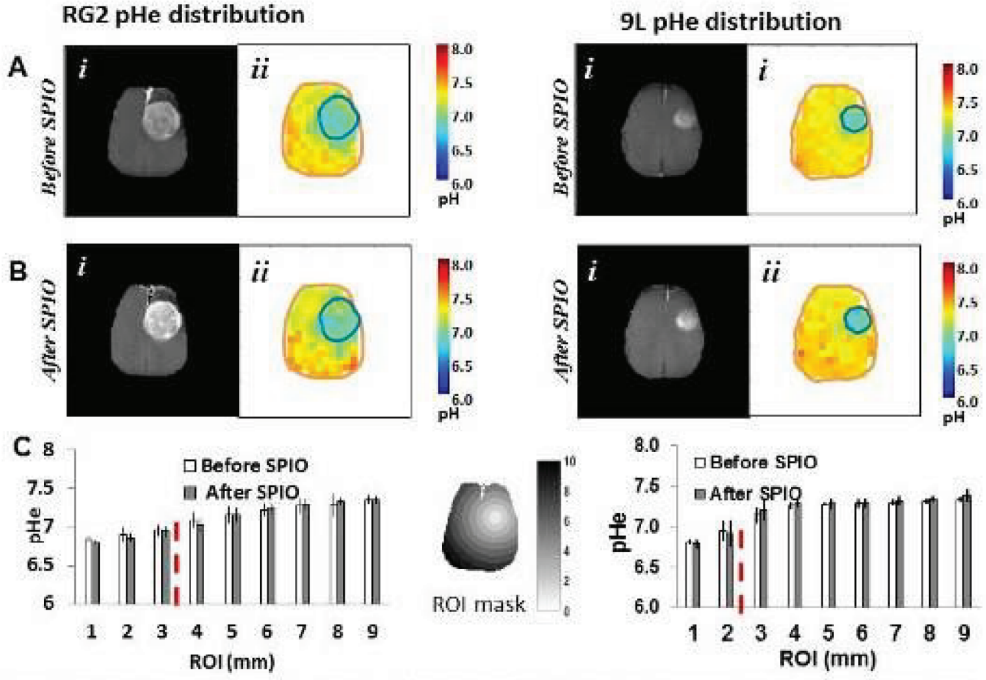

Structural and pHe maps of RG2 and 9L glioma-bearing rat brains obtained by BIRDS at 9.4 T using $TmDOTP^{5-}$ before (A) and after (B) infusion of superparamagnetic iron oxide, SPIO. The regional pHe distribution measured as a function of the distance from the center of mass of the tumor (C) were similar before and after infusion of SPIO. Acidification of pHe was restricted to within the tumor core (red line) in the non-aggressive 9L tumors but spread beyond the tumor boundary in the aggressive RG2 tumors

PS03-079

Poster Viewing Session III

Atlas registration to assess edema-corrected MRI lesion volume in experimental stroke

S. Koch[1,2], S. Mueller[1,2], M. Foddis[1,2], T. Bienert[3], D. von Elverfeldt[3], F. Knab[1], T.D. Farr[1,4], R. Bernard[1], U. Dirnagl[1], C. Harms[1] and P. Boehm-Sturm[1,2]

[1]Charité University Medicine Berlin, Department of Experimental Neurology, Center for Stroke Research and NeuroCure, Berlin, Germany
[2]Charité University Medicine Berlin, Charité Core Facility 7T Experimental MRIs, Berlin, Germany
[3]University Medical Center Freiburg, Department of Radiology, Medical Physics and BrainLinks-BrainTools Excellence Cluster, Freiburg, Germany
[4]University of Nottingham, School of Life Sciences, Nottingham, United Kingdom

Abstract

Introduction: MRI lesion size is an important readout in experimental stroke studies. However, vasogenic edema leads to an overestimation of lesion volume and dislocation of brain structures. A manual lesion correction (MLC) [1] assumes homogenous tissue compression outside the lesion and requires full-brain MRI. This has widely been neglected. Since atlas registration (AR) can more finely assess volume changes voxel-wise, we compared AR to MLC in a mouse stroke model.

Methods: T2-weighted MR images of C57/Black6 mice were acquired at 7T 24h after 45 min middle cerebral artery occlusion (MCAO n = 17, sham n = 17). For AR, images and lesion/hemisphere masks were registered to the Allen atlas [2] by in-house scripts based on SPMMouse and ELASTIX. The capacity of AR to correct for edema was assessed by comparison to MLC and reduction of hemispheric volume differences. Volume changes encapsulated in AR transformation were mapped voxel-wise.

Results: Significant part of lesion volume was due to swelling (MLC: 30 ± 14%, AR: 28 ± 7%) and lesion volumes correlated well between methods (r = 0.976,p = 2.265e-11). Hemispheric volume differences due to swelling were removed after AR (before: 3.74% ± 3.38%, after:0.65% ± 0.74%, T(16) = −4.39, p = 4.53e-4). For artificially generated non-full brain MRI, MLC overestimated lesion volumes up to 18% whereas AR values remained unchanged. Voxel-wise mapping of tissue volume changes visualized inhomogenous compression outside the lesion, the lateral ventricle acted as a buffer (Fig. 1).

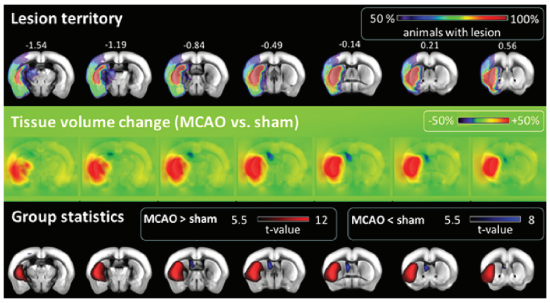

Fig.1: Lesion territory (top, 100% corresponds to n = 17), edema induced tissue volume changes (middle) and voxel-wise group t-test of these changes (bottom). Numbers above slices show distance from Bregma in mm.

Conclusions: MRI lesion volumes should be edema-corrected. Full-brain MRI coverage is required for MLC. AR outperforms MLC and can provide voxel-wise biomarkers of edema. These challenge simplified tissue models underlying MLC.

References

[1] Gerriets et al.;Stroke(2004);35: 566-571.
[2] Lein et al.;Nature(2007);445(7124):168–176.

PS03-080

Poster Viewing Session III

Cerebral assessment of pharmacological modulation of spinal $GABA_A$ receptor using Functional BOLD MRI in a rat model of postoperative pain

N. Just[1], D. Segelcke[2], C. Faber[1] and E. Pogatzki-Zahn[2]

[1]University of Münster, TRIC, Münster, Germany
[2]UKM, Klinik für Anästhesiologie, operative Intensivmedizin und Schmerztherapie, Münster, Germany

Abstract

Introduction: Recently, BOLD fMRI demonstrated its potential for the assessment of cerebral pain correlates and pain network in animal models[1]. Moreover, spinal GABAergic receptors were shown to mediate incisional

pain in rats. In the present study, BOLD fMRI was used to investigate the effects of $GABA_A$ modulation in the brain of rats during mechanical stimulation (MS).

Methods: SD rats (n = 15,180–250 g) underwent intrathecal (IT) catheterization. Three days later, their right hindpaw received a standardized incision. BOLD fMRI was conducted 24 hours later on a 9.4T scanner (Bruker) under medetomidine sedation. During MS of the right hindpaw EPI GRE were acquired (10 s ON-20 s OFF-paradigm, 10 minutes). Acquisitions were performed before and 60 minutes after IT injections of either Muscimol, Bicuculline or Saline (0.9%). After image preprocessing, first level analyses (SPM12) were performed followed by Group analysis (SPM12). Tvalue statistics were obtained with respective thresholds at $p < 0.01$.

Results: Upon MS, no significant difference between groups were found prior to injections. At 60 min after injection of Muscimol, the number of activated voxels was decreased compared to the Saline group (235 ± 114 vs. 898 ± 293 U-test $p < 0.05$). The number of deactivated voxels 60 min after Bicuculline injection was reduced (1058 ± 1122 vs 312 ± 225) while activated voxels increased (306 ± 269 vs 1114 ± 1278). MS induced activation of limbic regions (Insula, PFC) in Vehicle and Bicuculline groups. In the bicuculline group, somatosensory areas were positively activated (Thalamus and bilateral hindlimb regions) but also inhibitory areas such as the hypothalamus. In the Muscimol group, activity was reduced in limbic structures and somatosensory areas.An increased activity was detected in inhibitory structures (MnR, PAG).

Conclusion: The activation of spinal $GABA_A$-receptor in postoperative pain model reduced the cerebral activity after suprathreshold MS while inhibition of this receptor produced increased global brain activation, especially in limbic, sensory/discriminative and pain modulation regions.

Reference

1. Amirmohseni S. Neuroimage. 2016

PS03-081

Poster Viewing Session III

Ultra high-field cryocoil non-contrast-enhanced mouse brain DTI MRI: a novel method of image analysis and fibre tractography, and the effect of ageing on structural connectivity

R. Saggu[1] and G.C. Petzold[1]

[1]*German Center for Neurodegenerative Disease (DZNE), Bonn, Germany*

Abstract

Aims: To develop and optimise an *in vivo* mouse brain DTI MRI sequence using a cryogenic coil at ultra high-field (11.7T) such as to acquire high resolution diffusion tensor data in the shortest acquisition time possible. To develop and optimise a new method of analysing mouse brain DTI images to measure region-specific diffusivity parameters and generate fibre tractography objectively and accurately. To identify the consequences of ageing on diffusivity measures and fibre bundle connectivity.

Methods: A high-resolution DTI MRI sequence was developed and optimised for use with a transmit/receive ^1H surface cryocoil on an 11.7T horizontal small-bore magnet (Biospec 117/16, Bruker, Germany). 10-week-old and 14-month-old WT male C57BL/6J mice were imaged (n = 10 each group). A novel method of DTI MRI segmentation was developed for measuring DTI diffusivity parameters, which was used thereafter to generate fibre tractography and compare the different age groups.

Results: The novel objective method of DTI segmentation and analysis identified differences in DTI diffusivity measures in 14-month-old versus 10-week-old mice. Furthermore, fibre tractography identified age-related differences in the density of the fibres bundles between specific brain regions in young and old mice indicating a change in structural connectivity related to normal ageing.

Conclusions: Our high-resolution non-contrast-enhanced DTI MRI sequence and novel method of image analysis facilitate the noninvasive interrogation of mouse brain white and grey matter with unprecedented resolution, in vivo. Together, these methods have revealed differences in DTI diffusivity measures and fibre bundle connectivity related to normal ageing.

PS03-082

Poster Viewing Session III

Jugular vein collapse in upright and its relation to intracranial pressure regulation

P. Holmlund[1], E. Johansson[1], S. Qvarlander[1], A. Wåhlin[1], K. Ambarki[1], L.-O.D. Koskinen[1], J. Malm[1] and A. Eklund[1]
[1]*Umeå University, Umeå, Sweden*

Abstract

Objectives: The regulation of intracranial pressure (ICP) in the upright posture has recently been suggested to depend on hydrostatic effects in the venous system and the collapse of the internal jugular veins (IJVs) [1], but this regulatory mechanism is not fully understood. We evaluate a hypothesis of IJV collapse where balance of surrounding atmospheric pressure and internal venous pressure creates a zero pressure segment at neck level. This requires that hydrostatic effects are cancelled by the viscous losses in the collapsed segment, resulting in a predictable IJV cross-sectional area. The hypothesis was tested by comparing predicted area to measured IJV area in healthy.

Methods: Seventeen healthy volunteers (age 44 ± 9 years) were examined using ultrasound to assess IJV area, and 4D flow MRI to assess flow (used as input for the area prediction). Ultrasound measurements were performed for six upper body tilt angles, from supine to sitting (71°), and MRI scans were performed in supine and 16° tilt.

Results: Predicted and measured IJV area agreed well in sitting position, with small individual variation (predicted $6.4 \pm 2.2\,mm^2$ vs. measured $6.2 \pm 4.6\,mm^2$). Already at 24° agreement between measured and predicted area was seen for 48% of the IJVs, indicating IJV collapse. In sitting, agreement was seen for 94% of IJVs. Change in IJV area between supine and sitting was $93.0 \pm 50.9\,mm^2$ ($P < 0.01$).

Conclusions: The agreement between predicted and measured IJV area in sitting supports the hypothesis of a zero pressure segment in the neck, which is also supported by previous ICP observations [1]. This provides an explanation for how collapse of the IJVs could regulate cranial venous pressure and ICP in upright, which may improve our understanding of neurological diseases with suspected disturbances in the cerebrospinal fluid dynamics.

Reference

[1] Qvarlander et al. J Appl Physiol 115(10): 1474-1480.

PS03-083

Poster Viewing Session III

Noninvasive monitoring of critical closing pressure with near-infrared light

W.B. Baker[1], A.B. Parthasarathy[2], K.P. Gannon[3], V. Kavuri[2], D.R. Busch[4], M.T. Mullen[3], R. Balu[3], W.A. Kofke[1] and A.G. Yodh[2]
[1]*University of Pennsylvania, Anesthesiology and Critical Care, Philadelphia, United States*
[2]*University of Pennsylvania, Physics and Astronomy, Philadelphia, United States*
[3]*University of Pennsylvania, Neurology, Philadelphia, United States*
[4]*Children's Hospital of Philadelphia, Neurology, Philadelphia, United States*

Abstract

Objectives: We developed and validated a novel near-infrared optical technique for noninvasive, continuous measurement of the critical closing pressure (CrCP) of the cerebral circulation. CrCP is the arterial blood pressure (abp) at which cerebral blood flow approaches zero, and abp-CrCP is a noninvase proxy of cerebral perfusion pressure [1].

Methods: Diffuse correlation spectroscopy (DCS) employs near-infrared light to measure local, microvascular cerebral blood flow continuously at the bedside. DCS is noninvasive with deep tissue penetration (~1 cm) and excellent time resolution (20 Hz). We utilized DCS to measure pulsatile blood flow oscillations in cerebral arterioles in the prefrontal cortex for 5 minutes in 18 healthy adults. Simultaneously, middle cerebral artery flow velocity and abp in the finger were monitored noninvasively with transcranial Doppler ultrasound (TCD) and a Finapres, respectively. For each subject, we measured CrCP using two techniques, i.e., $CrCP_{TCD}$ and $CrCP_{DCS}$. $CrCP_{TCD}$ was obtained with Michel's method based on abp and flow velocity assessed with TCD [2]. $CrCP_{DCS}$ was calculated using DCS measurements of arteriole blood flow in place of the TCD data. We further measured $CrCP_{DCS}$ in two TBI patients.

Results: We found good agreement between the TCD and DCS measures of critical closing pressure ($R = 0.7$, slope $= 1.14 \pm 0.23$, mean difference $= -2 \pm 11$ mmHg).). The averages across healthy subjects are $CrCP_{DCS} = 11.1 \pm 5.0$ mmHg and $CrCP_{TCD} = 13.0 \pm 7.5$ mmHg

(mean ± SD). The $CrCP_{DCS}$ measurements in the two TBI subjects with normal ICP were 13.3 and 15.5 mmHg.
Conclusions: DCS is a novel technique for noninvasive, continuous monitoring of CrCP at the bedside. We validated it against TCD, and demonstrated its use in the neurocritical care environment. DCS probes are well-suited for continuous, long-term monitoring.

References

[1] Varsos GV, et al, *J Neurosurgery*. 2015; 123:638–48.
[2] Michel E, et al, *J Cereb Blood Flow Metab*. 1997; 17:1127–31.

PS03-084

Poster Viewing Session III

Experimental cerebral malaria: Mapping of Gd-DOTA leakage kinetics by MRI

T.-A. Perles-Barbacaru[1], E. Pecchi[1], M. Bernard[1], P. Cozzone[1] and A. Viola[1]
[1]*Aix Marseille University, CRMBM UMR 7339, Marseille, France*

Abstract

Increased permeability of the blood-brain barrier (BBB) has been suggested as one of the pathophysiological mechanisms in cerebral malaria (CM), an encephalopathy caused by Plasmodium infection. This study investigates whether quantification of endothelial permeability can be used as an early marker of disease progression.
Eight Plasmodium berghei ANKA infected (1) and two uninfected female C57BL/6J mice underwent dynamic magnetic resonance imaging (MRI) at 11.75T with intraperitoneal injection of 10 mmol/kg Gd-DOTA on up to 4 days using a quantitative technique designed for blood volume and permeability mapping (2). We quantified the spatial and temporal occurrence of endothelial permeability to Gd-DOTA and correlated it to general clinical and neurological signs during disease progression.
Infected mice progressed to experimental CM with overt neurological symptoms starting day 7 and reached the terminal stage at day 8–9 post infection. Abnormal permeability to Gd-DOTA appeared simultaneously with the first clinical signs and was quantitatively related to their severity. Spatial differences were observed with olfactive regions displaying the highest permeability and distribution volume fraction (DVf). The kinetics of Gd-DOTA accumulation in brain parenchyma was markedly different from those in high-grade tumors or extracerebral tissues such as muscle or skin (Figure 1).
This study reveals BBB impairment in experimental CM at an early stage of disease development and demonstrates quantitative differences in endothelial permeability to Gd-DOTA among brain regions as well as over time by following the same animals during disease progression. It also evokes a complex transport mechanism of Gd-DOTA across the BBB. This study might contribute to the understanding of the pathophysiological mechanism of CM.
Non-invasive quantitative mapping of the endothelial permeability by MRI can be used for follow-up and treatment monitoring in experimental CM.

Figure 2: Kinetics of Gd-DOTA accumulation

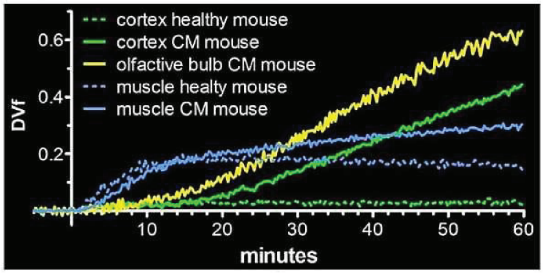

References

1. Penet et al. J Neurosci 2005; 25(32):7352–7358
2. Perles-Barbacaru et al. Magn Reson Med. 2015 Mar;73(3):1005–14

PS03-085

Poster Viewing Session III

Intraoperative assessment of cerebral blood flow changes in normal and pathological brain tissue, using an infrared camera

K. Kaczmarska[1,2], Ł. Przykaza[1], M. Zębala[3], T. Piątkowski[4], H. Polakowski[4], M. Kastek[4], J. Bogucki[1], Z. Czernicki[1,3], W. Koszewski[3] and E. Koźniewska[1,5]

[1]Mossakowski Medical Research Centre Polish Academy of Sciences, Department of Neurosurgery, Warsaw, Poland
[2]Warsaw University of Technology, Institute of Electronic Systems, Warsaw, Poland
[3]Medical University of Warsaw, Department of Neurosurgery, Warsaw, Poland
[4]Military University of Technology, Institute of Optoelectronics, Warsaw, Poland
[5]Medical University of Warsaw, Department of Experimental and Clinical Physiology, Warsaw, Poland

Abstract

The standard intraoperative monitoring of cortical blood flow which is essential for a successful surgery of cerebral pathology is still lacking. Present studies attempted to evaluate cerebrocortical microflow based on brain surface temperature recording using infrared thermography in patients with brain tumours, including those located in the vicinity of eloquent areas. The clinical application of this method was preceded by an experimental study of a correlation between microflow in the cerebral cortex and brain temperature.

The experiments were performed on 8 male, adult anaesthetized rats. After craniotomy the cerebrocortical microflow (LDF) was measured with a Laser-Doppler probe simultaneously with the registration of the thermal profile of the cortex with an infrared camera during baseline as well as during microflow increase (CO_2 inhalation) or short-lasting decrease (15 minutes occlusion/reperfusion of the middle cerebral artery). The same camera was used in the clinical study to measure temperature distribution in the cerebral cortex surface before, during, and after removal of a tumour in 16 patients. In six patients with tumours located close to the eloquent areas the temperature distribution was measured also during awake-part of surgical procedure.

A significant ($p < 0.01$) positive correlation was found between the LDF and brain temperature changes in rats. In patients, the temperature of the tumour was different from the temperature of the tissues adjacent to the resected pathology. The mean difference between the tumour and normal tissues temperatures was increasing during the tumour resection. In six patients subjected to the intraoperative awake procedure, the temperature increase in the activated motor cortex region during tumour removal was observed. The strong positive correlation between microflow and temperature of the cerebral cortex found in the preclinical study encourages the application of infrared thermography for non-invasive blood flow evaluation in patients during surgery.

PS03-086

Poster Viewing Session III

G-protein coupled receptor 39 expression and function in the microcirculation

N. Alkayed[1], Z. Cao[1], C. Davis[1], Z.Y. Qian[1], F. Xie[1], X. Liu[1], B. Li[2], D. Zeppenfeld[2], M. Grafe[2], J. Iliff[1], X. Xiao[2], A. Barnes[1] and S. Kaul[1]

[1]Knight Cardiovascular Institute, Portland, United States
[2]Oregon Health & Science University, Portland, United States

Abstract

Objectives: Epoxyeicosatrienoic (EETs) and hydroxyeicosatetraenoic acids (HETEs) are endogenous vasoactive P450 eicosanoids that play important roles in cerebrovascular physiology and disease, but their mechanisms of action are not fully understood (1,2). The current study was designed to investigate the molecular and cellular mechanisms of action of P450 eicosanoids in the microcirculation.

Methods: We developed a clickable photo-crosslinking probe (EET-P) based on EETs regio-isomer 14,15-EET, which allowed us to purify and enrich 14,15-EET binding proteins. We confirmed RNA and protein expression in isolated microvascular cells using RNAseq and mass spectrometry, and localized protein in mouse and human tissue using immunohistochemistry (IHC). The functional roles of EETs, HETEs and their putative receptors were examined in-vitro using live-cell calcium imaging and in-vivo using two-photon microscopy.

Results: Using photoaffinity labeling combined with mass spectrometry-based proteomics, we identified GPCR 39 (GPR39) as a potential mediator of EETs actions in the microcirculation. IHC staining of mouse and postmortem human tissue localized GPR39 in microvascular smooth muscle cells (mVSMCs) and peri-capillary pericytes. In primary cultured VSMCs, 15-HETE induced a rise in intracellular calcium ($[Ca^{2+}]i$), which was abolished by 14,15-EET and by a lentiviral-mediated short hairpin RNA (shRNA) knockdown of GPR39. In primary cultured pericytes, pretreatment with 14,15-EET prevents the rise in calcium induced by reoxygenation after oxygen-glucose deprivation (OGD). Finally, inhibition of EETs action on pericytes using 14,15-Epoxyeicosa-5(Z)-enoic acid (14,15-EEZE) constricted capillaries and reduced RBC flux in vivo.
Conclusions: Our results identify GPR39 as a mediator of the effects of 14,15-EET and 15-HETE on mVSMC and pericytes. Our findings suggest that GPR39 is antagonistically regulated in these cells by the balance between two endogenous P450 eicosanoids to fine-tune microvascular blood flow under physiological and post-ischemic conditions.

References

1. Prostaglandins Other Lipid Mediat. 2010 Apr; 91(3-4): 68–84
2. Curr Vasc Pharmacol. 2014;12(6):810–7.

PS03-087

Poster Viewing Session III

PGE_2 EP-1 receptors play an obligatory role in the increase of cerebral blood flow produced by hypercapnia in the mouse brain microcirculation

K. Uekawa[1], K. Koizumi[1], J. Hwang[1], N. Brunier[1], Y. Hattori[1], P. Zhou[1], C. Iadecola[1] and L. Park[1]
[1]Weill Cornell Medical College, Feil Brain and Mind Research Institute, New York, United States

Abstract

Hypercapnia is a potent vasodilator stimulus in the cerebral circulation. Although it has long been known that prostanoids participate in the cerebrovascular effects of hypercapnia, the role of prostaglandin E2 (PGE2) and PGE2 receptors have not been fully investigated. We sought to determine whether cyclooxygenase-1 (COX-1)-derived PGE2 and EP1 receptors are involved in the cerebrovascular response induced by hypercapnia. Male $EP1^{-/-}$ mice and wild type (WT) littermates (age 3–4 months; $n = 5$/group) were anesthetized and equipped with a cranial window overlying the somatosensory cortex. Cerebral blood flow (CBF) was recorded by laser-Doppler flowmetry with controlled blood pressure and physiological variables. In WT mice, neocortical superfusion of the EP1 receptor antagonist SC-51089 (10 μM) attenuated the increase in CBF elicited by systemic hypercapnia ($pCO_2 = 50–60$ mmHg) by 41% ($p < 0.05$ from no treatment) (Figure). These responses were also attenuated in $EP1^{-/-}$ mice. In contrast, in WT mice treated with SC-51089 or in $EP1^{-/-}$ mice the CBF increase elicited by neocortical application of acetylcholine (ACh) or adenosine was not affected ($p > 0.05$) (Figure). Similarly, the CBF increase evoked by whisker stimulation (WS) was not attenuated (Figure). In WT mice, the COX-1 inhibitor SC-560 (25 μM), but not the COX-2 inhibitor NS-398 (100 μM), attenuated the hypercapnic CBF increase by 50% ($p < 0.05$). Neocortical application of PGE2 (1 μM) did not affect resting CBF, but counteracted the attenuation of the hypercapnic response induced by SC-560 (SC-560, $44 \pm 4\%$; SC-560+PGE2, $66 \pm 6\%$; $p < 0.05$). In contrast, exogenous PGE2 did not rescue the attenuation in WT mice induced by SC-51089 or in $EP1^{-/-}$ mice, attesting to the obligatory role of EP1 receptors in the response. The findings indicate that the hypercapnic vasodilatation relies on COX-1-derived PGE2 acting on EP-1 receptors and underscore the critical role that COX-1 derived prostanoids and EP1 receptors play in the regulation of the cerebral circulation.

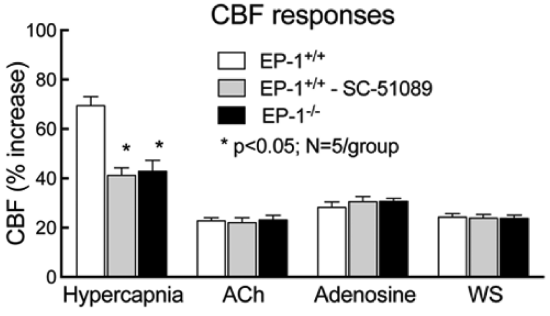

[Uekawa et al figure]

PS03-088

Poster Viewing Session III

Hemodynamic mapping of cell-specific and resting-state functional connectivity in the awake mouse brain

A. Bauer[1], A. Kraft[2], G. Baxter[1], P. Wright[1], M. Reisman[3], A. Bice[1], A. Snyder[1], M. Bruchas[4], J.-M. Lee[2] and J. Culver[1]

[1]*Washington University in St. Louis, Radiology, Saint Louis, United States*

[2]*Washington University in St. Louis, Neurology, Saint Louis, United States*

[3]*Washington University in St. Louis, Physics, Saint Louis, United States*

[4]*Washington University in St. Louis, Anesthesiology, Saint Louis, United States*

Abstract

Functional magnetic resonance imaging (fMRI) has transformed our understanding of the brain's functional organization. However, mapping subunits of a functional network using hemoglobin alone presents several disadvantages. Evoked and spontaneous hemodynamic fluctuations reflect ensemble activity from several populations of neurons making it difficult to discern excitatory vs inhibitory network activity. Still, blood-based methods of brain mapping remain powerful because hemoglobin provides endogenous contrast in all mammalian brains. To add greater specificity to hemoglobin assays, we integrated optical intrinsic signal(OIS) imaging with optogenetic stimulation to create an Opto-OIS mapping tool that combines the cell-specificity of optogenetics with label-free, hemoglobin imaging in awake mice (Fig. 1A). Before mapping, titrated photostimuli determined which stimulus parameters elicited linear hemodynamic responses in the cortex (Fig. 1B). Optimized stimuli were then scanned over the left hemisphere (Fig. 1C) to create a set of optogenetically-defined effective connectivity (Opto-EC) maps. For many sites investigated, Opto-EC maps exhibited higher spatial specificity than those determined using spontaneous hemodynamic fluctuations. For example, resting-state functional connectivity (RS-FC) patterns exhibited widespread ipsilateral connectivity while Opto-EC maps contained distinct short- and long-range constellations of ipsilateral connectivity (Fig. 1D). Further, RS-FC maps were usually symmetric about midline while Opto-EC maps displayed more heterogeneous contralateral homotopic connectivity. We also evaluated the connectivity structure of both modalities against structural connectivity

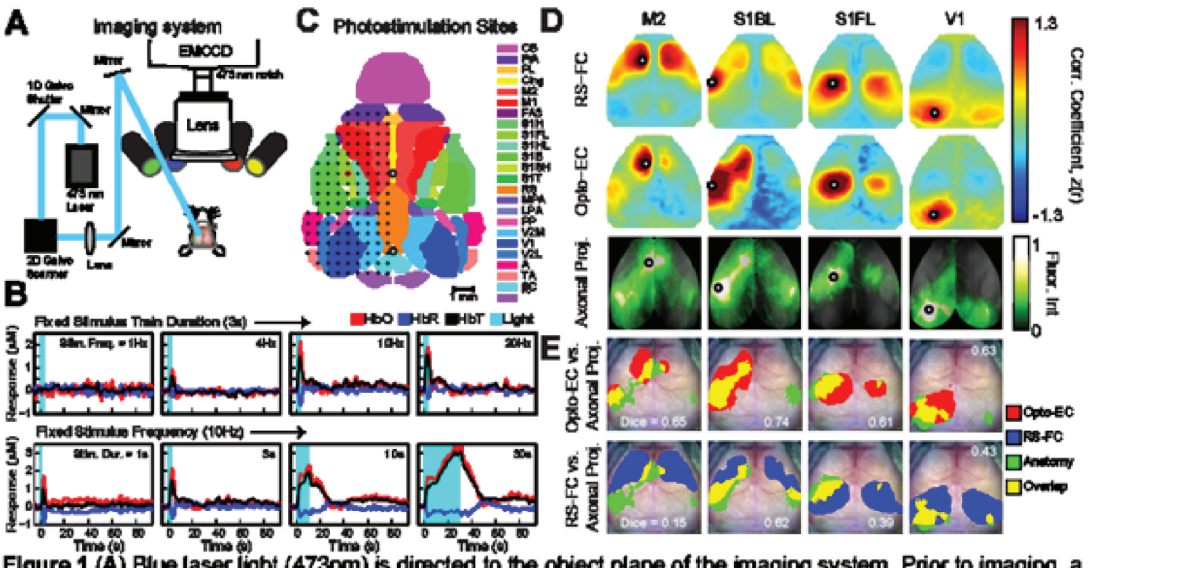

Figure 1 (A) Blue laser light (473nm) is directed to the object plane of the imaging system Prior to imaging, a small Plexiglas window glued to the intact mouse skull is used to secure the mouse head for imaging. (B) Hemodynamic responses to titrated doses of stimulus frequency (top) or duration (Bottom) reveal different temporal characteristics that what would otherwise be expected from physiological stimulation. (C) Sites selected for optogenetic mapping experiments. (D) Top Row: Resting state functional connectivity (RS-FC) maps using 20-30 min of data, Middle row: Maps of optogenetic effective connectivity (Opto-EC) using 25 seconds of data, and Bottom Row: Maps of axonal projections were collected from the Allen Mouse Brain Connectivity Atlas and co-registered to OIS imaging data. M2: secondary motor; S1Bl: primary somatosensory Barrel (lateral); S1FL: primary somatosensory forelimb; V1: primary visual. (E) In order to calculate the spatial overlap between maps, dice coefficients were calculated for Opto-EC and RS-FC maps thresholded at z(r)=0.3 and axonal projection images thresholded at 50% max fluorescence intensity. Opto-EC maps were found to be more topographically similar to structural connectivity images than RS-FC maps.

data from the Allen Institute Mouse Brain Atlas (Fig. 1E). Unlike RS-FC maps, Thy1-based maps collected in awake-behaving mice more closely recapitulated axonal connectivity patterns acquired using ex vivo tracer methods. Collectively these results suggest that Opto-OIS mapping provides a combination of both structural and functional connectivity information that complements analyses of task-evoked and spontaneous hemodynamics and could further the understanding of how the brain's structural framework influences its functional organization in models of disease and plasticity.
[BauerOptoMapping]

PS03-089

Poster Viewing Session III

Impaired hippocampal neurovascular coupling in a mouse model of Alzheimer's disease

L. Li[1], X.-K. Tong[2], E. Hamel[2] and H. Girouard[1]
[1]Université de Montréal, Department of Pharmacology, Montreal, Canada
[2]McGill University, Montreal, Canada

Abstract
Objectives: Alzheimer's disease (AD) is characterized by neuronal degeneration and cerebrovascular dysfunction. Increasing evidence indicates that cerebrovascular dysfunction may be a key or an aggravating pathogenic factor in AD, emphasizing the importance to investigate the tight coupling between neuronal activity and cerebral blood flow (CBF) termed neurovascular coupling (NVC) (1,2). Astrocytes are important players within NVC and in the progression of AD (2,3). Hence, the objective of this study was to characterize the hippocampal NVC in a mouse model of AD.
Methods: Hippocampal NVC was studied in 6-month-old APP transgenic and wild-type mice by *in vivo* laser Doppler flowmetry to measure Schaffer collateral-CA1 evoked CBF responses and *ex vivo* two-photon microscopy to determine astrocytic and vascular responses to electric field stimulation (EFS) in hippocampal slices. Neuronal synaptic transmission, astrocytic reactive oxygen species (ROS), and vascular reactivity were further investigated using electrophysiological, astrocytic Ca^{2+} uncaging or pharmacological approaches.
Results: Hippocampal evoked CBF and *in vitro* vascular responses to EFS were impaired in APP mice compared with age-matched controls, along with decreased basal synaptic transmission, a shorter astrocytic Ca^{2+} signal and altered vascular response to elevated perivascular K^+. However, neuronal long-term potentiation, astrocytic Ca^{2+} amplitude in response to EFS, together with vascular responses to nitric oxide or to the thromboxane receptor agonist U46619 remained unchanged. Importantly, we found a significantly increased resting and Ca^{2+} uncaging-induced ROS production in APP mice. Tempol, a superoxide dismutase mimetic, prevented NVC impairment in APP mice while normalizing astrocytic Ca^{2+} signaling.
Conclusions: Hippocampal NVC is altered at many levels in APP mice, at least in part through oxidative stress. This points out that therapies against AD should include an antioxidative component to protect the neurovascular unit.

References

1. Tong et al. *J Neurosci*. 2012;
2. Girouard et al. *PNAS*. 2010; 3. Osborn et al. *Prog Neurobiol*. 2016.

PS03-090

Poster Viewing Session III

Cerebral blood flow and oxygen delivery changes in response to oxygen inhalation: Impact from the genetic adaptation at high altitude

J. Liu[1,2], H. Wang[3], L.H. Ren[4], P. Zhao[1] and J.M. Serrador[2]
[1]Tangdu Hospital, Fourth Military Medical University, Department of Ultrasound Diagnostics, Xi'an, China
[2]New Jersey Medical School, Rutgers Biomedical Health Sciences, Department of Pharmacology, Physiology & Neuroscience, Newark, United States
[3]Jinling Hospital, Nanjing University School of Medicine, Department of Ultrasound Diagnostics, Nanjing, China
[4]General Hospital of Tibet Military Area Command, Lhasa, China

Abstract
Objectives: Our previous study[1] indicated that Tibetans might blunt total cerebral oxygen delivery (TCOD) response to long-term (>1 year) altitude change (from 400 m to 3658 m) as compared to Han Chinese. The

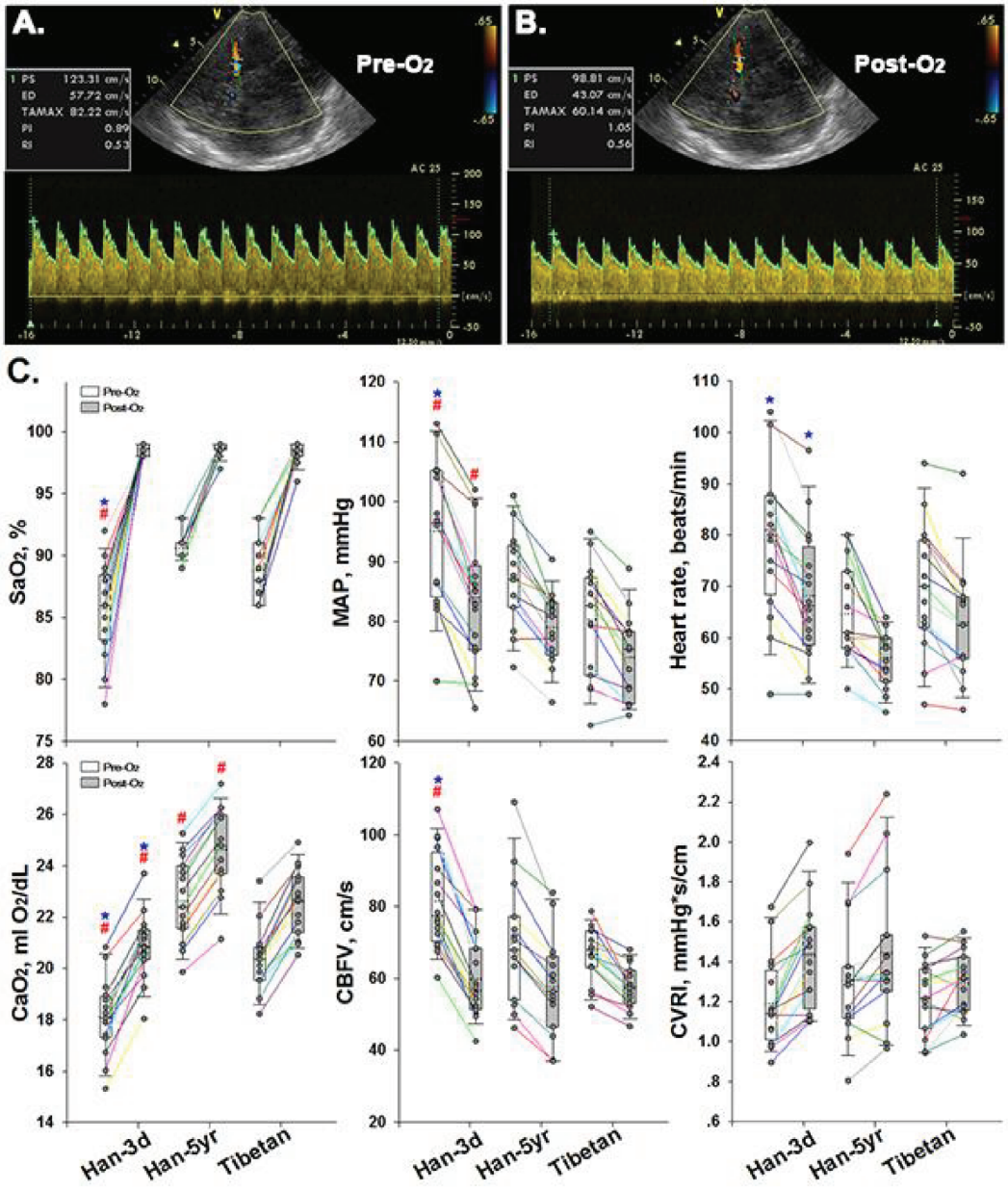

Figure-1. All variables changed significantly after O_2 inhalation as analyzed by paired t-tests.

#$P < 0.05$, *vs.* Tibetan; and *$P < 0.05$, Han-3d *vs.* Han-5yr, using one-way ANOVA with LSD post-hoc tests.

MAP = mean arterial pressure; CaO_2 = arterial oxygen content = 0.0136 × Hb (g/dL) ×SaO_2;

CBFV = TAMAX = time-averaged maximum velocity; CVRI = cerebrovascular resistance index = MAP/CBFV.

present study was aimed to determine whether the genetic adaptation would also impact the TCOD response to a rapid increase in arterial oxygen saturation (SaO_2) at high altitude (HA, 3658 m).

Methods: We enrolled 3 groups of young healthy males: Tibetans (n = 15) and Han Chinese with 5-year and 3-day stay at HA (Han-5yr and Han-3d, n = 15 and 16). The cerebral blood flow velocity (CBFV) was recorded beat-by-beat for 3 minutes at middle cerebral artery (MCA), just before and 4-min after continuous 100% O_2 inhalation (2 L/min) respectively, using transcranial color-coded duplex sonography (Figure-1-A&B). The simultaneous monitoring on finger SaO_2 and a measurement on the hemoglobin concentration (Hb, g/dL) were also performed. Thus when assuming the percentage change of CBFV (Δ%CBFV) approximate to that of total cerebral blood flow, the Δ%TCOD could be derived from a physiological formula.

Results: The 3 groups had similar demographic characteristics and time-course of SaO_2 change (all increased to a stable SaO_2 within 4 min after the O_2-inhalation), with expected among-group differences in Hb (16.9 ± 0.9, 18.4 ± 1.3, and 15.5 ± 1.0). All the measured physiological parameters changed significantly after the O_2-inhalation (Figure-1-C); however the Tibetans showed significantly reduced responses in CBFV and TCOD (assessed by Δ%CBFV/ΔSaO_2 and Δ%TCOD/ΔSaO_2) when compared to both Han-5yr and Han-3d groups (-1.50 ± 0.25 vs. -2.24 ± 0.25 and -2.23 ± 0.27; -0.52 ± 0.27 vs. -1.33 ± 0.26 and -1.38 ± 0.28; Mean $\pm$ SE, $P < 0.05$).
Conclusions: These findings confirmed the impact of genetic adaptation on the cerebral blood flow and oxygen delivery regulations at altitude.

Reference

1. Liu J, et al. 2016; doi: 10.1038/srep30500.

PS03-091

Poster Viewing Session III

Perivascular macrophages mediate vascular oxidative stress and neurovascular dysfunction induced by amyloid-β through CD36 and Nox2

L. Park[1], L. Garcia-Bonilla[1], K. Uekawa[1], P. Zhou[1], R. Pitstick[2], L. Younkin[3], S. Younkin[3], G. Carlson[2] and C. Iadecola[1]
[1]*Weill Cornell Medical College, Feil Brain and Mind Research Institute, New York, United States*
[2]*McLaughlin Research Institute, Great Falls, United States*
[3]*Mayo Clinic Jacksonville, Jacksonville, United States*

Abstract

Amyloid-β (Aβ) has harmful effects on the cerebral microcirculation, which may contribute to cognitive impairment in Alzheimer disease and mixed dementias. The cerebrovascular effects of Aβ are mediated by reactive oxygen species (ROS) from a NOX2-containing NADPH oxidase activated by the interaction of Aβ with the innate immunity receptor CD36. However, the cellular source(s) of the ROS have not been established. We tested the hypothesis that perivascular macrophages (PVM), myeloid cells located within the perivascular spaces and expressing CD36 and NOX2, contribute to the oxidative stress and cerebrovascular dysfunction induced by Aβ. Cerebral blood flow (CBF) was measured by laser-Doppler flowmetry in the somatosensory cortex of urethane-chloralose anesthetized male tg2576 and wild-type (WT) littermates (age 3–4 months; n = 5/group). Since PVM are bone marrow (BM) derived, we used transplant of CD36- or NOX2-negative BM to selectively delete CD36 or NOX2 in PVM. In WT mice transplanted with WT BM (WT⇒WT), superfusion of $A\beta_{1-40}$ (5 μM) attenuated CBF response induced by whisker stimulation (WS) ($p < 0.05$ from vehicle) or by superfusion of acetylcholine (ACh) ($p < 0.05$ from vehicle), which was associated with increase (80 ± 8%) in ROS in PVM (Figure A). However, in WT mice receiving $CD36^{-/-}$ or $Nox2^{-/-}$ BM Aβ failed to increase ROS and to impair the CBF increase ($p > 0.05$ from vehicle) (Figure A). Similarly, CBF responses were ameliorated in tg2576 mice receiving $CD36^{-/-}$ or $Nox2^{-/-}$ BM ($p > 0.05$ from WT⇒WT), an effect associated with reduced vascular oxidative stress (Figure B). Brain $A\beta_{1-40}$ levels did not differ between WT⇒tg2576 and $CD36^{-/-}$⇒tg2576 or $Nox2^{-/-}$⇒tg2576. We conclude that PVM are the critical cells required for the ROS production underlying the cerebrovascular dysfunction induced by Aβ, an effect mediated by CD36 and NOX2. These observations provide evidence that NOX2 and CD36 in PVM may be therapeutic targets to counteract the detrimental neurovascular effects of Aβ.

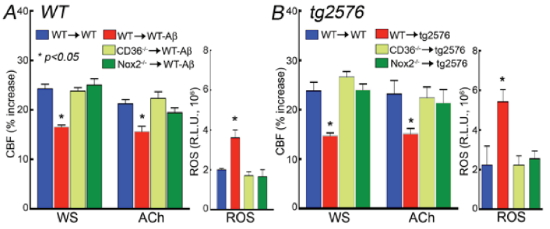

[Park et al Figure]

PS03-092

Poster Viewing Session III

High-resolution functional parcellation of the rat thalamus

B.G. Sanganahalli[1,2], P. Herman[1,2], G.J. Thompson[1] and F. Hyder[1,2,3]

[1]*Yale University, Radiology and Biomedical Imaging, New Haven, United States*

[2]*Yale University, Quantitative Neuroscience with Magnetic Resonance in Medicine, New Haven, United States*

[3]*Yale University, Biomedical Engineering, New Haven, United States*

Abstract

Objectives: The thalamus is a crucial node in cortical-subcortical circuits important for human emotion, cognition, and memory. While invasive studies in animals have revealed rich anatomical and functional separation of various thalamic nuclei, we sought to parse the different portions of the rat thalamus in relation to tactile (forepaw, whisker) and non-tactile (visual, olfactory) stimuli by fMRI.

Methods: We used adult male Sprague-Dawley rats (200–250 g) under α-chloralose and urethane anesthesia were used. Forepaw stimulation (2 mA, 0.3 ms, 3 Hz), whisker stimulation (4 Hz, air puff), visual stimulation (8 Hz and 1 Hz, blue light) and olfactory stimulation (methyl valerate, ethyl butyrate, isoamyl acetate) using custom built hardware. All fMRI data were obtained on a modified 11.7 T Bruker-horizontal-bore spectrometer (Billerica, MA) using a ^{1}H resonator/surface coil RF probe.

Results: Our results demonstrated reproducible thalamic activity during tactile (forepaw, whisker), and non-tactile (visual, olfactory) stimuli. Forepaw and whisker stimulation activated the broader regions within the thalamus: ventral posterior lateral (VPL), ventral posterior medial (VPM), posterior medial (POM) and dorsal and medial parts of lateral geniculate nucleus. Visual stimulation activated dorsal lateral geniculate nucleus (dLGN), whereas olfactory stimulation activated mediodorsal nucleus of the thalamus (MDT). This is the first fMRI study in rodents to show thalamic activation with olfactory stimuli reproducibility. Compared to cortical responses, these thalamic responses were much smaller.

Conclusion: Thalamic regions are difficult to detect because of low sensitivity and/or difficult access. We reproducibly detected BOLD activations of VPL, VPM, POM, dLGN, and MDT, where MDT activation is a novel indication of this structure's involvement during olfactory processing. Future studies of high-resolution neuroanatomy (e.g., DTI) can provide the morphological basis of the high-resolution functional parcellation of the rat thalamus. These results have significance in understanding the role of both cortical-subcortical circuits during sensory integration.

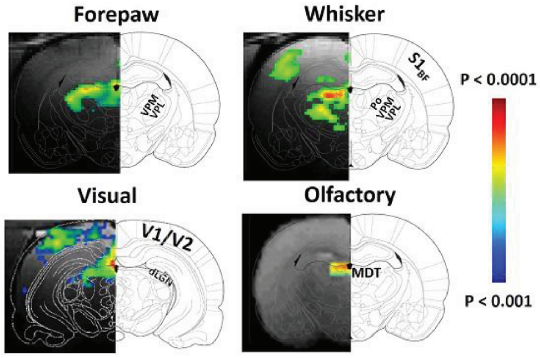

PS03-093

Poster Viewing Session III

Interferometric near-infrared spectroscopy (iNIRS) quantifies brain absorption, scattering, and blood flow index in vivo

D. Borycki[1], O. Kholiqov[1] and V. Srinivasan[1]

[1]*University of California Davis, Biomedical Engineering Department, Davis, United States*

Abstract

Objectives: Quantification of optical (absorption and scattering) and dynamical (blood flow index, BFI) properties of the brain *in vivo* are ongoing goals of near-infrared spectroscopy (NIRS) and diffuse correlation spectroscopy (DCS). While these methods provide a real-time assessment of tissue oxygenation and blood perfusion, quantification using the most widely-adopted implementations requires numerous assumptions, and may be susceptible to extracerebral confounds. Hence, quantitative baseline measurement of oxygen saturation and BFI remain challenging. To address these limitations, we have developed interferometric near-infrared spectroscopy (iNIRS), based on time-of-flight-(TOF-) resolved measurement of

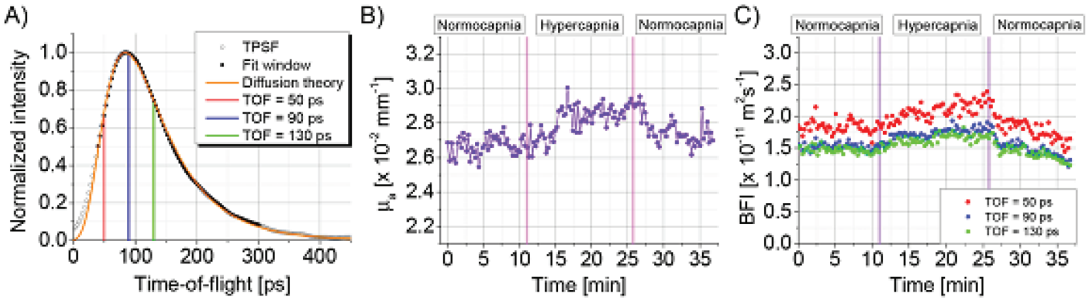

coherent light scattered from the brain. This method enables non-invasive quantification of absorption, scattering, and BFI *in vivo*.

Methods: Our approach is based on interferometry using a coherent tunable laser to achieve path length resolution. The reemitted optical field autocorrelation is measured over time with TOF-resolution; this two-dimensional measurement is then used to derive optical and dynamical properties in the medium. Temporal point spread functions (TPSFs), obtained from the zero-lag autocorrelations, are fitted with diffusion theory to derive optical properties, while BFI is extracted by fitting TOF-dependent field autocorrelation decay rates with diffusing wave spectroscopy (DWS) theory.

Results: We demonstrate that iNIRS can simultaneously quantify optical properties and BFI of the nude mouse brain during hypercapnia. The figure shows a measured representative TPSF and fits with diffusion theory (A). As expected, absorption increases during hypercapnia (B), while BFIs for three distinct path lengths (C) suggest that vasodilation during hypercapnia leads to increased cerebral blood flow.

Conclusions: iNIRS integrates the capabilities of NIRS and DCS techniques into a single modality, quantifying optical and dynamical properties in tissue, making it a promising approach for non-invasive and quantitative monitoring of oxygenation and metabolism *in vivo*.

PS03-094

Poster Viewing Session III

ASL combined with EEG for neurovascular coupling assessment in a clinical model of vascular dementia

C. Huneau[1,2], H. Benali[3] and H. Chabriat[2,4]

[1]*Université de Nantes, LS2N, Nantes, France*
[2]*Inserm U1161, Genetics and Pathogenesis of Cerebrovascular Diseases, Paris, France*
[3]*Concordia University, Department of Electrical & Computer Engineering, Montreal, Canada*
[4]*DHU NeuroVasc, Sorbonne Paris Cité, Paris, France*

Abstract

Neurovascular coupling (NVC) is responsible for local cerebral functional hyperemia in response to transient increase of neural activity. There is accumulating evidence suggesting that different physiological processes might be involved at different timing during prolonged neuronal stimulation. We hypothesized that dynamics of hyperemia might be altered in some specific human pathological conditions. For this purpose, we investigated NVC in CADASIL, a genetic disorder caused by NOTCH3 gene mutations and affecting early both pericytes and smooth muscle cells functioning within the cerebral microcirculation bed. Functional MRI using arterial spin labelling (ASL) providing enough time resolution for measuring the dynamics of functional hyperemia combined with Electroencephalogram (EEG) for measuring electrical activity were used in 30 CADASIL patients and 30 age-matched healthy controls subjects. Both motor and visual stimulations within primary cortical regions were obtained during stimulation blocks varying from 20s to 60s. Dedicated processing was used to detect

independently activated region without any prior on canonical hemodynamic responses. Although baseline blood flow values did not differ between patients and controls, a significant reduction of the amplitude of functional hyperemia was detected in patients, especially for longer stimulation blocks. This difference was observed both in visual and motor areas. In contrast, no difference was detected in the same cortical regions when measuring evoked potentials during simultaneous and identical visual stimuli, in line with previous data obtained in CADASIL. Our results strongly support that alterations of neurovascular coupling can be detected using ASL combined to EEG early in CADASIL and may represent a potential biomarker for evaluating microcirculatory alterations at early stage in this archetypal cerebral small vessel disease.

PS03-095

Poster Viewing Session III

Metabolic demand of neural-hemodynamic associated and disassociated areas with calibrated fMRI

P. Herman[1], B.G. Sangannahali[1], D.L. Rothman[1,2], H. Blumenfeld[3] and F. Hyder[1,2]

[1]*Yale University, Department of Radiology and Biomedical Imaging, New Haven, United States*

[2]*Yale University, Department of Biomedical Engineering, New Haven, United States*

[3]*Yale University, Department of Neurology, New Haven, United States*

Abstract

Objectives: In search of specific type of neuronal activity that is reflected by fMRI, Logothetis and colleagues found that the sensory-evoked BOLD response in primate cerebral cortex is better correlated to LFP than MUA[1]. While this result is used to argue that cortical BOLD signal primarily reflects LFP, another important implication is that MUA is disassociated from LFP which has been reported under a variety of other situations[2]. Regional dissociation of MUA from LFP, and hence BOLD or CBF, has been

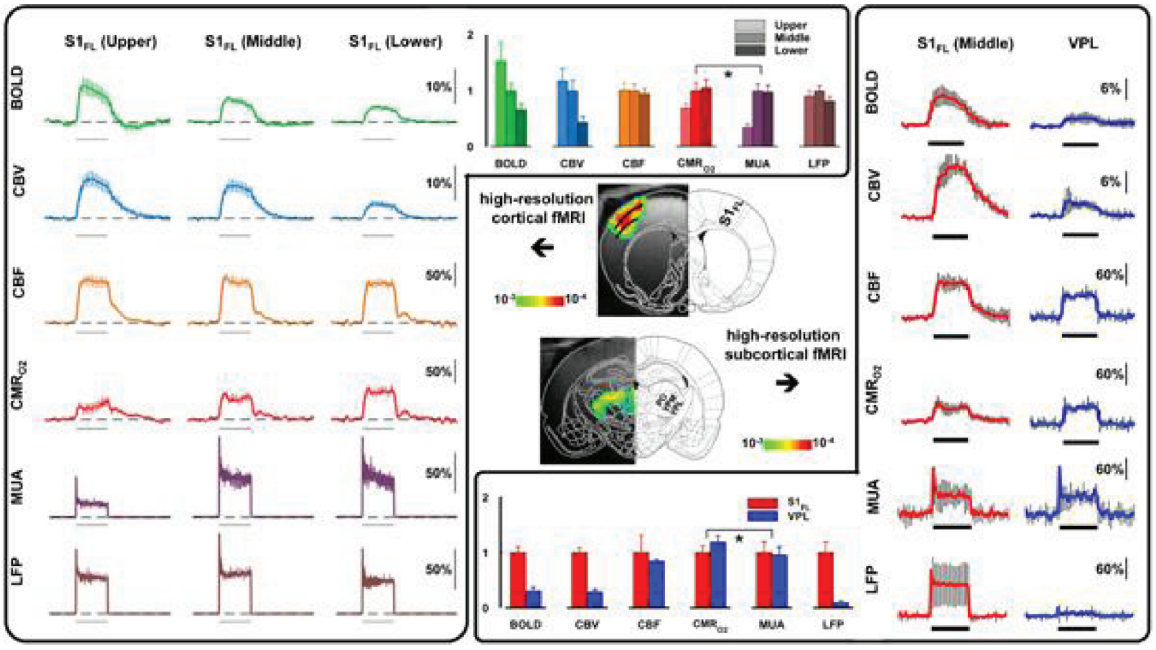

rationalized on both vascular-, and circuitry-based differences. To examine if neural-hemodynamic associated and disassociated areas have different metabolic demands, we used rat's thalamic VPL and laminae of the cortical $S1_{FL}$ as two model regions where LFP and MUA can be associated or disassociated from the respective BOLD responses.

Methods: At 11.7T we measured sensory-evoked responses of BOLD, CBF, CBV, and CMR_{O2} from rat's VPL and $S1_{FL}$ and compared them to extracellular recorded MUA and LFP[3,4].

Results: Calibrated fMRI and electrophysiology data in $S1_{FL}$ and VPL during sensory stimulation (Figure) showed that BOLD and CBV responses were greater in $S1_{FL}$ than in VPL, similar to LFP regional differences. CBF and CMR_{O2} responses were both comparable in both regions. Despite different levels of CBF-CMR_{O2} and LFP-MUA couplings in VPL and $S1_{FL}$, the CMR_{O2} was well matched with MUA in both regions and in cortical laminae.

Conclusions: These results suggest that neural-hemodynamic associated and disassociated areas in brain can have similar metabolic demands and therefore challenge the notion that conventional fMRI can accurately reflect regional changes in neuronal activity unless regionally calibrated.

References

1. Logothetis *et al. Nature* **412**:150–157 (2001).
2. Ekstrom *BrainResRev* **62**:233–244 (2010).
3. Herman *et al. PNAS* **110**:15115–15120 (2013).
4. Sanganahalli *et al. JCBFM* **36**:1695–1707 (2016).

Supported by NIH (R01 MH-067528, P30 NS-052519).

PS03-096

Poster Viewing Session III

Vascular tPA influences neurovascular coupling through an NMDA-receptor dependent mechanism

A. Anfray[1], D. Vivien[1] and C. Orset[1]
[1]INSERM U919/University of Caen Normandy, Caen, France

Abstract

Neurovascular coupling refers to the fact that neuronal activity leads to a local increase in cerebral blood flow. Beyond its roles in the vascular compartment, tissue-type Plasminogen Activator (tPA) influences NMDA-receptors signaling and subsequent brain physiological processes. Previous studies have reported an implication of tPA in the mechanisms of neurovascular coupling (Park et al., PNAS, 2008). The goal of our present study was to further investigate the role of the vascular tPA in the control of the neurovascular coupling. To address this question, we used a murine model of mechanical stimulations of vibrissae coupled with the recording of the cerebral blood flow by using the laser Doppler speckle. We first confirmed that tPA is involved in the increase of the cerebral blood flow evoked by somatosensory stimulations. Secondly, we demonstrated that this effect is mediated by the vascular tPA. Then, we used a protocol of hydrodynamic transfection in tPA-deficient mice, allowing a release of tPA and tPA variants in the circulation. We transfected mice with a plasmid containing the cDNA encoding for either the wild type tPA or for a tPA mutated on its Kringle 2 domain (a domain involved in the interaction of tPA with NMDA receptor). Modulation of the cerebral blood flow occurred with the wild type tPA in the blood stream, but not with the tPA mutated on its Kringle 2 domain. We then confirmed the role of the tPA-dependent NMDA receptor signaling in the modulation of the neurovascular coupling by using pharmacological approaches targeting NMDAR (AP-5) and the tPA-dependent NMDAR signaling (Glunomab). By using these strategies, we demonstrated the ability of the vascular tPA to increase blood flow after a somatosensory stimulation, a process involving its interaction with NMDA receptors expressed on endothelial cells.

PS03-097

Poster Viewing Session III

Brain endothelial $G\alpha_{q/11}$ signaling is involved in cerebral blood flow regulation

J. Wenzel[1], J.C. Assmann[1], S. Offermanns[2] and M. Schwaninger[1]
[1]University of Lübeck, Institute of Experimental and Clinical Pharmacology and Toxicology, Lübeck, Germany
[2]Max Planck Institute for Heart and Lung Research, Bad Nauheim, Germany

Abstract

Cerebral blood flow (CBF) is tightly regulated to meet the high metabolic demands of the brain. Different stimuli induce an increase in brain perfusion like neuronal activity or an increase in arterial CO_2 concentration. Whether brain endothelium is directly involved in the regulation of stimulated blood flow is unclear so far.

As $G\alpha_{q/11}$-coupled receptors are known to mediate CBF increase upon stimulation, we asked, whether this signaling pathway plays a role in brain endothelial cells. To test this concept we used $G\alpha_{11}$ knockout mice and crossed them with the *Slco1c1*-CreER^{T2} mouse line carrying a floxed $G\alpha_q$ gene. The generated mice ($G\alpha_{q/11}{}^{beKO}$) were deficient of $G\alpha_{q/11}$ signaling in brain endothelial cells. The same strategy was used to delete the $G\alpha_{q/11}$ signaling pathway in astrocytes by using a *Glast*-CreER^{T2} mouse line.

We used calcium imaging in primary brain endothelial cells to verify the knockout, showing an almost absent calcium increase in endothelial cells deficient of $G\alpha_{q/11}$ compared to control cells stimulated with ATP.

To induce a CBF increase in the cortex we used whisker pad stimulation and measured the CBF response by laser speckle imaging. We found a reduced CBF increase in $G\alpha_{q/11}{}^{beKO}$ mice, whereas astrocytic knockout of the $G\alpha_{q/11}$ signaling pathway had no effect on neurovascular coupling. Similarly, $G\alpha_{q/11}{}^{beKO}$ mice showed a reduced response upon CBF stimulation by increased inhaled CO_2 concentration. On the other hand, basal perfusion was the same in control and in $G\alpha_{q/11}{}^{beKO}$ mice, as well as blood flow response upon isoflurane inhalation.

To summarize, we found endothelial but not astrocytic $G\alpha_{q/11}$ signaling to be important for neurovascular coupling. In addition, endothelial cells mediate the CBF response upon increased CO_2 concentration by this signaling pathway. These findings imply a relevant contribution of endothelial cells to the cerebral blood flow regulation by G protein-coupled receptors and their downstream signaling.

PS03-099

Poster Viewing Session III

Montreal scale of cognitive functions in early diagnosis of constrictive cerebral arteries

M. Salohiddinov[1]
[1]*Tashkent Medical Academy, Neurology, Tashkent, Uzbekistan*

Abstract

Objective: To study the efficacy of diagnosis of the violation of cognitive functions in patients with chronic vascular – cerebral insufficiency (CHVCI) III-IV degree combined vascular dementia via Montreal cognitive assessment scale (MoCA test).

Methods: The study involved 60 patients (32 men and 28 women) aged 45 to 65 years (mean age 58,6 ± 5,3 years). Group I group CHVCI (III-IVst.) 30 patients with vascular dementia and 30 patients with CHVCI (III-IVst.) without cognitive impairment. As a method of research objective measures of cognitive functions we used MoCA- test. As a control group 30 healthy volunteers were involved with no pathology of the central nervous system.

Results: Study showed: in group I – hand- skills 2,9 ± 0,2, short-term memory 0, a test for attention 2.8 ± 0, 2, score on speech fluency test 0,9 ± 0,2, 0 points- abstract thinking, delayed reproduction 1,8 ± 0,2 points, the test for orientation in time 1,7 ± 0,3 points. In Group II – hand-executive skills averaged 4,9 ± 0,1 points, short-term memory 1 point, a test for attention 3,8 ± 0,4 points for fluency test speech 2,1 ± 0,3, the test for abstract thinking 1,9 ± 0,1, delayed reproduction 3,8 ± 0,3, test time orientation 4,7 ± 0,2 points.

Duplex scanning of neck vessels revealed the presence of hemodynamic significant deficiency in group I 65%, hemodynamic insignificant deficit in Group II 47% in the control group, 30–32% in the normal range.

Conclusions: The total score of Montreal Cognitive Scale is a sensitive indicator of cognitive impairment from mild to moderate to deep vascular dementia, is effective in determining the tactics of therapeutic approaches in patients with stenotic lesions of MCA.

References

1. Gomez-Pinilla, Fernando. "The Combined Effects of Exercise and Foods in Preventing Neurological and Cognitive Disorders".
2. Ferrara, Miranda. "Memory and Amnesia".

PS03-100

Poster Viewing Session III

Noradrenergic deficits in Parkinson's disease: Relations to cognitive and cortical oscillatory activity declines

A. Nahimi[1], M. Sommerauer[1], K. Østergaard[2], M.B. Kinnerup[3], M. Winterdahl[3], R. Krogbæk[2], J. Jacobsen[3], A. Schacht[3], P. Borghammer[3], M.F. Damholdt[1], B. Johnsen[4] and A. Gjedde[5,6]

[1]Aarhus University Hospital, Department of Clinical Medicine, Aarhus, Denmark
[2]Aarhus University Hospital, Department of Neurology, Aarhus, Denmark
[3]Aarhus University Hospital, Department of Nuclear Medicine and PET-Centre, Aarhus, Denmark
[4]Aarhus University Hospital, Department of Neurophysiology, Aarhus, Denmark
[5]University of Copenhagen, Department of Neuroscience and Pharmacology, Copenhagen, Denmark
[6]Johns Hopkins University School of Medicine, Department of Radiology and Radiological Sciences, Baltimore, United States

Abstract

Objectives: In vitro studies suggest that noradrenergic projections from locus coeruleus to subcortical and cortical brain structures, e.g., thalamus, undergo severe neurodegeneration in Parkinson's disease (PD). Loss of noradrenergic projections may alter oscillatory activity that in turn may be associated with cognitive decline. To test this hypothesis of the origin of cognitive decline in this disease, we used positron emission tomography (PET) to quantify the density of noradrenergic projections in groups of PD patients and healthy controls (HC), in combination with neuropsychological assessment and recording of quantitative electroencephalography (qEEG).

Methods: Following administration of ^{11}C-MeNER, the positron-emitting form of a selective noradrenaline reuptake transporter antagonist, 17 non-demented PD patients and 10 HC underwent 90–120 minutes' dynamic PET. The caudate was established as the reference region in datasets with arterial blood samples. The binding potential of ^{11}C-MeNER relative to non-displaceable tracer (BP_{ND}) was estimated with the simplified reference tissue model 2 (SRTM2), correlated to cognitive function in four domains, and to changes of cortical oscillatory activities measured with qEEG.

Results: Global ^{11}C-MeNER BP_{ND} values were reduced numerically in the PD group, with regionally significant declines in the thalamus, hypothalamus, and nucleus ruber. Tremor was associated with attenuated decline of tracer binding. The value of thalamic ^{11}C-MeNER BP_{ND} was associated with cognitive performance, independent of premorbid cognitive function or disease. PD patients had significant slowing of qEEG, e.g., the background alpha rhythm, but only EEG reactivity upon eye opening correlated with thalamic ^{11}C-MeNER BP_{ND} in PD patients.

Conclusion: This is the first direct quantification of noradrenergic denervation in vivo in PD patients. In agreement with predictions from in vitro studies, we discovered a global decline of noradrenergic projections in the brains of PD patients in vivo. Noradrenergic degeneration in PD may explain perturbed cognition associated with the reduced cortical oscillatory activity.

PS03-101

Poster Viewing Session III

Elicitation of cortical spreading depolarization (CSD) in adult rats by substance P – a mechanism to aggravate secondary cortical damage after brain injury or infection?

F. Richter[1], J. Leuchtweis[1], A. Eitner[1], A. Lehmenkühler[2] and H.-G. Schaible[1]

[1]University Hospital Jena – Friedrich Schiller University, Institute of Physiology I, Jena, Germany
[2]Pain Institute & Center for Medical Education, Düsseldorf, Germany

Abstract

It is assumed that substance P (SP) critically contributes to secondary damages in the brain. In this study we tested, whether SP could induce CSD, an energy consuming process particularly in a previously damaged brain.

We recorded in spontaneously breathing anesthetized adult rats (sodium thiopentone, 100 mg/kg, i.p.) CSD in cerebral cortex with two pairs of glass micropipettes (distance 5–6 mm) at depths of 400 and 1200 μm in two separated areas of the brain. In one area, CSD was elicited by a microinjection of 1 M KCl (tip diameter 5 μm, 100 kPa, 300 ms-1 s) into the grey matter at intervals of 30 min.

100 μl of 10^{-5} M SP were applied topically to the remote cortical surface and left there. In another group of rats, we performed microinjections of 10^{-5} M SP into the grey matter at different depths starting from 1200 μm up to 200 μm.

In all rats tested, the topical application of SP induced a series of CSD (3–7 within the first 30 min of application). Amplitudes of CSD did not differ from those elicited by KCl and 87% propagated into the untreated cortical area. The application of SP did not significantly interfere with the CSD amplitudes induced by KCl in the untreated area, slightly increased the amplitudes in the treated area (400 μm depth: control 21.3 ± 3.0 mV, after two hours 23.2 ± 4.8 mV; 1200 μm depth: control 21.7 ± 1.4 mV, after two hours 27.4 ± 4.0 mV), and did not change propagation velocity. Microinjections of 10^{-5} M SP with pulses of 300 ms-1 s in cortical depths between 600 and 1200 μm failed to elicit CSD.

Our results confirm that SP is a candidate to elicit CSD independently from other depolarizing agents. CSD might contribute to secondary brain damage besides the other pathophysiological effects of SP.